MASTERARBEIT

Titel der Masterarbeit

„The Role of Mitogen Activated Protein Kinase-Activated Protein Kinase 2 in Proliferation and Migration of Gastroesophageal Cancer Cells"

verfasst von

Jasmin Stieger, BSc

angestrebter akademischer Grad

Master of Science (MSc)

Wien, 2014

DANKSAGUNG

Mein größter Dank gilt meinen Eltern, die mich während meines gesamten Studiums unterstützt haben und immer an mich glauben.

Weiters möchte ich mich bei meiner Betreuerin Frau ao. Univ.-Prof. Dr. Christine Brostjan bedanken, die mich herzlich in ihr Team aufgenommen und exzellent betreut hat. Ich habe sehr viel gelernt - danke!
Mein Dank ergeht auch an meinen Betreuer Herrn ao. Univ.-Prof. Dr. Peter Birner, MSc.
Außerdem möchte ich den Kooperationspartnern dieses Projekts, Herrn Univ.-Prof. Dr. med. univ. Berthold Streubel und Herrn ao. Univ.-Prof. Dr. med. univ. Sebastian Schoppmann, sowie Frau Dr. Ursula Vinatzer, meinen Dank aussprechen.

Frau Ao. Univ.-Prof. Dipl.-Biol. Dr. Angela Witte möchte ich für die Betreuung meiner Masterarbeit an der Universität Wien danken.

Ein herzliches Dankeschön auch an alle Mitarbeiter der Abteilung für Chirurgische Forschung für eine unvergessliche Zeit! Frau Dipl.-Ing. Elisabeth Buchberger sei gedankt für die geduldige Beantwortung aller meiner Fragen und ihre technische Unterstützung. Vielen Dank an Katrin Gitschtaler, MSc und Anna Zommer - lustig war's mit euch!

Zum Schluss möchte ich noch meinem Partner Stefan danken - für all seinen Zuspruch, seine Unterstützung und Motivation. Tack för allt!

TABLE OF CONTENTS

1 INTRODUCTION

1.1 Mitogen Activated Protein Kinase-Activated Protein Kinases

Mitogen activated protein kinase-activated protein kinases (MAPKAPKs) represent a signaling step downstream the cascades of mitogen activated protein kinases (MAPKs) and transmit signals initiated by extracellular stimuli into diverse cellular responses and processes like proliferation and differentiation, protein synthesis and chromatin remodeling, apoptosis, immunity, motility and tumor progression [1].

15 MAPKs have been comprehensively investigated and they can be divided into seven groups [2]. The following kinases belong to the subdivision of conventional MAPKs: the extracellular signal-regulated kinases 1/2 (ERK1/2), c-Jun amino (N)-terminal kinases 1/2/3 (JNK1/2/3), p38 isoforms (α, β, γ, and δ), and ERK5. The group of atypical MAPKs comprises ERK3/4/7/8, and the Nemo-like kinase (NLK). When MAPKs forward a signal triggered by a stimulus, they phosphorylate various substrates including the MAPKAPK subgroups of p90 ribosomal S6 kinases (RSKs), mitogen- and stress-activated kinases (MSKs), MAPK-interacting kinases (MNKs), and the MAPK-activated protein kinases 2/3/5 (MK2/3/5) (Fig. 1) [1].
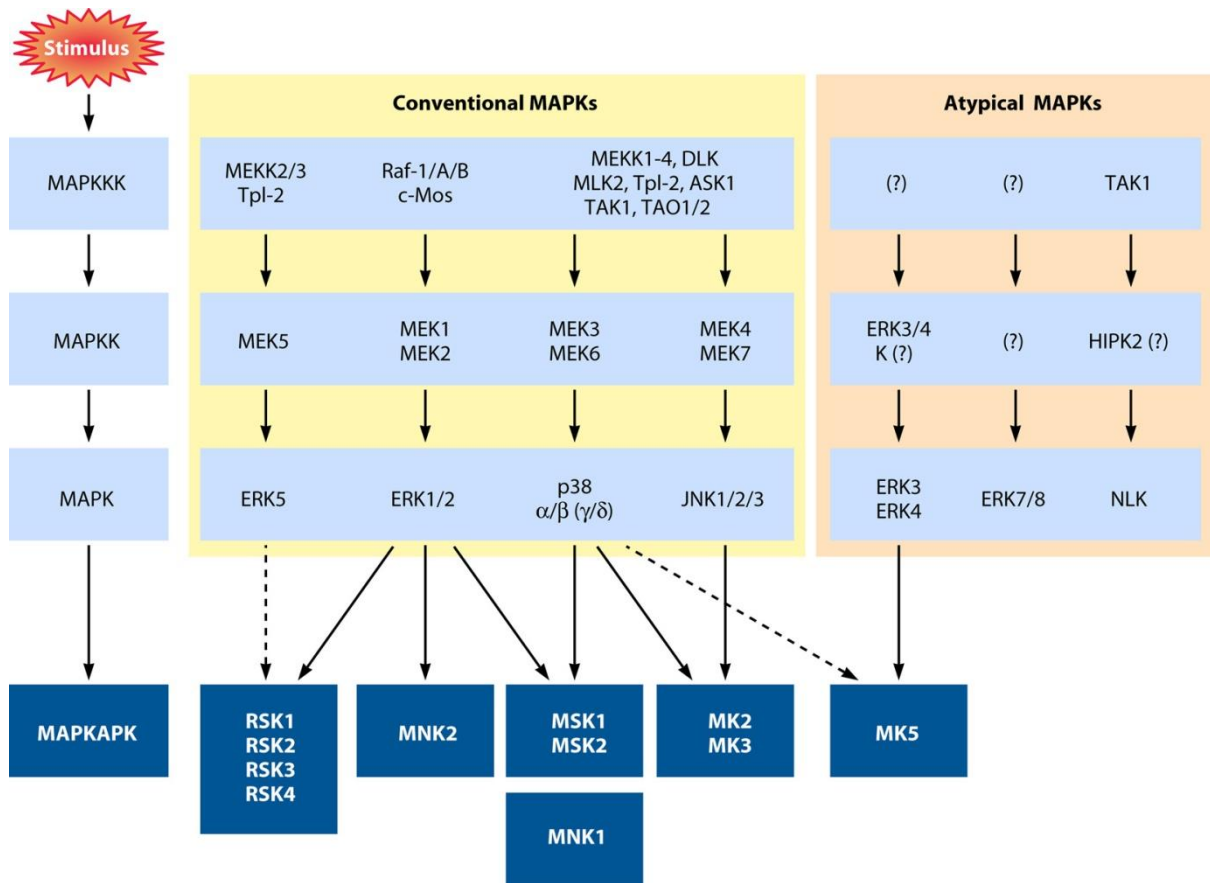
Fig. 1 Conventional and atypical MAPKs and their upstream and downstream pathway steps. Stimuli trigger the phosphorylation and activation of different MAPK pathways which then phosphorylate the family of MAPKAPKs, including RSKs, MNKs, MSKs and MKs [2].

MAPKAPKs belong to the family of calcium/calmodulin-dependent protein kinases and contain the same activation loop sequence which is necessary for phosphorylation by the corresponding upstream MAPK [3]. In MK2 and MK3 there is an additional regulatory phosphorylation site which is located in the hinge region between the catalytic and the C-terminal domain (Fig. 2) [4, 5]. The C-terminus of MNK1, MK2, MK3, and MK5 contains a nuclear export signal (NES) responsible for the export of the kinases from the nucleus into the cytosol, see Fig. 2 [6, 7]. In case of MK2/3 the exposition of the NES after phosphorylation leads to nuclear export of the complex of active p38α and MK2/3. MNK2 also comprises an NES, but this signal sequence is not functional due to the lack of certain residues which are important for NES function [8]. The sequences of MSK1, MSK2, MK2, MK3, and MK5 contain a nuclear localization signal (NLS) at the C-terminal domain, whereas RSK3 includes an NLS at its N-terminus.

The basic residues in the NLS of MK2 and MK3 are responsible for enabling binding of p38 MAPKs as well as modulating the NLS function [9] (Fig. 2).

Fig. 2 Schematic drawing of the protein structure of MAPKAPKs. RSK1/2/3/4 and MSK1/2 comprise two different N-terminal and C-terminal kinase domains (NTKD and CTKD), whereas MNK1/2 and MK2/3/5 have a single kinase domain. NES and NLS are denoted above, as well as respective phosphorylation sites and the D domain or MAPK docking site [2].

The N-terminal region of MK2 and MK3 also contains a proline-rich sequence which is responsible for interaction with Src-homology-3 (SH3) domains *in vitro.* MNK1 and MNK2 own a polybasic region (PBR) which is not only important in the recognition of the eukaryotic initiation factor 4G, but also functions as an NLS for promoting nuclear import by importin α [7].

1.2   Mitogen Activated Protein Kinase-Activated Protein Kinase 2

The mitogen activated protein kinase-activated protein kinase 2 (MK2) was first described by Stokoe et al. in 1992 [5] where they identified MK2 as the kinase which modifies the heat shock protein 27 (Hsp27) or its murine homologue heat shock protein 25 (Hsp25) [10].
In their work they demonstrated that MK2 is able to phosphorylate all serine residues of Hsp27 and Hsp25 in response to heat shock or mitogens.

MK2 is 400 amino acids long and present in two splice variants where only one version owns an NLS and a p38 binding domain [11]. The second splice variant represents a shortened version which can still be phosphorylated by p38α but resulting in a less efficient signal transduction. As depicted in Fig. 2, MK2 possesses a proline-rich sequence for interaction with SH3 domains at its N-terminus, followed by a kinase domain, an NES and an NLS which is divided into two parts, the NLS itself and a domain (D) for attachment of p38 [2, 11].

MK2 is expressed in most tissues [12]. A high level of expression can be found in the heart and in whole blood, more specifically in CD34$^+$ hematopoietic stem cells, CD19$^+$ B cells, CD56$^+$ natural killer cells, and CD33$^+$ myeloid granulocyte precursor cells. Furthermore, MK2 is highly expressed in BDCA4$^+$ dendritic cells [12]. In pathological situations, MK2 may be elevated and activated in rheumatoid arthritis [13], inflammatory bowel disease [14], Burkitt's lymphoma [12], gastro-intestinal stromal tumors (GISTs) [15], colon cancer [16], Kaposi's sarcoma [17], lung cancer [18], prostate carcinoma [19], bladder cancer [20], and nasopharyngeal tumors [21, 22].

In resting cells a stable nuclear heterodimer of p38α and MK2 with an active NLS is present [23, 24] (Fig. 3). After phosphorylation of mitogen-activated protein kinase kinase 6 (MKK6) by stress stimuli or cytokines, MKK6 phosphorylates p38α which then in turn activates MK2 via phosphorylation of Thr^{25}, Thr^{222}, Ser^{272}, and Thr^{334} [2, 9, 11]. The phosphorylation of Thr^{334} is critical for a conformational change of MK2 exposing the NES, masking the NLS and subsequent export of the active p38α-MK2 complex to the cytoplasm. A steady-state with a mainly cytoplasmatic localization of active p38α-MK2 is then reached [9, 23].
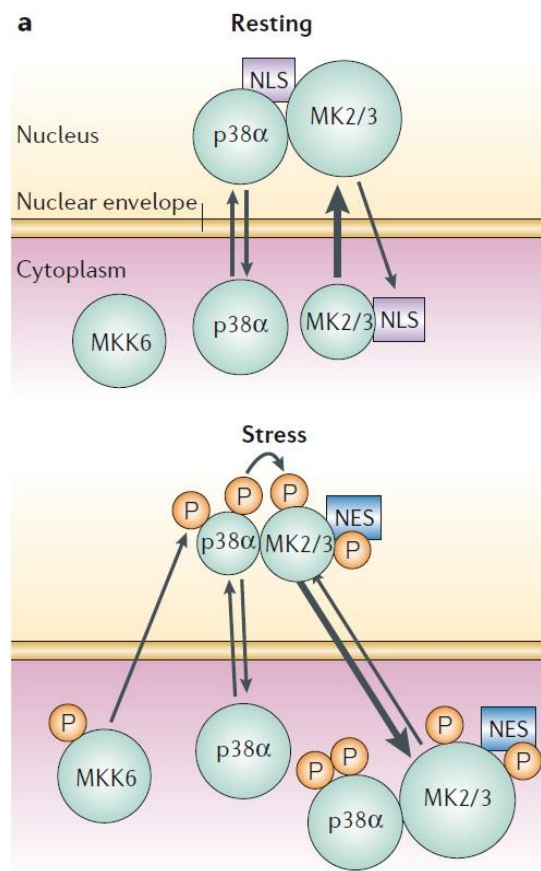
Fig. 3 Activation and nuclear export of MK2. The p38α-MK2 complex is present in the nucleus of resting cells until p38α is activated by MKK6. This then leads to an activation of MK2 and a following export of the p38α-MK2 complex to the cytosol [9].

In their experiments, Engel et al. showed that a constitutively active green fluorescent protein (GFP)-MK2 fusion molecule in 3T3 fibroblasts, containing a functional NES as well as an NLS, is localized in the cytoplasm to a large extent, but is rapidly reimported into the nucleus after treatment with leptomycin B, a nuclear export inhibitor. Their study further demonstrated that MK2 contains a constitutively active NLS signal but requires a stress-regulated signal for nuclear export [23].

MK2 is not solely activated by p38α, but also phosphorylated by ERK1/2 at the same residues, although most of the *in vivo* studies focused on p38α-MK2 signaling [5].

1.2.1 MK2 in Cell Cycle Control and Proliferation

Two kinases are responsible for signal transduction after DNA damage: Ataxia telangiectasia mutated (ATM) phosphorylates its downstream target checkpoint kinase 2 (Chk2) and ataxia telangiectasia and Rad3-related protein (ATR) is responsible for activation and phosphorylation of checkpoint kinase 1 (Chk1) (Fig. 4) [25]. The phosphatase cell division cycle 25B (Cdc25B) can be inactivated by both Chk1 and Chk2, whereas cell division cycle 25A (Cdc25A) is inactivated only by Chk1-mediated phosphorylation.

Beside Chk1 and Chk2, MK2 is the third checkpoint effector involved in mediating DNA damage response and it is acting in parallel to these two kinases. MK2 is able to phosphorylate and therefore inactivate both, Cdc25A and Cdc25B [25]. Loss of Cdc25 activity results in cell cycle arrest, as the target Cdk (cyclin-dependent kinase) molecules remain phosphorylated and hence blocked. The cell cycle arrest is intended to allow for DNA repair and promote cell survival after DNA damage.
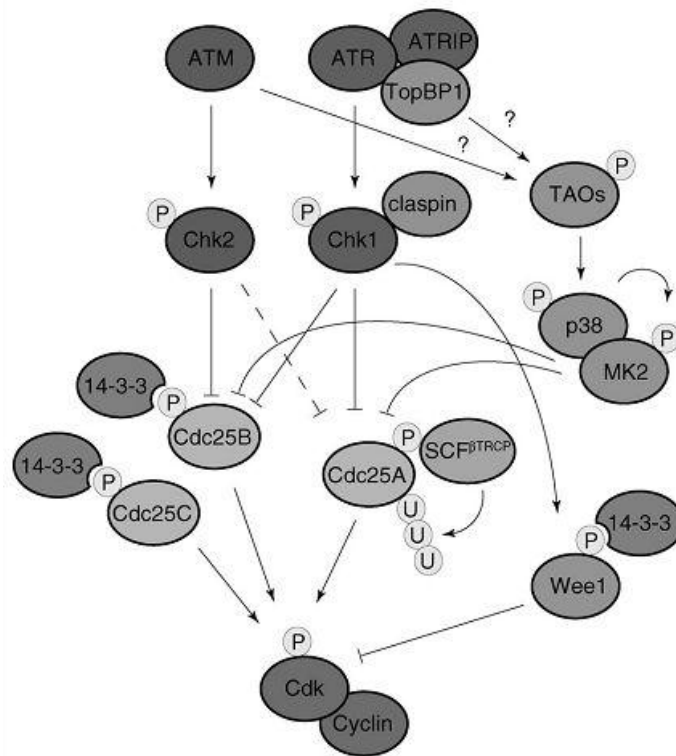
Fig. 4 Activation of ATM- and ATR-dependent and -independent pathways leading to Cdk inhibition after DNA damage. Chk1, Chk2, and p38/MK2 are activated by their upstream effectors and then lead to phosphorylation of the Cdc25 phosphatases. Cdc25 family members then in turn are not able to dephosphorylate Cdk anymore. As a result, cell cycle is arrested [25].

Thus, MK2 contributes to cell cycle arrest in phase G2 after cell damage caused by e.g. UV irradiation or exposure to viral protein R (VPR) [26]. Experiments showed that after induction of vpr expression, the amount of cells in G2/M phase was significantly higher compared to untreated cells. The underlying VPR-triggered process was the MK2-mediated phosphorylation of Cdc25.

After DNA damage by the chemotherapeutics cisplatin, camptothecin, and doxorubicin the p38/MK2 module is activated via ATR, and doxorubicin additionally involves ATM [27]. Of interest, MK2 is specifically required to promote cell survival after chemotherapeutic DNA damage in p53 mutant cancer cells [27]. Furthermore, UV irradiation is able to activate p38 and MK2 in a way independent of ATM or ATR which might be due to different kinds of DNA damage introduced by UV irradiation and chemotherapeutics [25, 27].

1.2.2 MK2 in Cell Motility and Invasion

After activation of MK2 by p38, the capping protein Hsp27 is phosphorylated at the residues Ser[15], Ser[78], and Ser[82] and as a result it is no longer able to block actin polymerization [28-31]. This then leads to remodeling of actin filaments and cell migration. To guarantee a coordinated process of Hsp27 activation and inactivation, reversible modification of MK2 by small ubiquitin-like modifiers (SUMOs) is an important step. MK2 contains a SUMOylation site at Lys[339] which acts like a switch for a controlled phosphorylation and dephosphorylation of Hsp27 by affecting the kinase activity of MK2. Thus, SUMOs are capable of MK2 inhibition which then allows Hsp27 to block actin polymerization again [29].

Xu et al. showed that in prostate cancer cells stimulation of p38 by transforming growth factor beta (TGFβ) led to an activation of MK2 as well as Hsp27, followed by an increase of MMP2 (matrix metalloproteinase 2) activity and cell invasion [19]. Experiments with *MK2* dominant-negative cells showed that there was no upregulation of MMP2 activity after TGFβ treatment, whereas in cells with constitutively active MK2 there was no response beyond basal expression of MMP2 after stimulation with TGFβ. Kumar et al. investigated the impact of MK2 on bladder cancer cell invasion by upregulation of MMP2 and MMP9 [20]. They could show that p38 and MK2 are important regulators of MMP2 and MMP9 by stabilizing their mRNA. MMPs generally contribute to the degradation of extracellular matrix components thereby facilitating cell invasion into the tissue.

A more detailed insight to the role of MK2 in cancer is given in the Introduction section 1.2.4.

1.2.3 MK2 in Cytokine and Chemokine Regulation

MK2 plays a crucial role in the regulation of various cytokines, for example tumor necrosis factor alpha (TNFα), interferon gamma (IFNγ), interleukin 6 (IL6) or interleukin 8 (IL8) [32-34]. Mainly, the stabilization of mRNA is a key component for cytokine control by MK2.

Several experiments by Winzen et al. demonstrated that IL6 and IL8 possess AU-rich elements (AREs) in their 3' untranslated region and those AREs are essential to mRNA stabilization [34]. The MAP kinase kinase kinase 1 (MEKK1) is activated via stress stimuli and acting upstream of MKK6 which is the activator of the p38/MK2 module. As a result of constitutively active MEKK1 and MK2, IL6, and IL8 mRNA transcripts are stabilized via AREs. Moreover, active MEKK1 and MK2 do not only stabilize IL6 and IL8 mRNA, but also the transcripts of the central pro-inflammatory regulators IL1 and TNFα [34].

MK2 does not act directly on AREs in mRNAs, but via ARE-binding proteins like tristetraprolin (TTP) [35]. Normally, TTP destabilizes TNFα mRNA which results in a decrease of transcript levels [35, 36]. After phosphorylation by MK2, TPP cannot efficiently bind to ARE and hence does not act as TNF suppressor anymore. Furthermore, TTP mRNA is also regulated in a feedback loop which results in an increased production of TTP (Fig.5). As a result, TNF mRNA is stabilized and TNFα and other cytokines are efficiently produced.
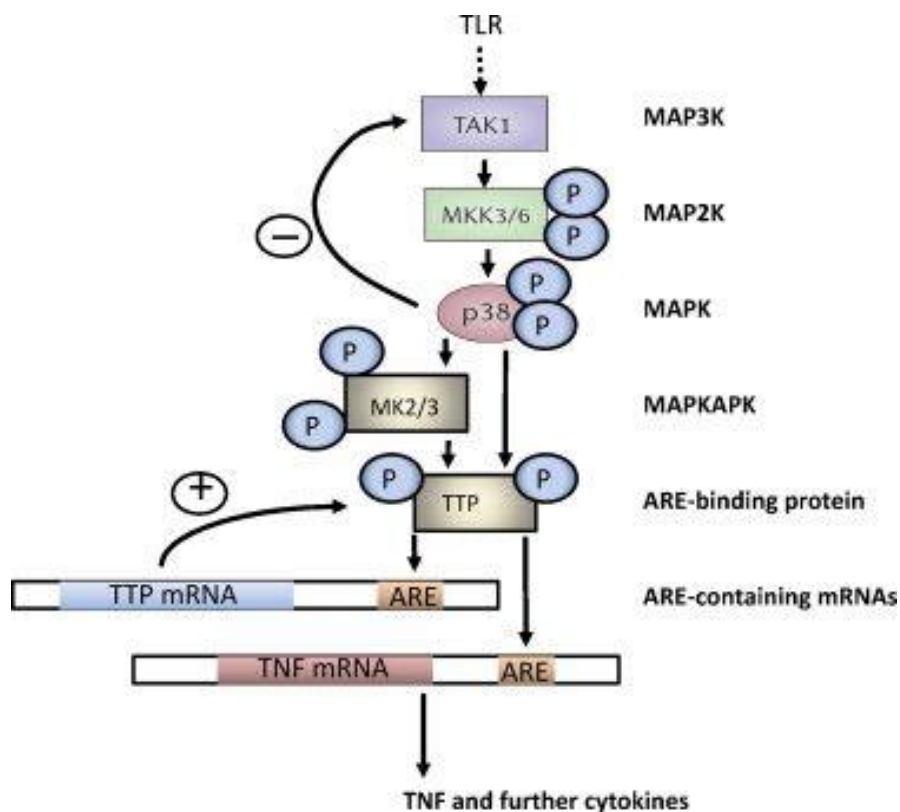

Fig. 5 Regulation of TNFα biosynthesis via MKK6, p38 and MK2. TNFα mRNA is destabilized by TTP. This effect is abolished through the phosphorylation of TTP by MK2 [35].

Brooke et al. observed that the stimulation of cells with LPS led to a stabilization of TNFα mRNA and that the treatment with the p38 inhibitor SB203580 reduced TNFα mRNA stability [37]. In experiments conducted by Neininger et al. the increase in TNFα production after LPS stimulation was lost in *MK2*-deficient mice but could be restored upon deletion of the *ARE* sequence, indicating that AREs are acting downstream of MK2 in the control of TNFα expression [33].

Kotylarov et al. were able to show that after injection of LPS, *MK2*-knock out mice displayed less severe effects and 50% of them survived, whereas the mice with functional MK2 died of the endotoxic shock [32]. Furthermore, when TNFα was administered, both *MK2*-deficient and wildtype mice died which proved that TNFα signaling was not affected, but TNFα production was controlled by MK2 and central to the endotoxic shock. Further tests confirmed that the TNFα levels were lowered to a substantial extent after LPS stimulation in *MK2*-deficient mice.

1.2.4   MK2 in Cancer

Ricci-Vitiani et al. reported that **colon cancer** cells comprise a subset of undifferentiated cells which are CD133$^+$ and functioning as cancer stem cells or tumor-inducing cells (TICs) [38]. Development of cancer is probably linked to deregulation in the TIC self renewal system and it is known that TICs survive under high levels of stress [39]. Serum depletion and hypoxia are stress signals which may drive colon cancer cells into apoptosis. However, the population of CD133$^+$ cells shows higher resistance to apoptosis as a result of downregulated caspase 3 and caspase 9 expression as well as a reduction in the cleavage of caspase molecules. Further studies showed, that the level of Hsp27 phosphorylation was 8.6 fold higher in CD133$^+$ cells compared to CD133$^-$ cancer cells, whereas Akt and ERK displayed no difference in their phosphorylation status. Also, MK2 and p38 were activated to a higher extent in CD133$^+$ cancer cells [39]. Thus, by efficiently triggering the p38-MK2 pathway under stress conditions, CD133$^+$ cancer stem cells increase Hsp27 phosphorylation which is required to inhibit caspase 9 and 3 cleavage and protect them from apoptosis.

Recent studies by Kobayashi et al. showed that MK2 is able to increase the growth of Ras-dependent as well as Ras-independent colon cancer cells [40]. In experiments it was shown that after ERK stimulation by Ras MK2 was phosphorylated and activated. This emphasizes that MK2 is a dual-responsive kinase which is not only activated via p38, but also after stimulation by ERK. After inhibition of ERK with PD98059 there was a reduction in MK2 and a reduced growth of cancer cells, whereas inhibition of p38 with SB203580 did not lead to a reduction of growth and upregulation of MK2. The study also included the investigation of the impact of MK2 on reactive oxygen species (ROS) produced after Ras activation [40]. The accumulation of ROS after Ras stimulation is required for Ras oncogenesis [41]. In case of constitutively active MK2, the human colon cancer cell lines displayed a significantly elevated production of ROS. Further experiments revealed that MK2 promotes the progression of colon cancer by an upregulation of the ROS production [40].

Kumar et al. discovered that treatment of **bladder cancer** cell lines with the p38 inhibitor SB203580 led to a lowered MK2 activity in bladder cancer [20]. They could also show that SB203580 blocked MMP9 expression and decreased MMP2 expression partially. In further experiments, they found that cells with constitutively active MK2 displayed the highest MMP2 and MMP9 activities. The authors came to the conclusion that p38 as well as MK2 were responsible for the regulation of MMP2 and MMP9 via stabilization of their transcripts resulting in enhanced invasiveness of bladder carcinoma cells [20].

With respect to the relevance of MMPs in tumor invasion, another study reported that MMP2 protein levels as well as mRNA expression were significantly higher in the high-invasive bladder cancer cells compared to the low-invasive cells [42]. Summarizing it can be said that MK2 plays an important role in MMP2/9 signaling and the subsequent invasiveness of bladder cancer cells.

Liu and colleagues discovered that the CNV-30450 copy number variation, which duplicates the MAPKAPK2 promoter has a marker potential in predicting **lung cancer** risk in the Chinese population [18]. Individuals who possessed four copies of CNV-30450 had a higher risk of developing lung cancer than those with two or three copies.

Also, four copies of CNV-30450 led to a shorter median survival time of the patients (9 months) compared to those with two or three copies (14 months). Furthermore, the higher the number of copies of CNV-30450 was, the higher was the expression of MK2 mRNA and MK2 protein [18].

MK2 is, moreover, an important factor in the initiation and early stages of **skin tumors** [43]. In experiments tumors were chemically induced in three groups of laboratory animals: *MK2*-deficient, *TNFα*-deficient, and wild-type mice. First papillomas emerged in 93% of the wild-type mice, whereas in the group with the *TNFα*-deficient mice 18% exhibited skin papillomas after week 18 and *MK2*-deficient mice showed only one animal with a single papilloma after 18 weeks. The inflammatory response to the tumor promoting stimulus was both reduced in the *MK2* -and the *TNFα*-deficient group. Additionally, the investigations revealed that *MK2*-deficient mice displayed more p53 expression and more apoptotic cells which points to a role of MK2 in preventing cell apoptosis.

When Birner et al. originally investigated the role of ETV1 (E twenty-six translocation variant 1) in **gastrointestinal stromal tumors** (GISTs) they found that the ETV1 inhibitor MK2 was highly activated in this cancer type [15]. *In vitro* studies demonstrated that ETV1 was phosphorylated by MK2 leading to an inactivation [44]. 139 patients were included in the study by Birner et al., where 22 suffered a relapse and 12 died of the GIST. 44.6% of the cases displayed a high cytoplasmic expression of MK2 which was accompanied by p-p38 expression. Staining for phosphorylated MK2 (phospho-MK2) revealed that there was no cytoplasmic staining, and nuclear staining was only detected in a few cases.

When investigating the potential of MK2 as a prognostic factor, the evaluation revealed that patients with high MK2 expression showed metastases which were already present when they were diagnosed with GIST. Additionally, MK2 overexpression was linked to cancer recurrence as well as a shorter disease-free survival time which was approximately 30% lowered in patients with high MK2 expression. Based on these findings, it was pointed out that MK2 inhibitors like PF-3644022 [35] or pyrrolopyridine inhibitors [45] which were originally developed for the treatment of rheumatoid arthritis, might constitute possible alternatives to tyrosine kinase inhibitors in the treatment of GISTs [15].

Several MK2 inhibitors exist, for example PF-3644022, a benzothiopene tested for the treatment of acute as well as chronic inflammation in experiments [46]. PF-3644022 is ATP-competitive and binds to MK2 with a high selectivity, resulting in the downregulation of TNFα production after stimulation with lipopolysaccharide (LPS). Moreover, it is able to inhibit MK5 as well as MK3 but at substantially higher concentrations. The IC_{50} value of PF-3644022 for MK2 equals 5.2 nM, which implies that at a concentration of 5.2 nM half of MK2 is inhibited. Additionally, this compound is able to block TNFα production in U937 monocytic cells after LPS stimulation with an IC_{50} of 159 nM. In animal experiments it was demonstrated that PF-3644022 is rapidly absorbed after administration in suspension and leads to a dose-dependent TNFα inhibition [46].

1.3 Aims of Study

Similar to the report on the prognostic potential of MK2 overexpression in GIST [15], Birner *et al.* observed that high levels of cytosolic MK2 protein in gastroesophageal cancer tissue was associated with a poor prognosis of tumor patients (unpublished data). As the functional role of MK2 in esophageal cancer has not been revealed to data, an explorative study was initiated at the Medical University of Vienna by Berthold Streubel from the University Clinic of Gynecology and Peter Birner from the Department of Pathology and realized as a collaboration project between the University Clinic of Surgery (groups Brostjan and Schoppmann) and the Department of Pathology (Peter Birner).

The purpose of this diploma study was to investigate the role of MK2 in gastroesophageal cancer cells *in vitro*, with a particular emphasis on cell proliferation and migration. To address this question, the project involved testing of two chemical MK2 inhibitors as well as three different small interfering RNAs (siRNAs) to study the downregulation of MK2. Further experiments were performed where MK2 was overexpressed using an MK2 cDNA plasmid. For the assessment of the effects of MK2 inhibition or silencing as well as overexpression, migration and proliferation assays, immunoblotting, and quantitative polymerase chain reaction (qRT-PCR) were implemented. Additionally, to evaluate the cellular expression of MK2 and phospho-MK2 confocal laser scanning microscopy (CLSM) was carried out for cell cultures and clinical specimens of esophageal cancer tissue were stained immunohistochemically.

The major questions to assess the role of MK2 in gastroesophageal cancer cells were defined as follows:

- How are MK2 and phospho-MK2 protein expressed and distributed in gastroesophageal cancer cells?

- Do MK2 inhibitors and siRNAs regulate the expression of MK2 and display effects on cell proliferation and migration?

- In turn, does MK2 overexpression influence the migrational and proliferative behavior of gastroesophageal carcinoma cells?

2   METHODS AND MATERIALS

2.1   *Immunohistochemistry*

Glass slides with tissue specimens from patients with esophageal cancer were obtained from the Clinical Institute of Pathology and stained with the use of the MaxPoly-One Polymer HRP Universal Detection Kit with AEC (MaxVision Biosciences, Washington, USA). Paraffin melting was performed overnight at 56 °C. For rehydration the slides were put into xylene for 20 min and subsequently into 100%, 96%, 70%, 50%, and 30% ethanol for 2 min each, completed by rinsing in Dulbecco's phosphate-buffered saline without Ca^{2+} and Mg^{2+} (PBSdef) for 15 min. As a next step, endogenous peroxidase activity was blocked by addition of solution C diluted 1:50 with distilled water (aqua dest.).

After a rinsing step with aqua dest. the antigen retrieval was performed. Therefore, antigen retrieval buffer (TE buffer or citrate buffer) was filled into a plastic cuvette containing the tissue slides and heated in an autoclave at 135 °C and 2.5 bar for 20 min.

After cooling down to room temperature (RT) two rinsing steps with PBSdef were performed, followed by incubation with protein blocking solution for 10 min in a moist chamber. Afterwards the specimens were incubated with the primary antibodies for 1 hour in a wet chamber. Next, after 3 washing steps with PBSdef for 2 min each, horseradish peroxidase (HRP) conjugated anti-mouse & rabbit secondary antibody solution was added to cover the tissue sections and incubated for 15 min under humid conditions. Subsequent to that, again 3 washing steps with PBSdef for 2 min each were performed and the AEC chromogen working solution was freshly prepared. For this purpose, a working solution containing reagent A and B diluted with aqua dest. at a ratio of 1:25 and reagent C diluted 1:50 with aqua dest. was prepared and mixed in a reaction tube in equal volumes. Incubation with AEC chromogen working solution was performed for 5 to 30 min, while color development was monitored under a light microscope. When red staining was clearly visible the color reaction was stopped by putting the slides into aqua dest. Counterstaining was carried out with hemalum diluted 1:3 with aqua dest. followed by a short washing step with tap water, incubation with PBSdef for 1 min and rinsing with Aqua dest.

Afterwards the specimens were ready to be mounted with Aquatex®. Therefore, excess water was removed from the slides before a drop of Aquatex® was applied directly onto the specimen and a glass cover slip was put on top. The mounting medium was allowed to set for 24 hours before the specimens were analyzed.

Materials

Solutions:

TE buffer:

    10 mM tris(hydroxymethyl)aminomethane (TRIS) (Merck, Darmstadt, Germany)

    1 mM ethylenediaminetetraacetic acid (EDTA) (Merck, Darmstadt, Germany)

    in aqua dest., adjusted to pH 9, stored at 4 °C

Citrate buffer:

    10 mM citric acid (Merck, Darmstadt, Germany)

    0.05% Tween-20 (Sigma-Aldrich, St. Louis, MO, USA)

    in aqua dest., adjusted to pH 6, stored at 4°C

PBSdef (Invitrogen, Carlsbad, CA, USA)

Mayer's hemalum solution (Merck, Darmstadt, Germany)

Aquatex® (Merck, Darmstadt, Germany)

Primary antibodies:

Anti-human MAPKAPK-2 rabbit polyclonal antibody, 1 mg/ml, #ab63574 (1:200) (Abcam, Cambridge, UK)

Anti-human MAPKAPK-2 rabbit polyclonal antibody, 10 µg/ml, #3042 (1:200)

Anti-human phospho-MAPKAPK-2 (Thr334) rabbit monoclonal antibody (mAb) 27B7, 99 µg/ml, #3007 (1:50)

Anti-human phospho-MAPKAPK-2 (Thr334) rabbit polyclonal antibody, 75 µg/ml, #3041 (1:50)

(all from Cell Signaling Technology, Danvers, MA, USA)

diluted in PBSdef

Plastic equipment:

Reaction tubes 1.5 ml (Greiner Bio-One, Frickenhausen, Germany)

Reaction tubes 2 ml (Eppendorf, Hamburg, Germany)

Glass cover slips (Marienfeld-Superior, Lauda Königshofen, Germany)

Kits & Devices:

MaxPoly-One Polymer HRP Universal Detection Kit with AEC (MaxVision Biosciences, Washington, USA)

Olympus BX61 microscope (Olympus, Hamburg, Germany)

Olympus DP72 camera with BX-UCB device (Olympus, Hamburg, Germany)

2.2   Cell Culture

To secure sterile work conditions, a biological safety cabinet as well as sterile instruments and solutions were used. All cells were cultured in a humidified atmosphere with 5% CO_2 at 37 °C.

2.2.1   Human Cancer Cell Lines

The following esophageal cancer cell lines were investigated for MK2 expression:
- FLO-1 (ECACC® #11012001)
- SK-GT-4 (ECACC® #11012007)
- TE-1 (kindly donated by the laboratory of Walter Berger from the Institute of Cancer Research, Vienna, Austria).

A human leukemic T cell lymphoblast line was used for comparison in selected experiments:
- Jurkat E6-1 (ECACC® #88042803).

2.2.2 Cell Propagation

Cells were cultured in T25 cm^2, T75 cm^2 or T150 cm^2 flasks and split two to three times per week. When the adherent cells (FLO-1, SK-GT-4, and TE-1) reached confluence, a washing step with PBSdef was performed, followed by addition of 1x trypsin-EDTA to detach the cells (see Tab. 1). The reaction was stopped with PBSdef supplemented with 10% heat-inactivated fetal calf serum (FCS) and the cell suspensions were centrifuged (190 x g, 5 min, RT).
The cell pellets were then diluted with appropriate cell culture medium and transferred to a new tissue culture flask.

	1x trypsin-EDTA	*10% FCS in PBSdef to stop reaction*	*total culture medium*
T25	1 ml	1 ml	4 ml
T75	3 ml	3 ml	10 ml
T150	6 ml	6 ml	20 ml

Tab. 1: Listing of reagent volumes applied in cell culture. Amounts of trypsin-EDTA for detachment of cells, 10% FCS/PBSdef for stopping the reaction, and the volume of total culture medium are indicated.

SK-GT-4 and TE-1 cells were grown in RPMI growth medium and propagated at a ratio of 1:3 to 1:6 two to three times a week. FLO-1 cells were cultured in DMEM growth medium and passaged at a ratio 1:3 to 1:6.

Jurkat cells were also cultured in RPMI growth medium. As these are suspension cells the process of detaching them with trypsin does not apply. Instead, passaging them at a ratio of 1:10 two to three times a week was performed by cell centrifugation, removing old and adding new culture medium.

Materials

Media & Solutions:

DMEM growth medium:

    DMEM high glucose medium

    + 10% heat inactivated FCS

    + 100 µg/ml streptomycin (stock 10000 µg/ml)

    + 100 U/ml penicillin (stock: 10000 U/ml)

    + 2 mM L-glutamine (stock: 200 mM)

RPMI 1640 growth medium:

    RPMI 1640 medium with GlutaMAX™   Invitrogen, Carlsbad, CA, USA

    + 10% heat inactivated FCS

    + 100 µg/ml streptomycin (stock 10000 µg/ml)

    + 100 U/ml penicillin (stock: 10000 U/ml)

    + 2 mM L-glutamine (stock: 200 mM)

PBSdef

10x trypsin-EDTA (0.5% trypsin, 5.3 mM EDTA-Na)

1x trypsin-EDTA (working solution):

    10x trypsin-EDTA diluted 1:10 in PBSdef

Heat inactivated FCS (Linaris, Wertheim-Bettingen, Germany)

10% FCS in PBSdef (working solution): 50 ml FCS in 500 ml PBSdef

Plastic equipment:

TPP® triangular angled neck cell culture flasks with vent cap (25 cm^2, 75 cm^2, and 150 cm^2)

(TPP, Trasadingen, Switzerland)

Reaction tubes for 50 ml and 15 ml, without skirt (Sarstedt, Nümbrecht, Germany)

2.3. Determination of Cell Proliferation

2.3.1 Cell Counting

Cell count was determined using a Neubauer improved hemocytometer (with 0.1 mm of depth and an area of 0.0025 mm² per smallest square) and a glass cover slip. Depending on the concentration of cells in the sample, a 1:2, 1:5 or 1:10 pre-dilution in PBSdef was performed in 1.5 ml reaction tubes. For an additional 1:2 dilution, 10 µl of sample were added to 10 µl of trypan blue solution, mixed and 10 µl of this solution were applied on the hemocytometer. Afterwards cell counting was performed using a light microscope and 100x magnification.
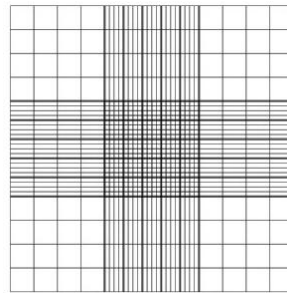
Fig. 6 Setup of a Neubauer improved hemocytometer grid. Picture shows 9 areas which are divided into 16 small squares each, where the centered small squares are further subdivided by cross-wise arranged lines.

For cell counting the cells in the 4 corner areas composed of 4x4 squares (Fig. 6) were counted. Cells which were located at the border lines were evaluated according to the following rule: cells at the left and the bottom line of every corner area were not included, whereas cells located at the right or the top line were counted. The cell concentration was determined based on the following equation:

cell count divided by 4 (corner areas) multiplied by the combined dilution factor (of pre-dilution and 1:2 trypan blue dilution) x 10^4 per milliliter.

Materials

Solutions:

PBSdef (Invitrogen, Carlsbad, CA, USA)

Trypan blue solution 0.4% (Invitrogen, Carlsbad, CA, USA)

Plastic equipment:

Reaction tubes 1.5 ml (Greiner Bio-One, Frickenhausen, Germany)

Devices:

Neubauer improved hemocytometer (Assistent, Sondheim/Rhön, Germany)

Glass cover slips (Menzel-Gläser, Braunschweig, Germany)

Axiovert 40 CFL inverted light microscope (Carl Zeiss Microscopy, Thornwood, NY, USA)

2.3.2 Cell Imaging

Examination of cells and capture of serial pictures to document cell growth was performed using a light microscope with objectives of 5x, 10x, and 20x magnification, the AxioCam ICc3, and AxioVision software.

Materials

Devices & Software:

Axiovert 40 CFL inverted light microscope

AxioCam ICc 3 digital microscope camera   Carl Zeiss Microscopy, Thornwood, NY, USA

AxioVision software Rel. 4.8

2.3.3 Metabolic Assay (EZ4U)

EZ4U is a non-radioactive cell proliferation and toxicity assay measuring metabolic cell activity which was used to monitor the proliferation of cells seeded into 6 wells. Therefore, the substrate contained in one vial was dissolved in 2.5 ml of activator substance and pre-warmed to 37 °C. The medium in the 6 wells was reduced to 1 ml and 100 µl of activated substrate were added to gain a 1:11 dilution of substrate solution. Next, the plates were incubated for 45 min to 1 hour, depending on the color development. Afterwards 300 µl of each 6 well were transferred into a 96 well and absorbance at 450 nm was measured with a photometric plate reader (Varioskan Flash Multimode Reader, Thermo Fisher Scientific, Waltham, MA, USA).

Materials

Plastic equipment:

TPP® 6 well tissue culture (TC)-treated microplates (30 mm wells)

TPP® 96 well clear flat bottom microplates

(both from TPP, Trasadingen, Switzerland)

Kits & Devices:

EZ4U Cell Proliferation Assay (Biomedica, Vienna, Austria)

Varioskan Flash Multimode Reader (Thermo Fisher Scientific, Waltham, MA, USA)

2.4. Determination of Cell Migration

2.4.1 Scratch-Wound Assay

For the scratch-wound assay cells were seeded into 6 wells and grown to confluence. Then a cross-shaped scratch was created with a 200 µl pipette tip in the middle of every 6 well. The old medium was aspirated, a washing step with PBSdef was performed and 2 ml of fresh cell culture medium were added.

Materials

Solutions:

DMEM growth medium

RPMI 1640 growth medium   Invitrogen, Carlsbad, CA, USA
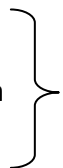
PBSdef

Plastic equipment:

TPP® 6 well tissue culture (TC)-treated microplates (30 mm wells) (TPP, Trasadingen, Switzerland)

2.4.2 Cell Imaging

The migration and proliferation of cells into the bare area was recorded with the use of a light microscope, the AxioCam ICc3, and the AxioVision software.

Devices & Software:

Axiovert 40 CFL inverted light microscope

AxioCam ICc 3 digital microscope camera   Carl Zeiss Microscopy, Thornwood, NY, USA

AxioVision software Rel. 4.8

2.5 Plasmid Propagation and Purification

2.5.1 Bacterial Transformation with Plasmid DNA

A piece of Whatman paper containing the plasmid DNA was put into a 2 ml reaction tube and 100 µl TE buffer were added. The paper was compressed, the tube was vortexed and briefly centrifuged. Then, the supernatant was transferred to a new reaction tube. Meanwhile, competent DH5α cells were thawed on wet ice. 50 µl of competent DH5α cells were transferred into a chilled polypropylene tube and 10 µl of plasmid-containing suspension were added. The solution was incubated on ice for 30 min and the cells were heat-shocked for 45 sec at 42 °C in a water bath without shaking. After that, the cells were placed on ice for 2 min, followed by addition of 1 ml LB medium and shaking for 1 hour at 225 rpm and 37 °C. Then the cell suspension containing the plasmid was diluted with LB medium at a ratio of 1:10. 100 µl and 200 µl of this dilution were plated on LB plates containing the required antibiotic (e.g. ampicillin) for selection of plasmid uptake, and plates were incubated overnight at 37 °C.

The following day, one single colony was picked and dispersed in 1 ml LB medium. The suspension was again spread on agar plates with ampicillin and incubated overnight at 37 °C.

The next day one colony was picked, transferred to 5 ml LB medium with antibiotics and incubated while shaking at 300 rpm and 37 °C for 7 hours. Afterwards, the suspension was transferred to an Erlenmeyer flask containing 500 ml LB medium with ampicillin and the incubation at 300 rpm and 37 °C was continued overnight.

2.5.2 Isolation and Purification of Plasmid DNA

Further plasmid preparation was based on the Plasmid Maxi Kit (Qiagen, Venlo, Netherlands). Therefore, the bacterial cells were centrifuged at 6000 x g and 4 °C for 15 min and the pellet was resuspended in 10 ml buffer P1. In the next step, 10 ml of buffer P2 were added, the tube was sealed with parafilm, inverted for a few times to ensure proper mixing and incubated for 5 min at RT. 10 ml of buffer P3 were then added, again mixed vigorously by inverting and the sample was incubated on ice for 20 min to precipitate DNA, proteins and cell debris. After mixing again, a centrifugation step at 20000 x g and 4 °C was performed for 30 min. The supernatant was removed immediately and centrifuged once more at 20000 x g and 4 °C for 15 min. Meanwhile, a Qiagen tip 500 was equilibrated with 10 ml of buffer QBT and then half of the supernatant was applied. After the supernatant had passed through the column, the Qiagen tip was washed twice with 30 ml buffer QC and DNA was eluted with 15 ml of buffer QF into a 30 ml Corex glass tube. DNA was precipitated by adding 10.5 ml of isopropyl alcohol at RT, mixed and centrifuged at 15000 x g and 4 °C for 30 min. Then the supernatant was carefully removed to retrieve the pellet containing the plasmid DNA.

Due to the large volume of initial bacterial cell suspension, the plasmid purification was performed in two runs, i.e., the column equilibration, sample application, wash and elution steps had to be repeated for the second half of bacterial culture supernatant. The second eluate was collected in the same Corex glass tube, and the plasmid DNA was again precipitated and centrifuged. The pellet containing the DNA was washed with 70% ethanol and a centrifugation step at 15000 x g for 10 min was performed. After decanting the supernatant the pellet was air-dried for 10 min and reconstituted in 300 µl TE buffer. In the next step, the dissolved DNA was centrifuged at 18000 x g for 5 min and the supernatant was retrieved and subjected to measurement of DNA content.

The DNA concentration was measured with a NanoDrop 8000 device (Thermo Fisher Scientific, Wilmington, DE, USA) at an absorption wavelength of 260 nm and adjusted to 1 µg/µl with TE buffer according to the following equation:

dsDNA concentration = 50 µg/ml × $absorption_{260\,nm}$ × dilution factor.

Materials

Media & Solutions:

LB medium:

 Lennox L Broth base (20 g/l) (Invitrogen, Walkersville, MD, USA) in aqua dest.,

 autoclaved and cooled down to 50 °C prior to addition of

 Ampicillin sodium salt (100 µg/ml) (Sigma-Aldrich, St. Louis, MO, USA)

LB Agar:

 Lennox L Broth base (20 g/l) (Invitrogen, Walkersville, MD, USA) and

 Select agar (15 g/l) (Sigma-Aldrich, St. Louis, MO, USA) in aqua dest., autoclaved

 and cooled down to 50 °C prior to addition of

 Ampicillin sodium salt (100 µg/ml) (Sigma-Aldrich, St. Louis, MO, USA)

 and casting into petri dishes

TE buffer:

 10 mM Tris(hydroxymethyl)aminomethane (Merck, Darmstadt, Germany)

 0.1 mM EDTA (Merck, Darmstadt, Germany)

 in Aqua dest., adjusted to pH 8, stored at 4 °C

Isopropyl alcohol (Sigma-Aldrich, St. Louis, MO, USA)

70% Ethanol in aqua dest. (Merck, Darmstadt, Germany)

DH5α competent cells (Invitrogen, Walkersville, MD, USA)

Plastic and glass equipment:

Reaction tubes 2 ml (Eppendorf, Hamburg, Germany)

Corning® 100 mm non TC-treated culture dish (Corning, Corning, NY, USA)

Corex® II glass centrifuge tubes (Corning, Corning, NY, USA)

Kits & Devices:

Plasmid Maxi Kit (Qiagen, Venlo, Netherlands)

NanoDrop 8000 (Thermo Fisher Scientific, Waltham, MA, USA)

2.6   Transient Gene Overexpression

2.6.1   Expression Constructs

EFpLink

EFpLink is a bacterial plasmid designed as an expression vector containing the elongation factor 1α promoter to drive expression of inserted eukaryotic genes [47]; it was kindly provided by Vivian Bardwell from the University of Minnesota (MN, USA).

MK2

The MK2 expression construct was kindly provided by Rachel Ben-Levy and her group from the Cancer Research Campaign Centre for Cell and Molecular Biology (London, UK). The MK2 cDNA was cloned into NcoI and BamHI sites of the EFp expression vector. Details on the inserted MK2 sequence can be found via the NCBI reference number NM_032960.

pEGFP-C3

This DNA vector (Clontech Laboratories Inc., Mountain View, CA, USA) is designed to drive expression of the EGFP (enhanced green fluorescent protein) reporter gene via the cytomegalovirus (CMV) promoter. It further contains a multiple-cloning site for insertion of genes downstream of EGFP and a neomycin-resistance cassette (Fig. 7).
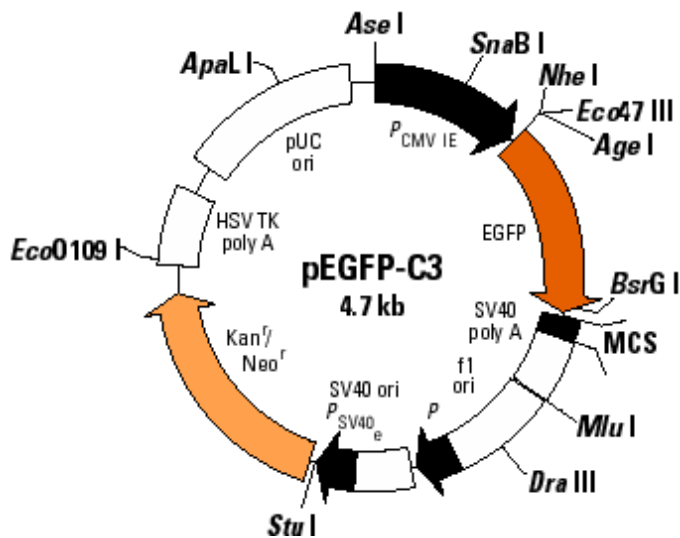
Fig. 7 Structure of the pEGFP-C3 vector. The plasmid includes the EGFP-coding sequence (dark orange) and a neomycin resistance cassette (light orange).

2.6.2 Electroporation for Transient Overexpression

$2*10^6$ cells per electroporation were calculated and seeded in tissue culture flasks the day before to gain a subconfluent, proliferating cell culture within 24 hours. The next day the cells were washed with PBSdef and detached with 1x trypsin-EDTA; the reaction was stopped with cold RPMI medium containing 10% FCS. Meanwhile, the centrifuge was pre-cooled to 4 °C. The cell suspension was then centrifuged for 5 min at 190 x g and 4 °C and the pellet was resuspended in 1 ml of cold RPMI medium. Then cell count was determined using a Neubauer hematocytometer (see Methods 2.2.1) and diluted to $5*10^6$ cells/ml in RPMI medium. 20 µg of plasmid DNA were transferred into a 1.5 ml reaction tube, mixed with 400 µl of cell suspension ($2*10^6$ cells) and the sample was transferred to a 4 mm electroporation cuvette. Electroporation was conducted immediately at 200 V and 1000 µF using a Gene Pulser Xcell Total System (Bio-Rad, Hercules, CA, USA). Afterwards the cell suspension was transferred into a reaction tube containing appropriate cell culture medium and seeded into culture plates.

Materials

Media & Solutions:

PBSdef (Invitrogen, Carlsbad, CA, USA)

1x trypsin-EDTA (Invitrogen, Carlsbad, CA, USA)

RPMI 1640 medium without phenol red and glutamine (Invitrogen, Walkersville, MD, USA) with 10% FCS (Linaris, Wertheim-Bettingen, Germany)

Plastic equipment:

Gene Pulser® cuvettes 4 mm gap (Bio-Rad, Hercules, CA, USA)

Reaction tubes 1.5 ml (Greiner Bio-One, Frickenhausen, Germany)

Device:

Gene Pulser Xcell™ Total System (Bio-Rad, Hercules, CA, USA)

2.7 Transient Gene Silencing

The siRNA oligoribonucleotides were diluted with RNase-free water to gain a 20 µM solution. As negative control, Stealth RNAi negative control duplex with low CG content was used.

Cells were seeded and harvested for electroporation as described in 2.6.2. 20 µl of MK2 siRNA (Tab. 2) or control siRNA were distributed to 1.5 ml reaction tubes. Afterwards 400 µl of cell suspension ($2*10^6$ cells) were transferred to each siRNA containing reaction tube, gently mixed and transferred to 4 mm electroporation cuvettes. Immediately, electroporation was conducted at 250 V and 1000 µF using a Gene Pulser Xcell Total System (Bio-Rad, Hercules, CA, USA). After electroporation the cell suspension was transferred into a reaction tube containing the corresponding cell culture medium and seeded into culture plates.

catalogue#	product#	sequence	amount
1299001	HSS190127	5'-GAGAACUCUUUAGCCGAAUCCAGGA-3' 5'-UCCUGGAUUCGGCUAAAGAGUUCUC-3'	20 µl
1299001	HSS190128	5'-GAAAGAGAAGCAUCCGAAAUCAUGA-3' 5'-UCAUGAUUUCGGAUGCUUCUCUUUC-3'	20 µl
1299001	HSS190733	5'-CCACUCCUUGUUAUACACCGUACUA-3' 5'-UAGUACGGUGUAUAACAAGGAGUGG-3'	20 µl

Tab. 2 Listing of MK2 siRNAs applied in gene silencing experiments. Catalogue and product number as well as siRNA sequences, and used amounts of siRNA are given.

Materials

Media & Solutions:

PBSdef

1x trypsin-EDTA

Stealth^{TM} RNAi Negative Control low GC Duplex

Stealth^{TM} siRNA HSS190127   Invitrogen, Carlsbad, CA, USA

Stealth^{TM} siRNA HSS190128

Stealth^{TM} siRNA HSS190733

RPMI 1640 medium without phenol red and glutamine (Invitrogen, Walkersville, MD, USA) with 10% FCS (Linaris, Wertheim-Bettingen, Germany)

Plastic equipment:

Gene Pulser® cuvettes 4 mm gap (Bio-Rad, Hercules, CA, USA)

Reaction tube 1.5 ml (Greiner Bio-One, Frickenhausen, Germany

Devices:

Gene Pulser Xcell™ Total System (Bio-Rad, Hercules, CA, USA)

2.8 RNA Isolation and Quantitation

The cell pellets from gene silencing and overexpression experiments were gained by trypsinization, centrifugation and were frozen at -20 °C directly after harvesting until further processing. For RNA isolation the RNeasy® Mini Kit (Qiagen, Venlo, Netherlands) was used. First, buffer RLT was supplemented with β-mercaptoethanol (10 µl per 1 ml buffer) and buffer RPE was diluted with 4 volumes of 100% ethanol to gain a working solution. To start with the RNA isolation, 350 µl of buffer RLT were added to each pellet (generally $2*10^5$ - $2*10^6$ cells) for cell extraction, and samples were centrifuged at 10000 x g for 3 min. The supernatant was retrieved carefully. In the next step, 350 µl of 70% ethanol were added to the lysate, mixed and applied on an RNeasy® Mini spin column which was placed in a 2 ml collection tube. Subsequently, a centrifugation step at 8000 x g for 15 sec was performed and the flow-through was discarded. Then 700 µl of wash buffer RW1 were added to the spin column, again centrifuged at 8000 x g for 15 sec and the flow-through was discarded. Afterwards, 500 µl of wash buffer RPE were applied onto the column which was then centrifuged at 8000 x g for 15 sec. Again, the flow-through was discarded. This step was repeated in the same way, except that centrifugation was performed for 2 min. Next, the RNeasy column was placed in a new 1.5 ml collection tube, 30-50 µl of RNase-free water were added, and centrifuged for 1 min at 8000 x g for RNA elution. RNA content was determined with a NanoDrop 8000 device (Thermo Fisher Scientific, Waltham, MA, USA) based on the equation:

RNA concentration = 40 µg/ml × $\text{absorption}_{260\ nm}$ × dilution factor.

Materials

Plastic equipment:

Reaction tubes 1.5 ml (Greiner Bio-One, Frickenhausen, Germany)

Reaction tubes 2 ml (Eppendorf, Hamburg, Germany)

Kits & Devices:

RNeasy® Mini Kit (Qiagen, Venlo, Netherlands)

NanoDrop 8000 (Thermo Fisher Scientific, Waltham, MA, USA)

2.9   cDNA Synthesis

cDNA synthesis was performed using the SuperScript® First-Strand Synthesis System (Invitrogen, Carlsbad, CA, USA). For each reaction the following RNA/primer mix was prepared in a sterile 0.2 ml tube:

RNA	500 ng - 1 µg
10 mM dNTP mix	1 µl
random hexamers (50 ng/µl)	1 µl
DEPC-treated water	to 10 µl

This RNA/primer mix was incubated at 65 °C for 5 min and afterwards placed on ice for 1 min.

In a separate tube, the following 2x reaction mix was prepared (indicated for 1 reaction):

10x RT buffer	2 µl
25 mM MgCl$_2$	4 µl
0.1 M dithiothreitol	2 µl
RNaseOUT™ (40 U/µl)	1 µl

In the next step, 9 µl of this 2x reaction mix were added to each RNA/primer sample, mixed and collected by short centrifugation. Incubation at RT for 2 min was carried out before addition of 1 µl SuperScript™ II reverse transcriptase to each tube. After 10 min of incubation at RT the mix was incubated at 42 °C for 50 min in a thermocycler. The reaction was terminated at 70 °C for 15 min, chilled on ice and harvested by brief centrifugation. Next, 1 µl of RNase H were added to each tube and incubated at 37 °C for 20 min. The reaction was then stored at -20 °C until analysis.

Materials

Plastic equipment:

PCR tubes 0.2 ml (Eppendorf, Hamburg, Germany)

SuperScript® First-Strand Synthesis System for RT-PCR, #11904-018 (Invitrogen, Carlsbad, CA, USA)

T1 Thermocycler (Biometra, Goettingen, Germany)

2.10   Quantitative Real Time-PCR

20 µl of cDNA obtained from cDNA synthesis were supplemented with 40 µl of H_2O and 3 µl of this solution were used for qRT-PCR which was carried out in duplicates. Beta-actin (ACTB) was used as a reference gene.

For each reaction the following components were added to 3 µl of cDNA template:

TaqMan® Universal PCR Master Mix	7.5 µl
TaqMan® gene expression assay (MK2 or ACTB)	0.75 µl
H_2O	3.75 µl

In the next step, the qRT-PCR (quantitative realtime polymerase chain reaction) was performed with a 7500 Fast Real-Time PCR System (Applied Biosystems, Foster City, CA, USA). Denaturation was carried out at 95 °C for 10 min, followed by 40 cycles of 95 °C for 15 sec and 60 °C for 1 min. To gain the values for relative MK2 expression, the received values for cycle threshold (Ct) were normalized to ACTB based on the $E^{-\Delta\Delta Ct}$ method [48].

Materials

Plastic equipment:

MicroAmp® Fast Optical 96-Well Reaction Plates (Life Technologies, Carlsbad, CA, USA)

Assays & Devices:

Hs01116946_m1 MK2 TaqMan® gene expression assay, #4331182

Hs99999903_m1 ACTB TaqMan® gene expression assay, #4331182

TaqMan® Universal PCR Master Mix, No AmpErase® UNG, #4324018

(all from Invitrogen, Carlsbad, CA, USA)

7500 Fast Real-Time PCR System (Life Technologies, Carlsbad, CA, USA)

2.11   Preparation of Cellular Protein Extracts

Cells were trypsinized, the reaction was stopped with 10% FCS in PBSdef and the cell suspension was centrifuged (190 x g, 5 min, RT). In the beginning of this project, RIPA buffer supplemented with protease inhibitor was used for cell lysis by simply adding 100 µl RIPA buffer to $2x10^6$ cells. Later, SDS (sodium dodecyl sulfate) lysis buffer in combination with sample heating and sonication was found to be more suitable. This method is a more harsh extraction procedure leading to a higher protein yield. For $2x10^6$ cells 200 µl of SDS lysis buffer were used to dissolve the pellet in a reaction tube. Subsequently, the sample was heated at 95 °C for 5 min and sonication was performed. The reaction tubes were put into the sonication device, power (amplitude) was set to 90% and cycle set to 0.3 (30% sonication). Sonication was then performed for 1 min and samples kept on ice until centrifugation (10000 x g, 10 min, 4 °C). After centrifugation the supernatant was transferred to a new reaction tube and frozen until further use.

Materials

Solutions:

RIPA buffer:

> 1% NP-40 (Life Technologies, Carlsbad, CA, USA)
>
> 0.5% deoxycholic acid (Life Technologies, Carlsbad, CA, USA)
>
> in PBSdef

SDS lysis buffer:

> 100 mM TRIS (Merck, Darmstadt, Germany)
>
> 1% SDS (Bio-Rad, Hercules, CA, USA)
>
> in aqua dest., adjusted to pH 9.5

cOmplete Protease Inhibitor Cocktail Tablets (F. Hoffmann La-Roche AG, Basel, Switzerland):
1 protease inhibitor tablet dissolved in 10 ml RIPA buffer

PBSdef

1x trypsin-EDTA   Invitrogen, Carlsbad, CA, USA

10% FCS in PBSdef

Plastic equipment:

Reaction tubes 1.5 ml (Greiner Bio-One, Frickenhausen, Germany)

Reaction tubes 2 ml (Eppendorf, Hamburg, Germany)

Device:

Sonication device UIS250L with sonotrode LTS24d10.4L2 and VialTweeter (Hielscher, Teltow, Germany)

2.12 Protein Quantitation

The BCA (bicinchoninic acid) method was used to quantify the amount of extracted protein. Therefore, the protein samples were thawed and a pre-dilution of 1:5 in SDS lysis buffer was performed. A working reagent was prepared from reagent A and reagent B contained in the BCA Protein Assay Kit at a ratio of 50:1. A standard series ranging from 2000 to 25 µg protein/ml was generated from an albumin stock solution. 200 µl of working reagent were added to 10 µl of diluted protein sample or standard and afterwards incubated for 30 min at 37 °C in reaction tubes on a thermomixer. Cu^{2+} then was reduced by proteins and blue BCA complexes with Cu^+ were formed. Those BCA complexes were detected via absorption at 562 nm in a photometric plate reader. With the use of measured absorption values a standard curve was generated and the protein concentration of samples was calculated accordingly and adjusted to the lowest sample concentration.

Materials

Solutions:

SDS lysis buffer:

    100 mM TRIS (Merck, Darmstadt, Germany)

    1% SDS (Bio-Rad, Hercules, CA, USA)

    in aqua dest., adjusted to pH 9.5

BCA Protein Assay Kit (Thermo Fisher Scientific, Waltham, MA, USA):

    reagent A and reagent B (50:1)

    albumin standard (2 mg/ml)

Reaction tubes 1.5 ml (Greiner Bio-One, Frickenhausen, Germany)

Reaction tubes 2 ml (Eppendorf, Hamburg, Germany)

96-well tissue culture test plates flat bottom (TPP, Trasadingen, Switzerland)

Device:

Thermomixer comfort (Eppendorf, Hamburg, Germany)

Varioskan Flash Multimode Reader (Thermo Fisher Scientific, Waltham, MA, USA)

2.13 *Sodium Dodecyl Sulphate Polyacrylamide Gel Electrophoresis*

2.13.1 Gel Preparation

The solutions for the running gel (10%) and stacking gel (4.5%) were prepared as listed in Tab. 3 and Tab. 4. Acrylamide/bis-acrylamide (AA/Bis), buffer, and aqua dest. were mixed in a 50 ml reaction tube. For the last two components (APS and TEMED) it was important to add APS (ammonium persulfate) first, because after addition of TEMED (tetramethylethylenediamine) gel polymerization started immediately.

component	amount
AA/Bis 40%	1.5 ml
4x Running Gel Buffer	1.5 ml
Aqua dest.	3 ml
APS (40%)	6 µl
TEMED	4 µl

Tab. 3: Components of running gel solutions.

component	amount
AA/Bis 40%	0.350 ml
4x Stacking Gel Buffer	0.750 ml
Aqua dest.	1.9 ml
APS (40%)	8 µl
TEMED	2 µl

Tab. 4: Components of stacking gel solutions.

At first, the running gel was prepared immediately before pouring it between an aluminum and a glass plate separated by 0.75 mm spacers. The running gel was then covered with water-saturated n-butanol to prevent the meniscus effect. After 1 hour of polymerization time the n-butanol was removed, the gel border was rinsed with aqua dest. and carefully dried with filter paper. Subsequently, the stacking gel solution was added onto the running gel and a 10-well comb was immediately inserted into the stacking gel for generating 5 mm sample wells. Again, the gel was allowed to polymerize for 1 hour. For electrophoresis, the plates containing the gel were transferred to an electrophoresis chamber.

2.13.2   Sample Preparation and Electrophoresis

5x SLAB was first supplemented with 4 M dithiothreitol (DTT) stock solution to a final concentration of 400 mM, and 2 µl of 5x SLAB were then added to 10 µl of every sample. Kaleidoscope prestained standard and biotinylated protein ladder were used for protein size determination. Samples and biotinylated protein marker were heated at 95 °C for 5 min and centrifuged shortly. The electrophoresis chamber was filled with tank buffer, the 10-well comb was removed from the stacking gel, and each well was rinsed carefully. Then 10 µl of every sample, 5 µl of Kaleidoscope prestained standard and 3 µl of biotinylated protein ladder were loaded onto the gel.

Electrophoresis was carried out with 15 mA per gel at 4 °C for 1 hour using an SE250 Mighty Small II Mini Vertical Electrophoresis Unit (Hoefer, Holliston, MA, USA).

Materials

Solutions:

4x Running Gel Buffer:

     1.5 M TRIS (Merck, Darmstadt, Germany)

     0.4% SDS (Bio-Rad, Hercules, CA, USA)

     in aqua dest., adjusted to pH 8.8, stored light-protected at 4 °C

4x Stacking Gel Buffer:

     0.5 M TRIS (Merck, Darmstadt, Germany)

     0.4% SDS (Bio-Rad, Hercules, CA, USA)

     in aqua dest., adjusted to pH 6.8, stored light-protected at 4 °C

Tank Buffer:

     0.025 M TRIS (Merck, Darmstadt, Germany)

     0.192 M glycine (Merck, Darmstadt, Germany)

     0.1% SDS (Bio-Rad, Hercules, CA, USA)

     in aqua dest., stored at RT

40% APS:

     0.8 g ammonium persulfate (Sigma-Aldrich, St. Louis, MO, USA)

     in aqua dest. added to 2 ml, stored in aliquots at -20 °C

5x SLAB:

     150 mM TRIS (Merck, Darmstadt, Germany)

     5% SDS (Bio-Rad, Hercules, CA, USA)

     25% glycerol (Merck, Darmstadt, Germany)

     11.5% ß-mercaptoethanol (Sigma-Aldrich, St. Louis, MO, USA)

     0.5% bromophenol blue (Serva, Heidelberg, Germany)

     in aqua dest., adjusted to pH 6.8, stored at -20°C

OmniPur® 40% acrylamide/bis-acrylamide (Merck, Darmstadt, Germany)

n-Butanol (Merck, Darmstadt, Germany)

Biotinylated protein ladder detection pack (New England Biolabs, Ipswich, MA, USA)

Kaleidoscope prestained standard (Bio-Rad, Hercules, CA, USA)

DL-Dithiothreitol (Sigma-Aldrich, St. Louis, MO, USA)

Plastic equipment:

Reaction tubes 1.5 ml (Greiner Bio-One, Frickenhausen, Germany)

Reaction tubes 50 ml without skirt (Sarstedt, Nümbrecht, Germany)

Device:

SE250 Mighty Small II Mini Vertical Electrophoresis Unit (Hoefer, Holliston, MA, USA)

2.14   Immunoblotting

The polyvinylidene fluoride (PVDF) membrane was activated with methanol for 15 sec, washed in aqua dest. for 2 min and equilibrated in semi-dry blotting buffer for at least 5 min. The polyacrylamide gel with the separated proteins was then removed from the electrophoresis chamber and the stacking gel was cut off. Afterwards the gel was equilibrated in semi-dry blotting buffer.

Then the blotting stack consisting of thick filter paper (soaked with semi-dry blotting buffer), the activated membrane, the gel and again a layer of thick filter paper was assembled and transferred to a Semi-Phor Transfer Unit (Hoefer, Holliston, MA, USA) where blotting was performed for 1 hour at 35 mA per membrane. Afterwards, blocking of free, unspecific protein binding sites on the membrane was carried out in a rotating 50 ml reaction tube at 4 °C overnight in 10 ml blocking solution.

The next day the primary antibodies were diluted in blocking solution and the membrane was incubated with 3 ml of antibody solution for 1 hour at RT on a rotating wheel (antibody dilutions as listed below). Therefore, the membrane was transferred into a 50 ml reaction tube and sealed with parafilm. Following primary antibody incubation, 4 washing steps with 5 ml of wash buffer each were performed for 5 min.

In the meantime, the secondary antibodies (anti-biotin and HRP-linked secondary antibody) were diluted 1:100000 and 1:5000, respectively. Next, incubation with 3 ml of secondary antibody solution was performed for 1 hour at RT on a rotating wheel, followed by 3 washing steps with 5 ml wash buffer and 1 wash step with PBSdef for 5 min each. During the last washing step the substrates of the ECL Advance Western Blotting Detection Kit were mixed at equal parts. Then the membrane was incubated with 500 µl of the substrate solution for 5 min in a plastic wrap. Next, the excess substrate was removed with filter paper, the membrane was transferred to a new plastic wrap and kept in the dark until exposure using a G:BOX EF2 with GeneSnap software (Syngene, Cambridge, UK).

Materials

Solutions:

Semi-dry blotting buffer:

    25 mM TRIS (Merck, Darmstadt, Germany)

    192 mM glycine (Merck, Darmstadt, Germany)

    0.1% SDS (Bio-Rad, Hercules, CA, USA)

    20% methanol (Merck, Darmstadt, Germany)

    800 ml aqua dest.

Blocking solution:

    5% Blotting grade blocker non fat dry milk (Bio-Rad, Hercules, CA, USA)

    0.05% Tween 20 (Sigma-Aldrich, St. Louis, MO, USA)

    in PBSdef (Invitrogen, Walkersville, MD, USA)

Wash buffer:

    0.05% Tween 20 (Sigma-Aldrich, St. Louis, MO, USA)

    in PBSdef (Invitrogen, Walkersville, MD, USA)

Lumigen® TMA-6 Chemiluminescent Reagent (Lumigen/Beckman Coulter, Southfield, MI, USA):

    50% Lumigen TMA-6 Solution A

    50% Lumigen TMA-6 Solution B

Methanol (Merck, Darmstadt, Germany)

Primary antibodies:

Anti-human MAPKAPK-2 rabbit polyclonal antibody, 1 mg/ml, #ab63574 (1:1000) (Abcam, Cambridge, UK)

Anti-human MAPKAPK-2 rabbit polyclonal antibody, 10 µg/ml, #3042 (1:1000)

Anti-human phospho-MAPKAPK-2 (Thr334) rabbit monoclonal antibody 27B7, 99 µg/ml, #3007 (1:2000)

Anti-human phospho-MAPKAPK-2 (Thr334) rabbit polyclonal antibody, 75 µg/ml, #3041 (1:1000)

(all from Cell Signaling Technology, Danvers, MA, USA)

diluted in blocking solution

Secondary antibodies:

Anti-rabbit goat immunoglobulin (IgG) - HRP conjugate, 200 µg/ml, sc-2030 (1:5000) (Santa Cruz Biotechnology, Dallas, TX, USA)

Anti-biotin, HRP-linked secondary antibody, 17 µg/ml, #7075 (1:100000) (Cell Signaling Technology, Danvers, MA, USA)

diluted in blocking solution

Materials:

Immobilon-P Membrane, PVDF, 0.45 µm (Millipore, Billerica, MA, USA)

Extra thick blot paper, #170-3966 (Bio-Rad, Hercules, CA, USA)

Parafilm (Pechiney Plastic Packaging, Chicago, IL, USA)

Reaction tube 50 ml without skirt (Sarstedt, Nümbrecht, Germany)

Devices:

Semi-Phor Transfer Unit (Hoefer, Holliston, MA, USA)

G:BOX EF2 Imaging System (Syngene, Cambridge, UK)

GeneSnap software (Syngene, Cambridge, UK)

2.15 Confocal Laser Scanning Microscopy

2.15.1 Staining of Esophageal Cancer Cells

Glass cover slips were rinsed in 96% ethanol and allowed to dry before they were put into 6-wells (30 mm wells). Next, 300 µl of gelatine were evenly layered on top of every glass cover slip and aspirated after 10 min. 300 µl of cell suspension containing 200000 cells were then seeded on each glass cover slip and incubated at 37 °C with 5% CO_2 until the cells had attached to the glass. Afterwards the amount of corresponding cell culture medium was adjusted to 2 ml.

The next day the cells were washed with PBS^{++} and fixed with 1 ml 4% paraformaldehyde per 6-well for 10 min followed by 3 washing steps with PBS^{++}. Then permeabilization with 1 ml 0.5% Triton-X 100 per well was performed for 7 min at RT and the cells were again washed with PBS^{++} 3 times. Next, 1 ml blocking solution was added to every well and incubated for 20 min at RT. Then the cells were incubated with 100 µl of primary antibody solution (dilutions as listed below) for 1 hour, followed by 3 washing steps with PBS^{++}. Afterwards, the cells were incubated in the dark for 1 hour at RT with 100 µl of the appropriate secondary antibody solution and Hoechst 33342 DNA stain, all diluted 1:1000. Again the cells were washed 3 times with PBS^{++} and fixed with 1 ml 4% paraformaldehyde for 5 min at RT. This was followed by 3 washing steps with PBS^{++}. Then the cover slips were allowed to dry before mounting them upside down with ProLong Gold antifade solution on a silane-coated object slide. The next day the specimens were examined with a laser scanning microscope LSM 780 (Carl Zeiss Microscopy, Thornwood, NY, USA).

2.15.2 Staining of Jurkat cells

$5*10^5$ Jurkat cells were seeded per 24-well (15 mm well) containing 0.5 ml RPMI growth medium. TNFα stock solution was added to a final concentration of 100 ng/ml, (control wells remained untreated) and cells were incubated for 20 min at 37 °C. Afterwards, cells were fixed by adding 0.5 ml of 8% paraformaldehyde for 10 min at 37 °C and then transferred into reaction tubes for centrifugation at 190 x g and RT for 5 min.

The pellet was resuspended in 30 µl blocking solution and the cell suspension was applied onto a coated glass slide and air-dried.

Next, the dried cell suspension was circled with a PAP pen (to create a hydrophobic border line) and subjected to rehydration in 100 - 200 µl PBS++ for 10 min and permeabilization with 100 µl 0.5% Triton-X 100 for 7 min. Subsequently, 3 washing steps with PBS++ for 5 min each were performed, followed by blocking for 20 min with 100 µl of blocking solution. Afterwards, 100 µl of primary antibody solution were added for 1 hour, where antibodies were diluted as listed below.

Next, 3 washing steps with PBS++ were carried out before addition of 100 µl secondary antibody solution and a following incubation in the dark for 1 hour. After that the slides were washed 3 times with PBS++, rinsed in aqua dest. and air-dried before they were mounted with ProLong Gold antifade solution.

Materials

Solutions:

4% or 8% paraformaldehyde solution:

    4% or 8% paraformaldehyde (Sigma-Aldrich, St. Louis, MO, USA)

    in PBSdef (Invitrogen, Carlsbad, CA, USA)

    dissolved and heated to 65 °C while stirring

    heat reduction and addition of 1 to 2 ml 1 M NaOH dropwise until solution cleared

    filtered and stored in aliquots at -20 °C

Blocking solution:

    1.5% bovine serum albumin (Sigma-Aldrich, St. Louis, MO, USA)

    0.1% NaN_3 (Merck, Darmstadt, Germany)

    in PBSdef (Invitrogen, Carlsbad, CA, USA)

    sterile filtered and stored at 4 °C

ProLong Gold antifade solution (Invitrogen, Carlsbad, CA, USA)

0.5% Triton-X 100 (Sigma-Aldrich, St. Louis, MO, USA) in PBSdef (Invitrogen, Carlsbad, CA, USA)

0.2% gelatine type B (Sigma-Aldrich, St. Louis, MO, USA) in aqua dest.

PBS++ (Invitrogen, Carlsbad, CA, USA)

TNFα, stock 100 µg/ml (kind gift of H.R. Alexander, National Cancer Institute, Bethesda, MD, USA)

Primary antibodies:

Anti-human MAPKAPK-2 rabbit polyclonal antibody, 1 mg/ml, #ab63574 (1:100) (Abcam, Cambridge, UK)

Anti-human MAPKAPK-2 rabbit polyclonal antibody, 10 µg/ml, #3042 (1:100)

Anti-human phospho-MAPKAPK-2 (Thr334) rabbit mAb 27B7, 99 µg/ml, #3007 (1:200)

Anti-human phospho-MAPKAPK-2 (Thr334) rabbit polyclonal antibody, 75 µg/ml, #3041 (1:200)

Anti-human phospho-p38 MAPK (Thr180/Tyr182) mouse mAb 28B10, 305 µg/ml, #9216 (1:1000 for Jurkat cells and 1:500 for esophageal cancer cells)

(all from Cell Signaling Technology, Danvers, MA, USA)

diluted in blocking solution

Secondary antibodies:

Alexa Fluor® 546 goat anti-rabbit IgG (H+L), 2 mg/ml, A-11010 (1:1000)

Alexa Fluor® 488 goat anti-rabbit IgG (H+L), 2 mg/ml, A-11008 (1:1000)

Alexa Fluor® 555 donkey anti-mouse IgG (H+L), 2 mg/ml, A-31570 (1:1000)

Hoechst 33342, trihydrochloride, trihydrate, 10 mg/ml, H-3570 (1:1000)

(all from Invitrogen, Carlsbad, CA, USA)

diluted in blocking solution

Plastic and glass equipment:

6-well tissue culture (TC)-treated microplates (30 mm wells)

24-well TC-treated microplates (15 mm wells)

(both from TPP, Trasadingen, Switzerland)

Reaction tubes 1.5 ml (Greiner Bio-One, Frickenhausen, Germany)

Glass cover slips (Marienfeld-Superior, Lauda Königshofen, Germany)

StarFrost® adhesive silane-treated glass slides (Knittel, Braunschweig, Germany)

Super PAP PEN, 4 mm tip (Polysciences, Inc., Warrington, PA, USA)

Zeiss LSM 780 confocal laser scanning microscope (Carl Zeiss Microscopy, Thornwood, NY, USA)

2.16   Flow Cytometry

Cells transfected with pEGFP-C3 expression plasmid and seeded in 6-wells the day before were washed with PBSdef and detached with 0.5 ml 1x trypsin-EDTA. The reaction was stopped with 0.5 ml 10% FCS in PBSdef and the cell suspension was centrifuged at 480 x g and 4 °C for 5 min. Next, the supernatant was removed and the pellet was resuspended in 200 µl 5% FCS in PBSdef and transferred to flow cytometry tubes already containing 200 µl of 2x FIX buffer. The sample was then subjected to flow cytometric analysis for detection of intracellular EGFP fluorescence.

Materials

Solutions:

2x FIX buffer:

    0.5% Formaldehyde (Sigma-Aldrich, St. Louis, MO, USA)

    in PBSdef (Invitrogen Carlsbad, CA, USA)

PBSdef

1x trypsin-EDTA   Invitrogen, Carlsbad, CA, USA

10% FCS in PBSdef

5% FCS in PBSdef

Plastic equipment:

1.4 ml standard U-bottom tubes for flow cytometry (Micronic, Aston, USA) inserted into

5 ml polypropylene tubes round bottom (Greiner Bio-One, Kremsmünster, Austria)

Device:

Gallios flow cytometer (Beckman Coulter, Brea, CA, USA)

3   RESULTS

3.1   *Immunohistochemical Staining of MK2 and phospho-MK2 in Esophageal Cancer Tissue*

Since Birner et al. had previously analyzed the expression of MK2 in GIST [15] and in esophageal carcinoma (unpublished data) using immunohistochemistry, the first step in this project was to reproduce these findings with antibodies used by them as well as with two other antibodies. Thus, two distinct antibodies for MK2 (ab63574, #3042) and two different antibodies for phospho-MK2 (#3041, #3007) were included in this study.

Esophageal cancer specimens were obtained from Peter Birner at the University Clinic of Pathology. The antigen retrieval procedure was performed according to data sheets and personal correspondence with the manufacturing company. The conditions were optimized in the course of the project by testing the antibodies with TE as well as citrate buffer, different temperatures (121 or 135 °C), pressure (1.5 or 2.5 bar), and exposure time (1, 6, 10, and 20 min) for antigen retrieval.

After antigen retrieval with TE buffer and autoclaving at 135 °C and 2.5 bar for 20 min it was possible to detect cytoplasmic staining of MK2 in cancer tissue (Fig. 8) using the MK2 antibody ab63574 which had previously been applied by Birner et al. [15].
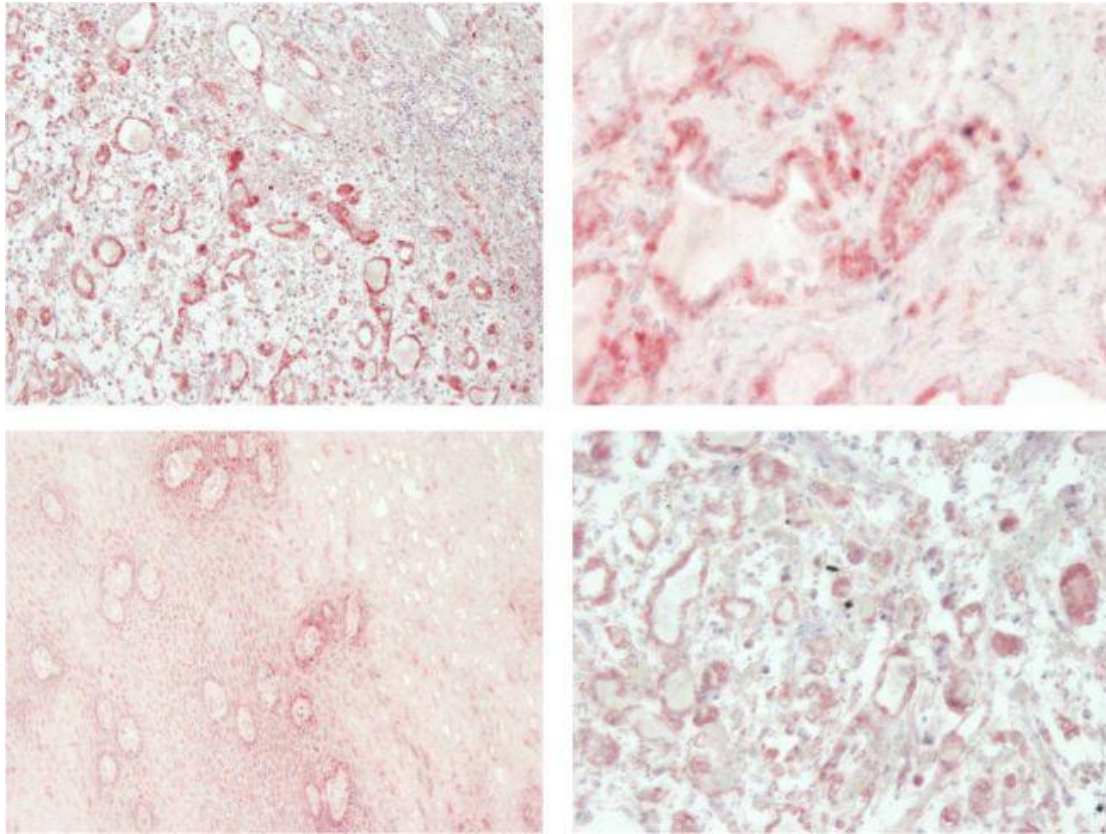
Fig 8. Positive red staining of an esophageal cancer specimen adenocarcinoma with MK2 antibody ab63574 and blue counterstaining of nuclei with hematoxylin. Left panels 40x magnification, top right panel 400x magnification, bottom right panel 200x magnification.

Antigen retrieval at 135 °C and 2.5 bar for 20 min in citrate buffer and staining with phospho-MK2 antibody #3041 also displayed a positive, i.e. diffuse red, staining of cells. However, rather than the esophageal cancer cells it was the normal epithelial and basal cell layer which presented positive for phospho-MK2 (Fig. 9).
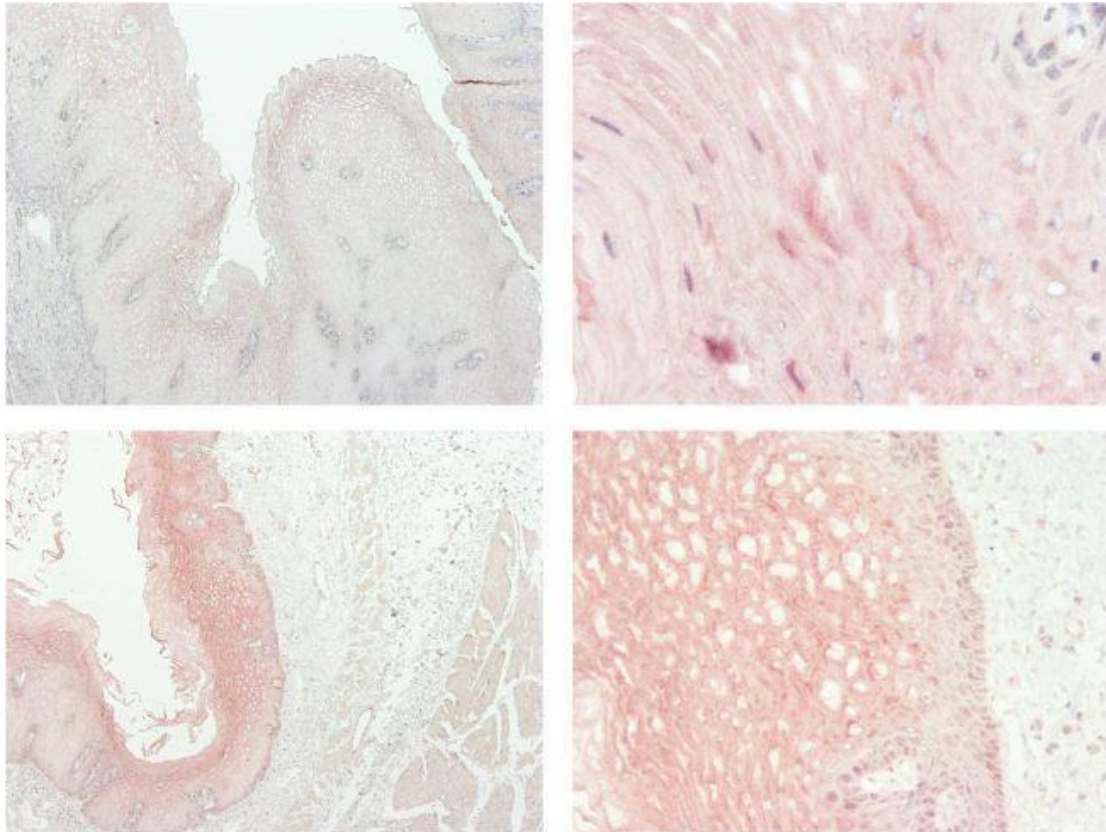
Fig. 9 Staining of a cancer-unaffected epithelial cell layer with phospho-MK2 antibody #3041. Left panels 40x magnification, top right panel 400x magnification, bottom right panel 200x magnification.

Incubation of tissue slides with MK2 antibody #3042 after antigen retrieval at 135 °C and 2.5 bar for 20 min using citrate or TE buffer led to no positive staining (Fig. 10).
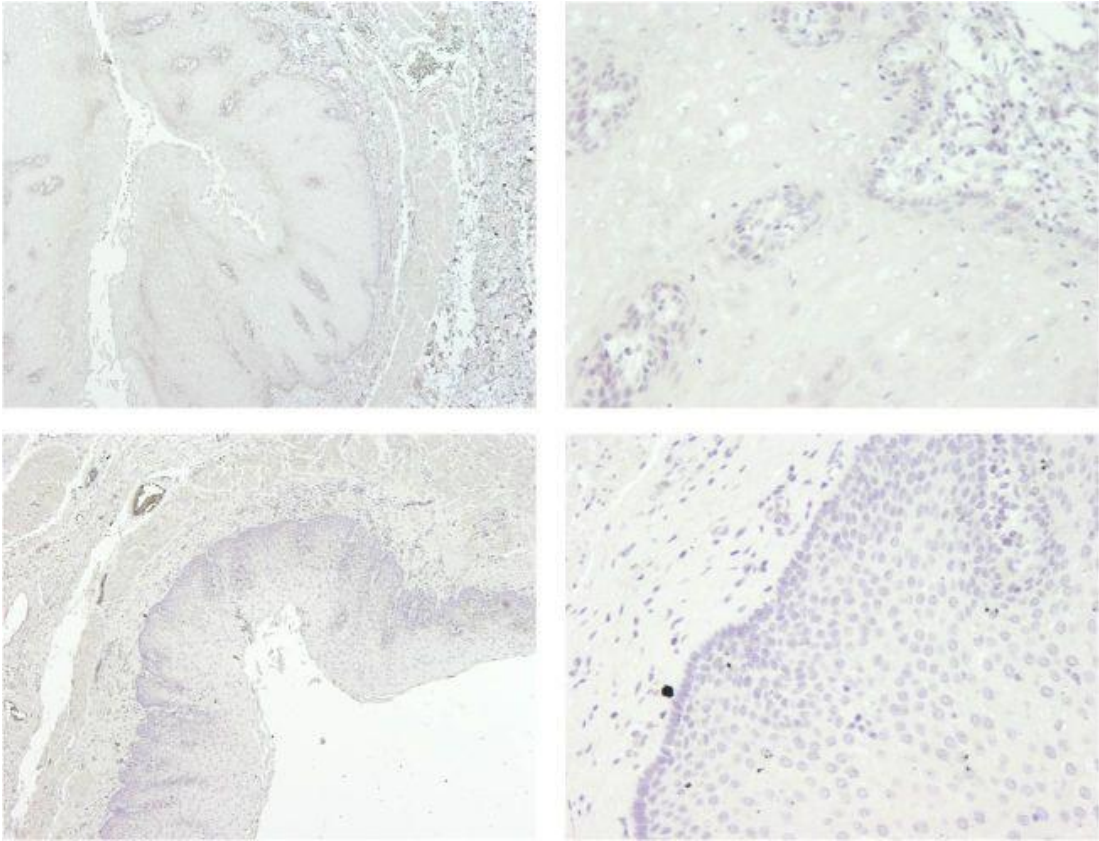
Fig. 10 Negative staining of a cancer specimen with MK2 antibody #3042. Left panels 40x magnification, right panels 200x magnification.

For the phospho-MK2 antibody #3007 it was indicated in the datasheet to use citrate buffer for antigen retrieval. In this project, citrate as well as TE buffer were tested. The results showed a positive staining of the cancer-unaffected epithelial cell layer when TE buffer was used for antigen retrieval at 135 °C and 2.5 bar for 20 min (Fig. 11). In contrast to this, pretreatment with citrate buffer (as recommended by the company) and the same parameters as indicated above led to no positive staining with only a few red dye aggregates (data not shown).
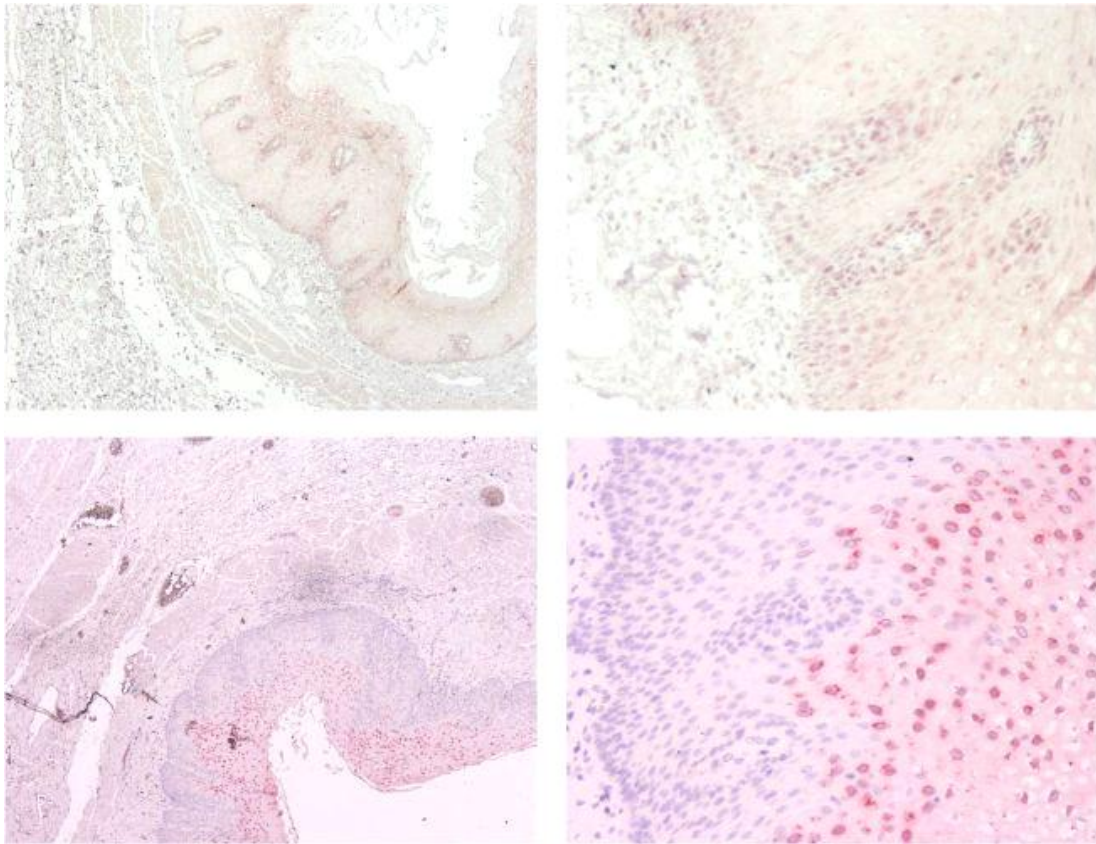
Fig. 11 Staining of a normal esophageal squamous epithelium with phospho-MK2 antibody #3007. Left panels 40x magnification, right panels 200x magnification.

3.2 Selection of Esophageal Cancer Cell Lines

Since there is a considerable number of available esophageal cancer cell lines, it was necessary to focus on a few selected ones. A literature search to find out which cell lines are common in studying esophageal cancer revealed that cell lines like FLO-1, KYAE-1, TE-1, SK-GT-4 or variants of the OE (OE19, OE33) and the ESO cancer cell line (ESO26, ESO51) were widely used.

The criteria for further selection of cell lines were on the one hand the expression level of MK2 and on the other hand the rate of cell growth. Here it was planned to obtain at least one MK2 low-expressing and one MK2 high-expressing cell line, both growing fast in culture. SK-GT-4 was chosen as MK2 high-expressing cell line [49] (NCBI GEO profile ID 11619989), whereas TE-1 was selected because it expressed MK2 at a low level [50] (NCBI GEO accession number GSM887695). Jurkat E6-1 cells were used as control cells expressing MK2 [50]. Unfortunately, for the FLO-1 cell line no MK2 expression data could be found.

According to ECACC® growth profiles, the esophageal carcinoma cell lines SK-GT-4 and FLO-1 were known for rapid growth, i.e. they reached confluence within 100 to 120 hours, when split at a 1:4 to 1:6 ratio. Preliminary tests in our laboratory confirmed those statements, and for TE-1 a similar growth rate was observed (data not shown). FLO-1 [51] as well as SK-GT-4 cells [52] display p53 mutations, whereas TE-1 is a cell line with p53 wildtype configuration [53].

3.3 Immunofluorescent Staining of MK2 and phospho-MK2 in Cancer Cell Lines

3.3.1 MK2, phospho-MK2, and phospho-p38 Staining in Esophageal Cancer Cells

In order to investigate the distribution of MK2 and phospho-MK2 in the chosen esophageal cancer cell lines FLO-1, SK-GT-4, and TE-1, fluorescence staining with the MK2 antibodies (ab63574 and #3042), and the phospho-MK2 antibodies (#3041 and #3007) was performed and samples were analyzed by confocal laser scanning microscopy.

Since Birner et al. had been using the antibodies MK2 ab63574 and p-MK2 #3041 in their previous work [15], our initial stainings were performed with these reagents. As shown in Fig. 12, the MK2 ab63574 antibody displayed a mainly cytosolic staining in all cell lines (Fig. 12A, 12C, 12E), whereas p-MK2 #3041 led to a primarily nuclear staining (Fig. 12B, 12D, 12F) with the exception of SK-GT-4 (Fig. 12D) where an additional cytoplasmic staining was observed.
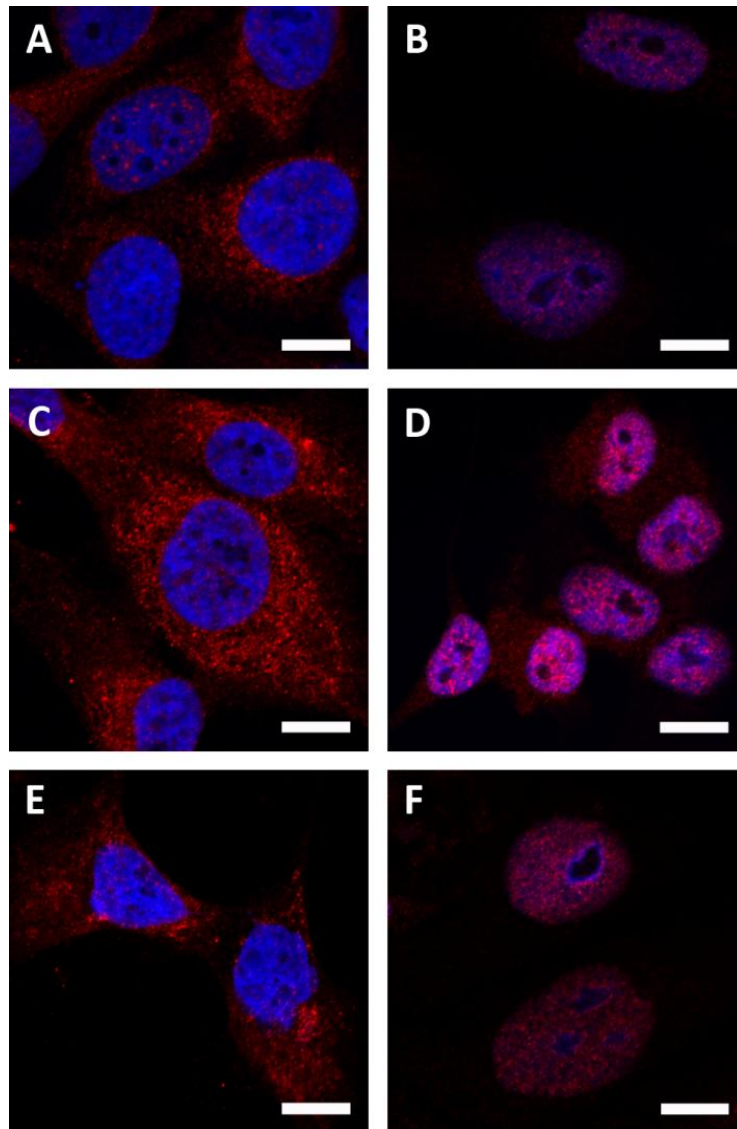

Fig. 12 CLSM imaging of MK2 expression in FLO-1 (A+B), SK-GT-4 (C+D), and TE-1 cells (E+F): MK2 detection in red and staining of nuclear DNA by Hoechst dye in blue. Left panels show staining with MK2 ab63574, right panels show phospho-MK2 #3041 antibody staining. Scale bar 10 μm.

Further experiments revealed that all three cell lines showed similar results concerning the detection with antibodies MK2 #3042 and phospho-MK2 #3007. Thus, only the results of FLO-1 cells are depicted in Fig. 13 below as compared to immunofluorescent analysis with antibodies MK2 ab63574 and p-MK2 #3041.

While MK2 antibody ab63574 led to a mainly cytoplasmic MK2 staining (Fig. 13A), the FLO-1 cells treated with MK2 antibody #3042 displayed a mainly nuclear staining with a weak signal in the cytosol (Fig. 13C). In contrast, p-MK2 #3007 antibody led to a strong signal, both in the nucleus and the cytoplasm (Fig. 13D), while p-MK2 detection by #3041 antibody was largely restricted to the nucleus (Fig. 13B). Additionally, it seemed that both, MK2 and phospho-MK2 signals were strongly increased in the cytosol of dividing cells (data not shown).
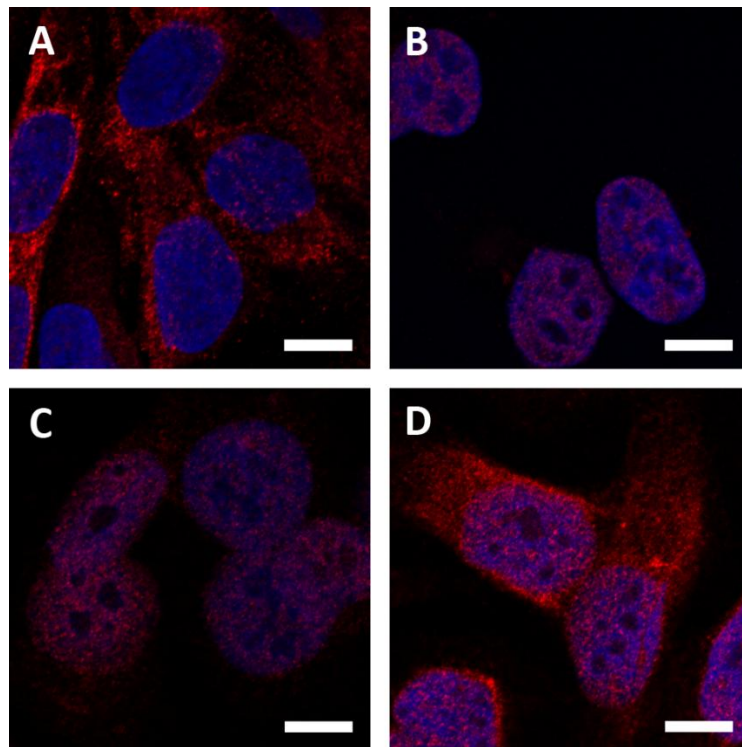
Fig. 13 MK2 and phospho-MK2 immunfluorescence staining of FLO-1 cells. (A) MK2 ab63574, (B) phospho-MK2 #3041, (C) MK2 #3042, (D) phospho-MK2 #3007 antibodies were applied. Scale bar 10 μm.

To investigate if the cell lines FLO-1, SK-GT-4, and TE-1 show a co-localized distribution of phospho-MK2 and phospho-p38, a co-staining was performed. Therefore, the antibodies phospho-MK2 #3007 and phospho-p38 #9216 were used.

The results (Fig. 14-16) demonstrated that phospho-MK2 expression (shown in green) was mainly limited to the nuclear region where it was co-localized with phospho-p38 (shown in red). Furthermore, phospho-MK2 showed an intense, compact and dense staining pattern.

FLO-1 cells (Fig. 14C) displayed the highest expression of phospho-MK2 when compared to SK-GT-4 (Fig. 15C) and TE-1 cells (Fig. 16C). Phospho-p38 by contrast exhibited a diffuse staining which was also present in the cytosol to a minor degree, but with a stronger signal in the nucleus. Here, TE-1 cells showed the weakest staining (Fig. 16D), whereas SK-GT-4 cells expressed a high amount of phospho-p38 (Fig. 15D) which was present in the nuclear region to a high extent and showed spotty accumulation.
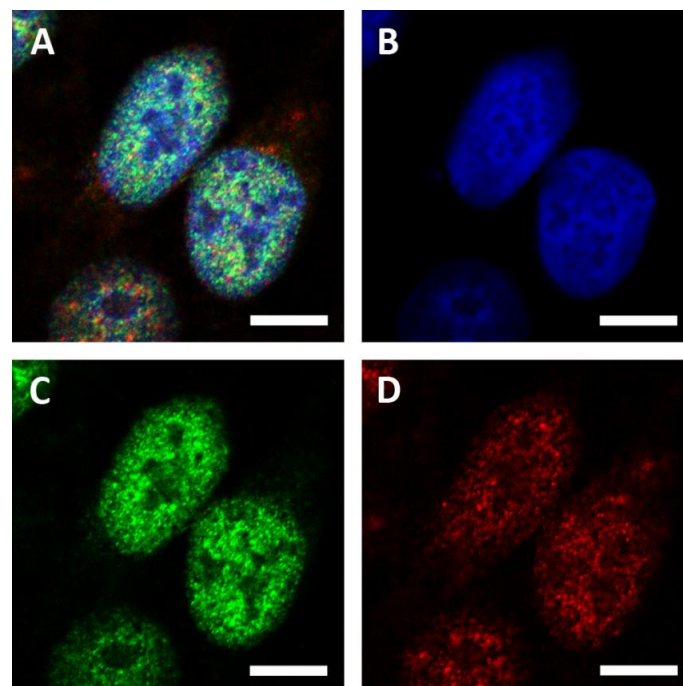
Fig. 14 Co-staining of phospho-MK2 #3007 and phospho-p38 #9216 in FLO-1 cells. Phospho-MK2 #3007 shown in green (C), phospho-p38 #9216 shown in red (D), nuclear Hoechst staining in blue (B) and merged images (A). Scale bar 10 μm.
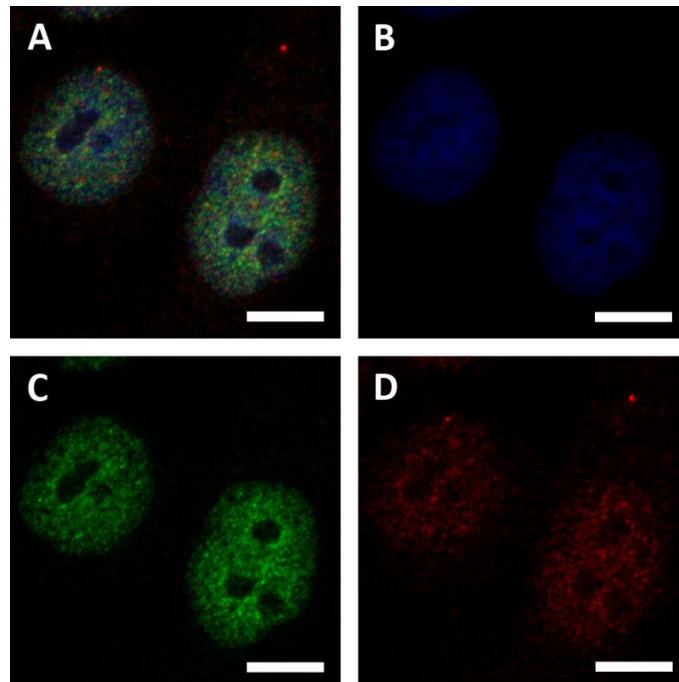
Fig. 15 Co-staining of phospho-MK2 #3007 and phospho-p38 #9216 in SK-GT-4 cells. Phospho-MK2 #3007 shown in green (C), phospho-p38 #9216 shown in red (D), nuclear Hoechst staining in blue (B) and merged images (A). Scale bar 10 μm.
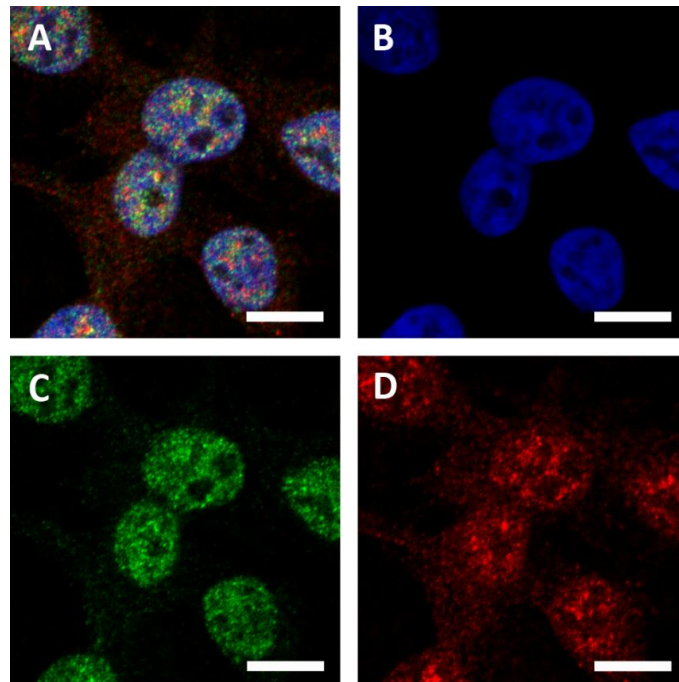
Fig. 16 Co-staining of phospho-MK2 #3007 and phospho-p38 #9216 in TE-1 cells. Phospho-MK2 #3007 shown in green (C), phospho-p38 #9216 shown in red (D), nuclear Hoechst staining in blue (B) and merged images (A). Scale bar 10 μm.

3.3.2 MK2, phospho-MK2, and phospho-p38 Staining in Jurkat Cells

Because the findings depicted in Fig. 13A and 13B were unexpected and contrary to the established literature [2, 9, 11], which describes that MK2 is expressed in the nucleus and only after phosphorylation (activation) is transported into the cytosol, control experiments with Jurkat cells were performed. The Jurkat suspension cells were either left untreated or stimulated with TNFα and applied onto coated glass slides for further fluorescence staining with MK2 antibodies (ab63574 and #3042), phospho-MK2 antibodies (#3041 and #3007), and the phospho-p38 antibody (#9216).

The results depicted in Fig. 17 showed primarily cytoplasmic MK2 expression in Jurkat cells and only marginal differences between MK2 (Fig. 17A-D) and phospho-MK2 (Fig. 17E-H) stainings. TNFα stimulation did not trigger major changes in MK2 or phospho-MK2 signals indicating constitutive MK2 activation in Jurkat cells. The phospho-MK2 #3007 antibody (Fig. 17G and 17H) displayed a generally more intense pattern when compared to phospho-MK2 #3041 (Fig. 17E and 17F) including nuclear detection of phospho-MK2.
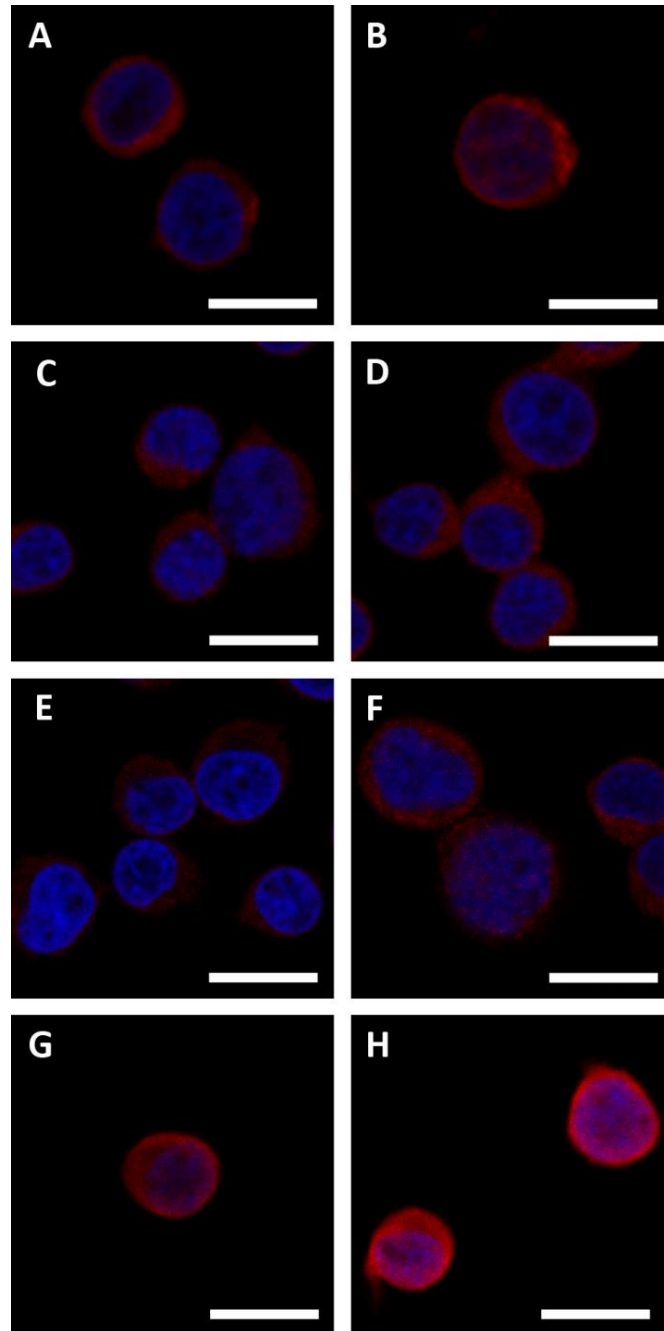
Fig. 17 CLSM imaging of MK2 expression in Jurkat cells. (A, B) MK2 ab63574, (C, D) MK2 #3042, (E, F) phospho-MK2 #3041, (G, H) phospho-MK2 #3007 staining of untreated (A, C, E, G) and TNFα-stimulated (B, D, F, H) Jurkat cells. Scale bar 10 μm.

The analysis also revealed that in some specimens a very strong phospho-MK2 staining in mitotic cells was found (Fig. 18.).
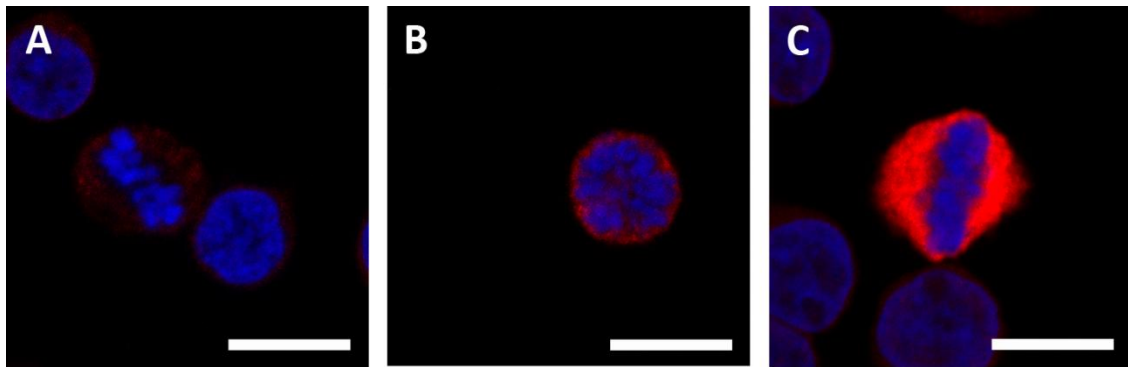

Fig. 18 Jurkat cells showing condensed DNA (B) or chromosomes arranged in the metaphase plate (A and C). (A and B) Immunofluorescent staining with phospho-MK2 #3041 and (C) with phospho-MK2 #3007 antibody. Scale bar 10 μm.

Staining with phospho-p38 #9216 antibody displayed a strong cytosolic signal present in unstimulated Jurkat cells (Fig. 19A) which was highly increased in TNFα stimulated cells (Fig. 19B).
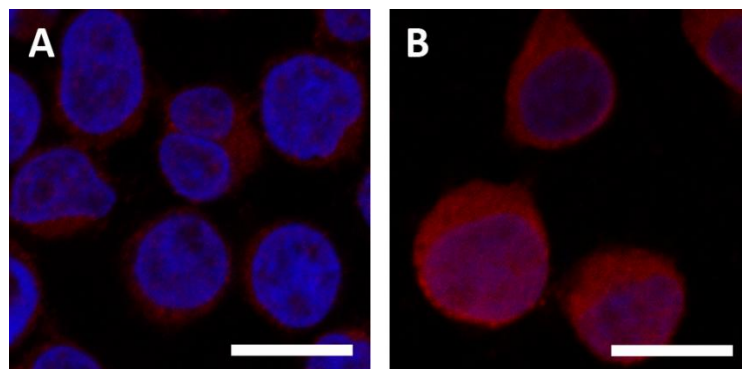

Fig. 19 Unstimulated and TNFα stimulated Jurkat cells stained with phospho-p38 #9216. (A) Phospho-p38 staining of control cells, (B) phospho-p38 staining of stimulated cells. Scale bar 10 μm.

Also for the phospho-p38 antibody an especially high signal was found in cells which were undergoing mitosis (Fig. 20).
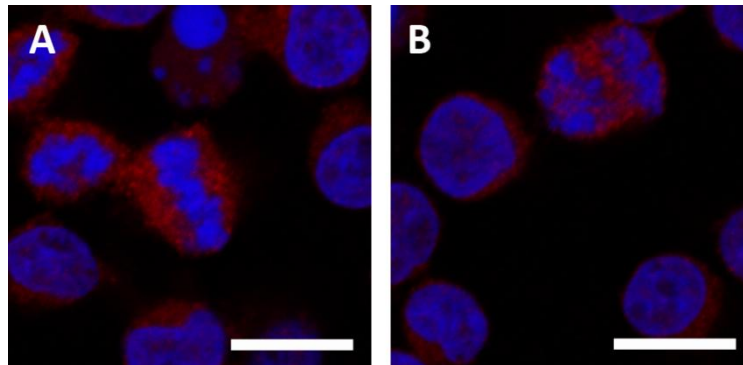

Fig. 20 Jurkat cells stained with phospho-p38 #9216. Cells show Hoechst staining of chromosomes arranged in the metaphase plate (A, center) or anaphase (B, top right). Scale bar 10 µm.

3.4 Detection of MK2 and phospho-MK2 in Cancer Cell Extracts by Immunoblotting

To evaluate MK2 and phospho-MK2 levels in FLO-1, SK-GT and TE-1 cells, cell extracts were prepared using RIPA buffer, and SDS-PAGE under reducing conditions followed by immunoblotting was chosen as further detection method. The first antibody to be tested was the MK2 antibody ab63574.

As depicted in Fig. 21 it was not possible to detect a distinct band at 46 kDa, the predicted size of MK2. A strong unspecific band was detected at approximately 70 kDa. This band was also visible when incubating the membrane with the secondary antibody alone (Fig. 21A) which was performed to determine background or "ghost bands".
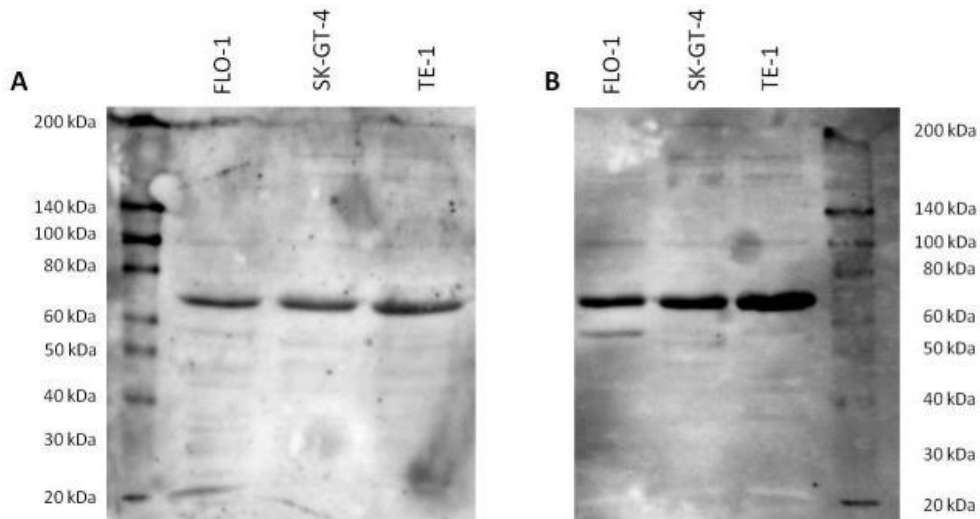
Fig. 21 Immunoblotting of cancer cell extracts without (A) and with (B) the primary antibody MK2 ab63574 and anti-rabbit secondary antibody. Expected molecular weight of MK2: 46 kDa.

Next, overexpression of MK2 was performed to facilitate the identification of the correct MK2 band at 46 kDa. Hence, cells were transfected with 20 µg EFpLink control vector or MK2 expression plasmid. Also two additional antibodies, MK2 #3042 and phospho-MK2 #3007, were tested.

As shown in Fig. 22 there was no distinct upregulation of MK2 protein in FLO-1 cells, but in case of MK2 transfected SK-GT-4 and TE-1 cells weak double bands at 46 kDa were detected.
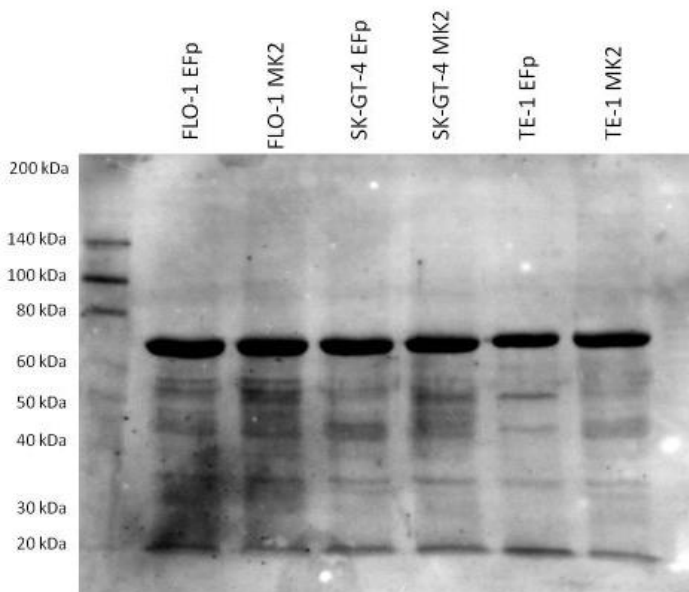
Again, the artifact band at 70 kDa was very prominent and 2 bands at 55 kDa seemed to be more intense in FLO-1 cells.

Fig. 22 Immunoblotting of MK2 in EFpLink or MK2 transfected cells using the antibody MK2 #3042.

Experiments with the phospho-MK2 antibody #3007 revealed that at 46 kDa only one weak band was visible (Fig. 23). An upregulation of MK2 after transfection with the expression plasmid was only seen in case of TE-1 cells.
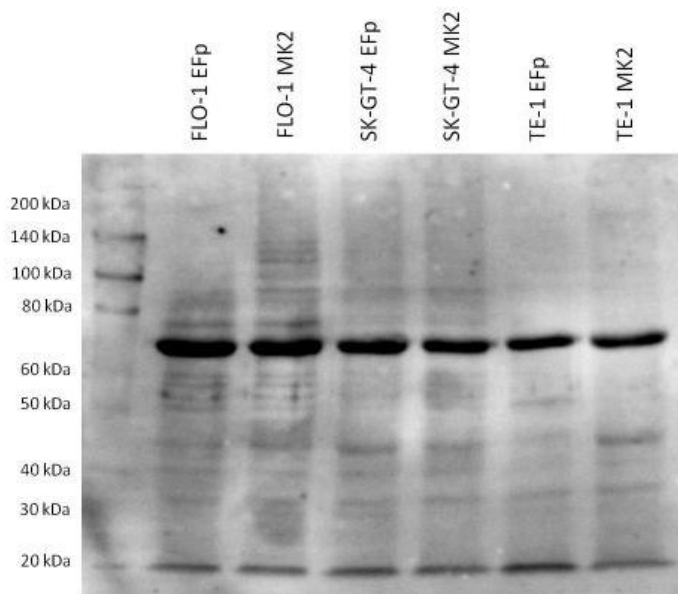

Fig. 23 MK2 overexpression in esophageal cancer cell lines as detected by immunoblotting of cell extracts with the phospho-MK2 antibody #3007.

Because preparation of cellular extracts for immunoblotting using RIPA buffer led only to very weak MK2 bands, we changed the protein extraction procedure: Next SDS lysis buffer plus heating and sonication were used to increase the protein yield and in further consequence the band intensity. In addition, Jurkat cell extracts were included as a positive control.

To further address the question if MK2 overexpression is transient and possibly rapidly downregulated, MK2 expression of all three esophageal cancer cell lines was investigated over time using 12, 24 and 48 hour points, where here only results for FLO-1 cells are represented.

When FLO-1 cell extracts were probed with the MK2 #3042 antibody, the plots displayed prominent double bands at 46 kDa (Fig. 24). At 12 hours MK2 expression was identical in control and MK2 transfected FLO-1 cells (bands at 46 kDa). After 24 hours MK2 expression was higher in MK2 plasmid-transfected than in control cells, but at 48 hours the MK2 level in MK2 plasmid-transfected cells was lower than in the control. Jurkat cells displayed the strongest double band at 46 kDa with a weak upper but intense lower band. An additional band at approximately 55 kDa was further observed in all cell extracts which was particularly prominent in Jurkat cell extracts.
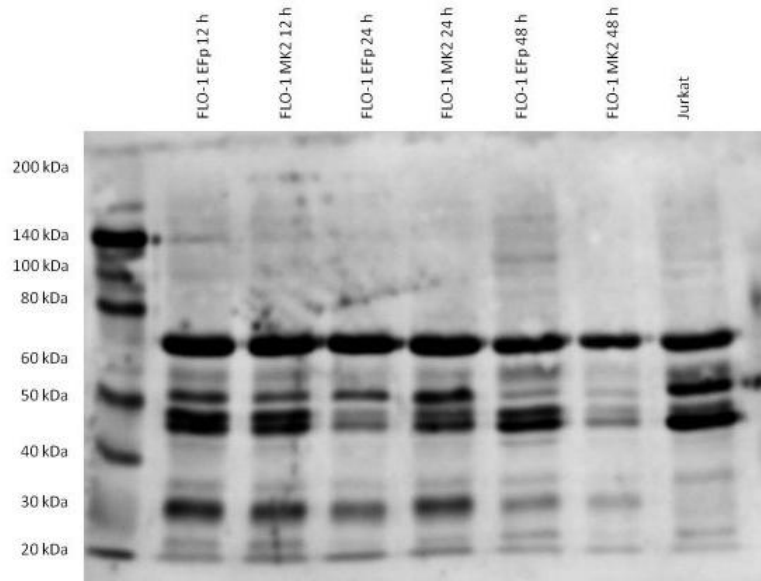
Fig. 24 Cell extracts analyzed at 12, 24, and 48 hours after FLO-1 cell transfection with MK2 expression plasmid or EFpLink control vector. Immunoblotting with antibody #3042.

Incubation of FLO-1 protein lysates with phospho-MK2 antibody #3007 revealed a single band at 46 kDa which again was of identical intensity at 12 hours, stronger in MK2-transfected cells at 24 h and diminished in MK2-transfected cells again after 48 hours. Jurkat cells displayed only a weak signal for phosph-MK2 (Fig. 26). However, it should be noted that protein loading or membrane transfer seemed to be weaker for the last two lanes as judged by the 70 kDa "ghost band".
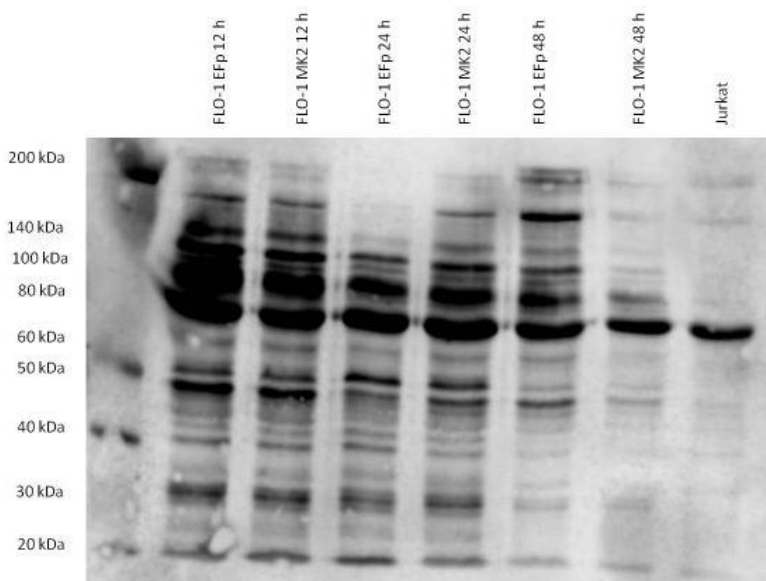

Fig. 25 Cell lysates of MK2 or control plasmid transfected FLO-1 cells, immunoblotted with the phospho-MK2-specific antibody #3007.

Furthermore, it is important to remark that the efficiency of cell transfection with MK2 expression plasmids was additionally verified by measuring the levels of MK2 mRNA by qRT-PCR. It was found that all three cell lines presented with very high levels of overexpressed MK2 mRNA (see Results 3.7.1), even though MK2 overexpression was hardly detectable at the protein level.

3.5 Effect of Pharmacological MK2 Inhibitors on Proliferation and Migration of Esophageal Cancer Cells

To investigate the effects of pharmacological MK2 inhibitor substances on proliferation and migration of the chosen esophageal cancer cell lines, the Hsp25 kinase inhibitor (#385880, Merck, Darmstadt, Germany) and PF-3644022 hydrate (#PZ0188, Sigma-Aldrich, St. Louis, MO, USA) were used. In short, 100000 cells per 6 well were seeded and cultured at 37 °C overnight in 2 ml cell culture medium. On the next day, the medium was reduced to 1 ml and the inhibitor which had been dissolved in DMSO (dimethyl sulfoxide) was added at different concentrations. After 24, 48, and 72 hours microscopic images were taken, a metabolic EZ4U assay was performed, and cell count was determined.

3.5.1 Hsp25 Kinase Inhibitor

The Hsp25 kinase inhibitor was added in the following concentrations: 0.5 µM, 2 µM, and 10 µM. Negative controls with 2 µl DMSO/ml (for the conditions with 0.5 µM and 2 µM inhibitor) and 10 µl DMSO/ml (for 10 µM of inhibitor) were also included.

Fig. 26-28 illustrate that Hsp25 kinase inhibitor did not affect the growth or survival of esophageal cancer cell lines. There were only minor differences between the different concentrations of inhibitor and the corresponding DMSO controls in FLO-1 cells. SK-GT-4 and TE-1 cells (Fig. 27 and Fig. 28, respectively) were sensitive to high levels of DMSO, i.e., showed a reduced cell growth in the 10 µM condition as well as its DMSO control sample.
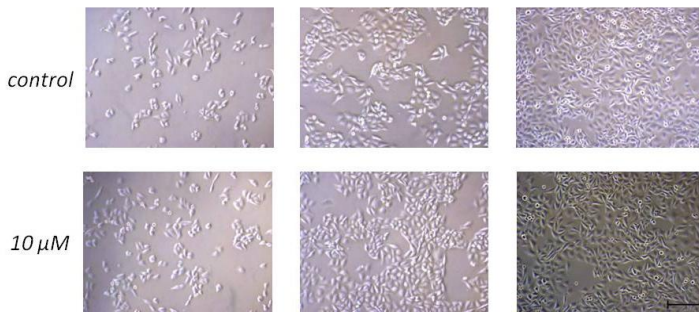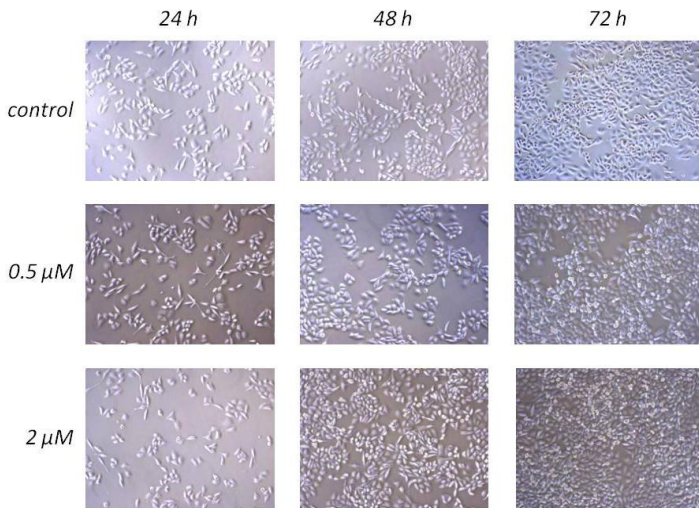
Fig. 26 Cell growth of FLO-1 cells 24, 48, and 72 hours after Hsp25 kinase inhibitor addition. Pictures of DMSO control samples are depicted above the corresponding test conditions. Scale bars 100 μm, valid for all images.
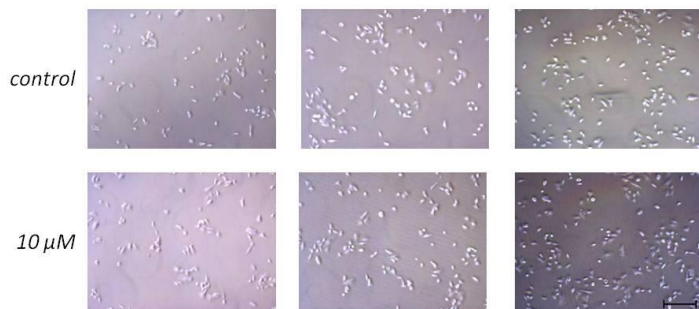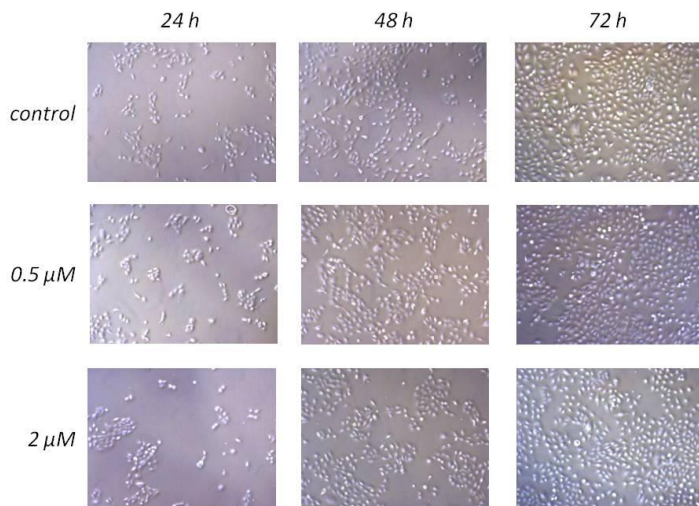
Fig. 27 Cell growth of SK-GT-4 cells 24, 48, and 72 hours after Hsp25 kinase inhibitor addition. Pictures of DMSO control samples are depicted above the corresponding test conditions. Scale bars 100 μm, valid for all images.
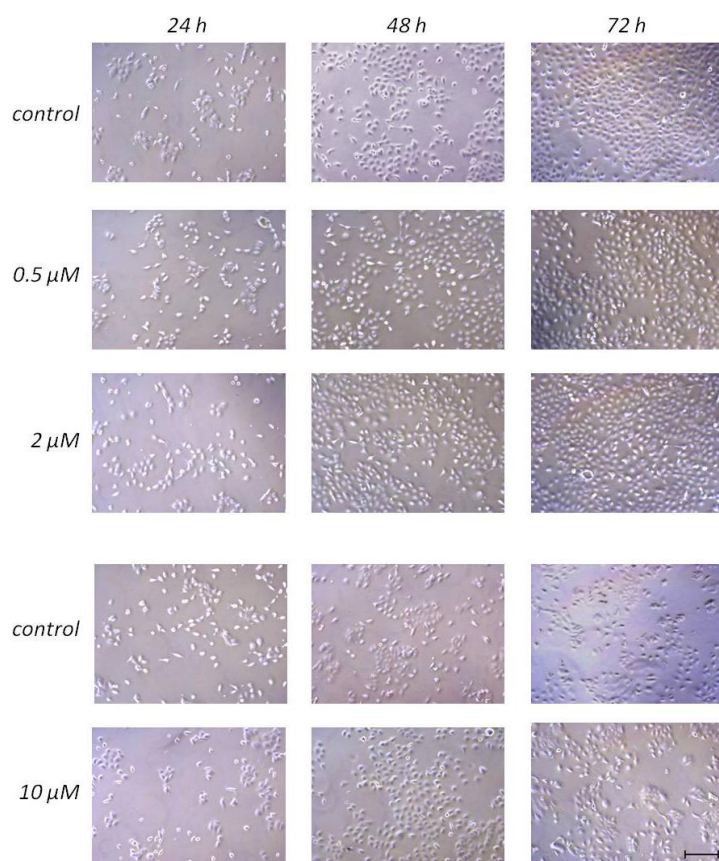
Fig. 28 Cell growth of TE-1 cells 24, 48, and 72 hours after Hsp25 kinase inhibitor addition. Pictures of DMSO control samples are depicted above the corresponding test conditions. Scale bars 100 μm, valid for all images.

These findings were confirmed by the results of the EZ4U assay which reflects cell survival and growth by metabolic activity (Fig. 29A, 29C, and 29E). FLO-1 cells (Fig. 29A) exhibited unrestricted growth at all conditions, while the metabolic activity of SK-GT-4 (Fig. 29C) and TE-1 cells (Fig. 29E) was reduced by the highest amount of DMSO (10 μl/ml) added to the culture. There was no time or dose dependent effect of the Hsp25 kinase inhibitor on the growth of FLO-1, SK-GT-4, and TE-1 cells.

Determination of cell concentrations by manual counting seemed to be more prone to variation, in particular for TE-1 cells (Fig. 29F). Overall, cell counts were only found to be increased after 72 hours of culture. There was no effect of treatment with Hsp25 kinase inhibitor on the number of FLO-1 cells. Cell growth of SK-GT-4 cells at 72 h was blocked by the highest concentration (10 μl/ml) of DMSO control. Again, there was no blocking effect of the Hsp25 kinase inhibitor on cell growth observed for any of the three investigated cell lines.
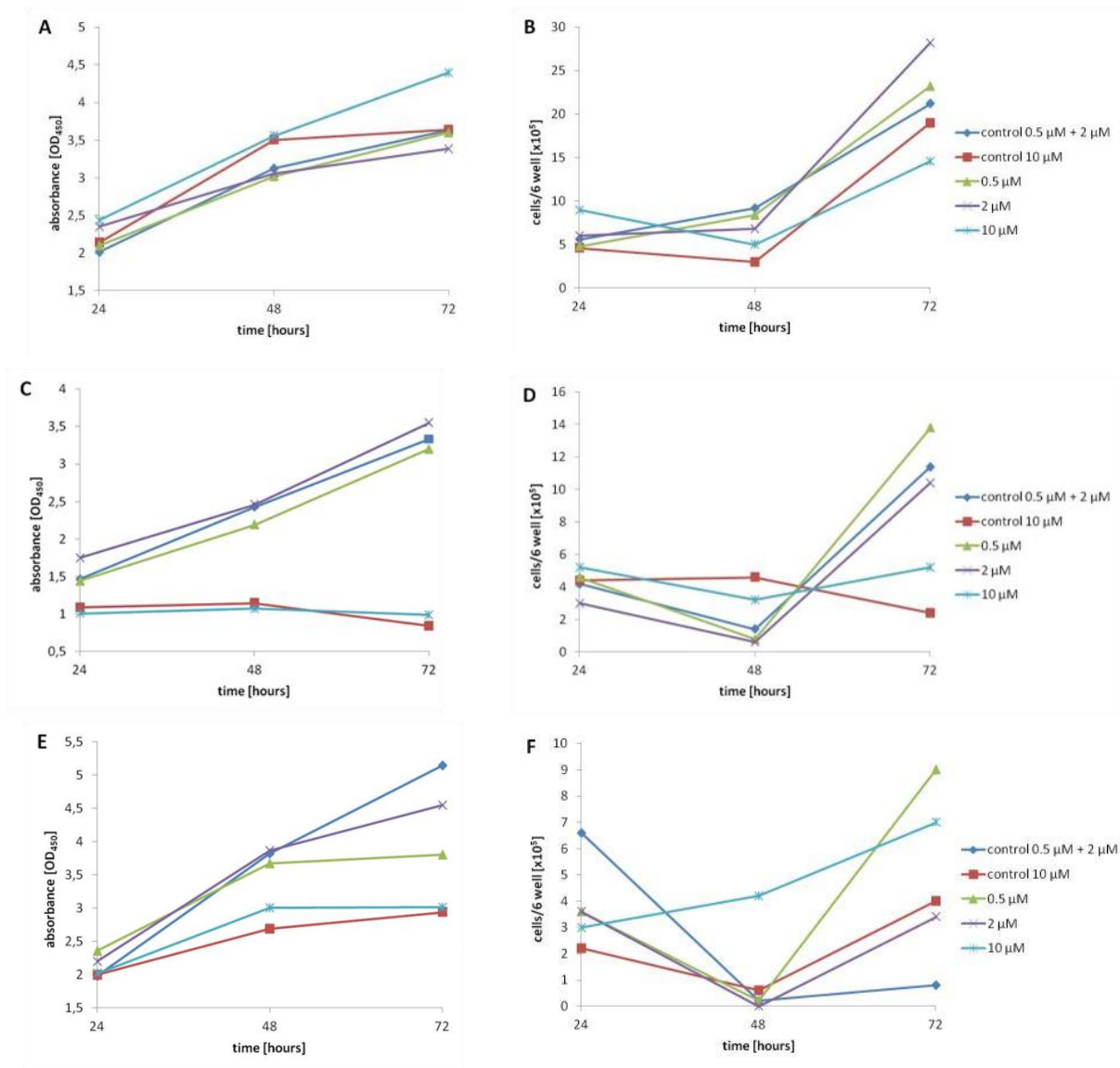
Fig. 29 EZ4U assay results (left panels) and cell count (right panels) of FLO-1 (A, B), SK-GT-4 (C, D), and TE-1 cells (E, F) after 24, 48, and 72 hours of Hsp25 kinase inhibitor treatment.

3.5.2 PF-3644022 Hydrate

With respect to PF-3644022 hydrate the applied inhibitor concentrations were 2 µM, 6 µM, and 20 µM. The required DMSO controls were also included: 2 µl DMSO for the 2 µM and 20 µM conditions and 6 µl DMSO for the condition with 6 µM inhibitor.

FLO-1 cells (Fig. 30) showed a considerably reduced cell growth at the concentrations of 6 µM and 20 µM. Especially, the effect of 20 µM inhibitor was already visible after 48 hours, whereas the proliferation inhibiting effect of 6 µM was only observed after 72 hours. Also for SK-GT-4 (Fig. 31) microscopic images displayed a remarkable reduction of cell number at 6 µM and 20 µM. The influence of PF-3644022 hydrate on the proliferation of TE-1 cells (Fig. 32) was already detectable at 2 µM inhibitor concentration.
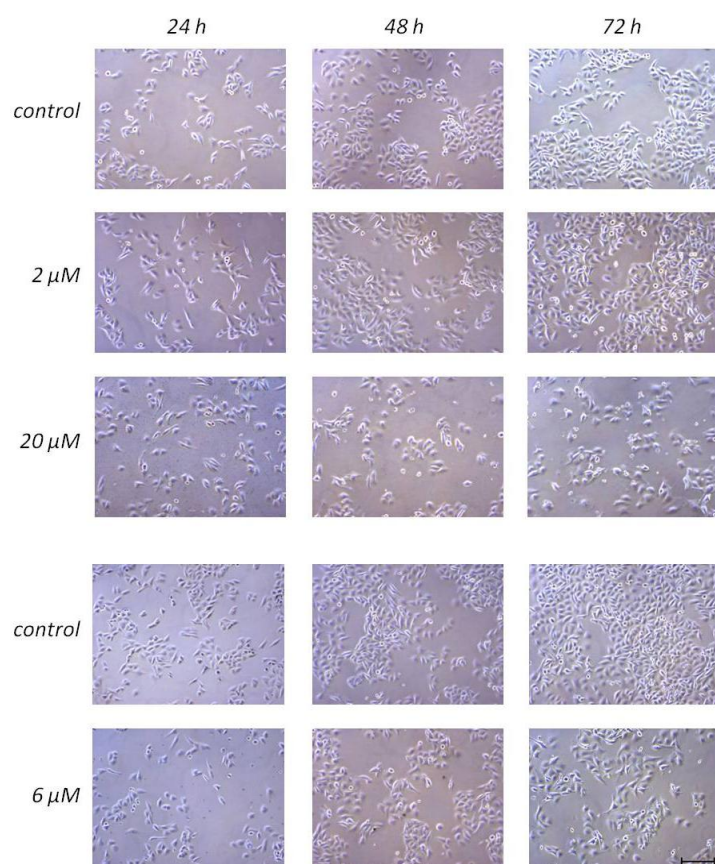
Fig. 30 Cell growth of FLO-1 cells 24, 48, and 72 hours after PF-3644022 hydrate addition. Pictures of controls depicted above the corresponding conditions. Scale bars 100 µm, valid for all images.
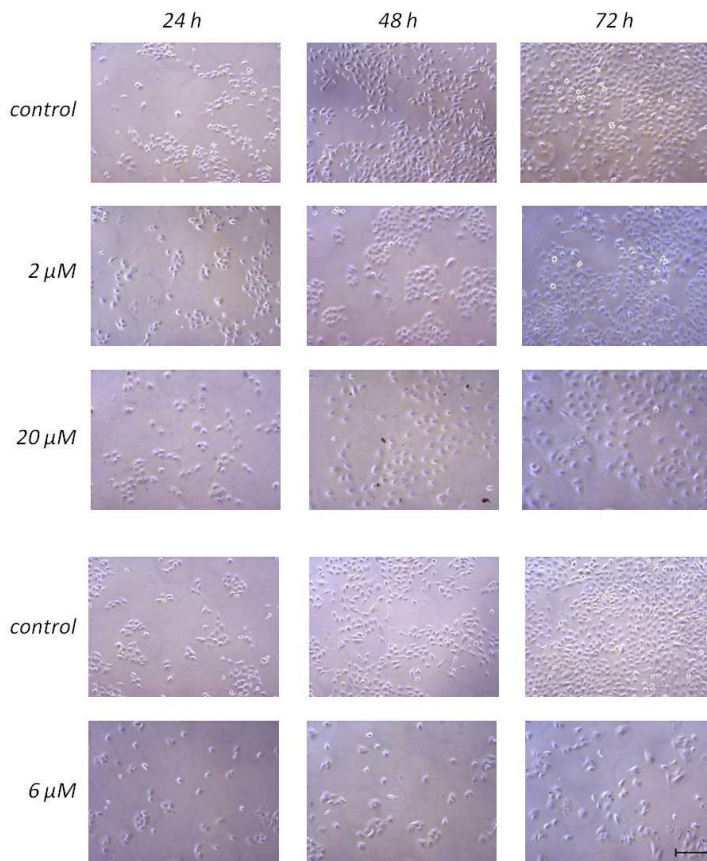
Fig. 31 Cell growth of SK-GT-4 cells 24, 48, and 72 hours after PF-3644022 hydrate addition. Pictures of DMSO control samples are depicted above the corresponding test conditions. Scale bars 100 μm, valid for all images.
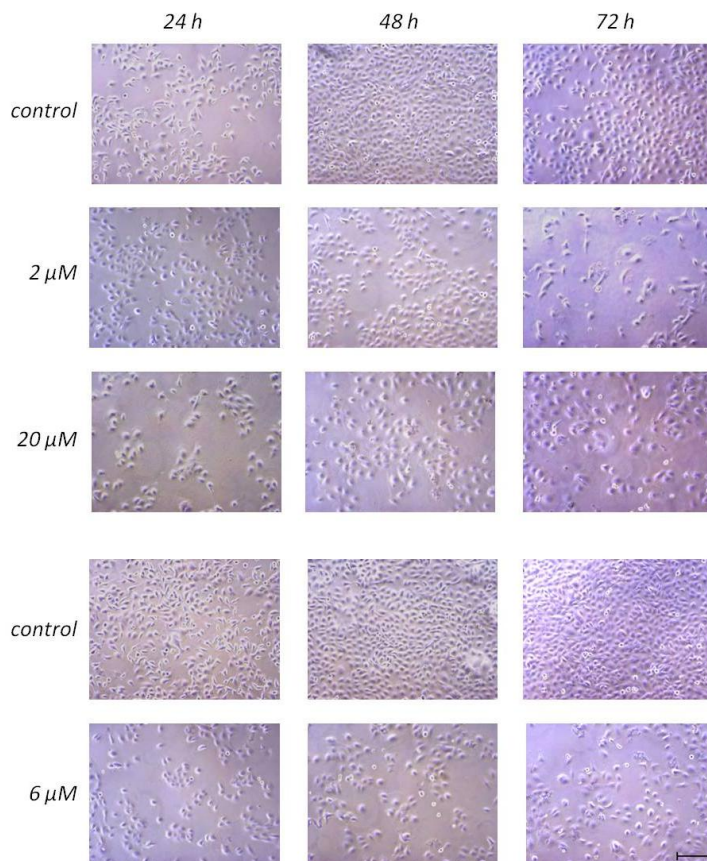

**Fig. 32 Cell growth of TE-1 cells 24, 48, and 72 hours after PF-3644022 hydrate addition. Pictures of DMSO control samples are depicted above the corresponding test conditions. Scale bars 100 μm, valid for all images.**

Results for the EZ4U assays of FLO-1 (Fig. 33A) and SK-GT-4 cells (Fig. 33C) confirmed the reduction in cell proliferation and metabolism by treatment with PF-3644022 hydrate over time. Cell counts for FLO-1 cells (Fig. 33B) were decreased at all inhibitor concentrations, while the values for SK-GT-4 (Fig. 33D) displayed a reduction of cell count in case of 6 µM and 20 µM PF-3644022 hydrate.

Again, the EZ4U measurements and cell count determination for TE-1 cells (Fig. 33E and F) did not match the microscopic observations and seemed to be more error prone.
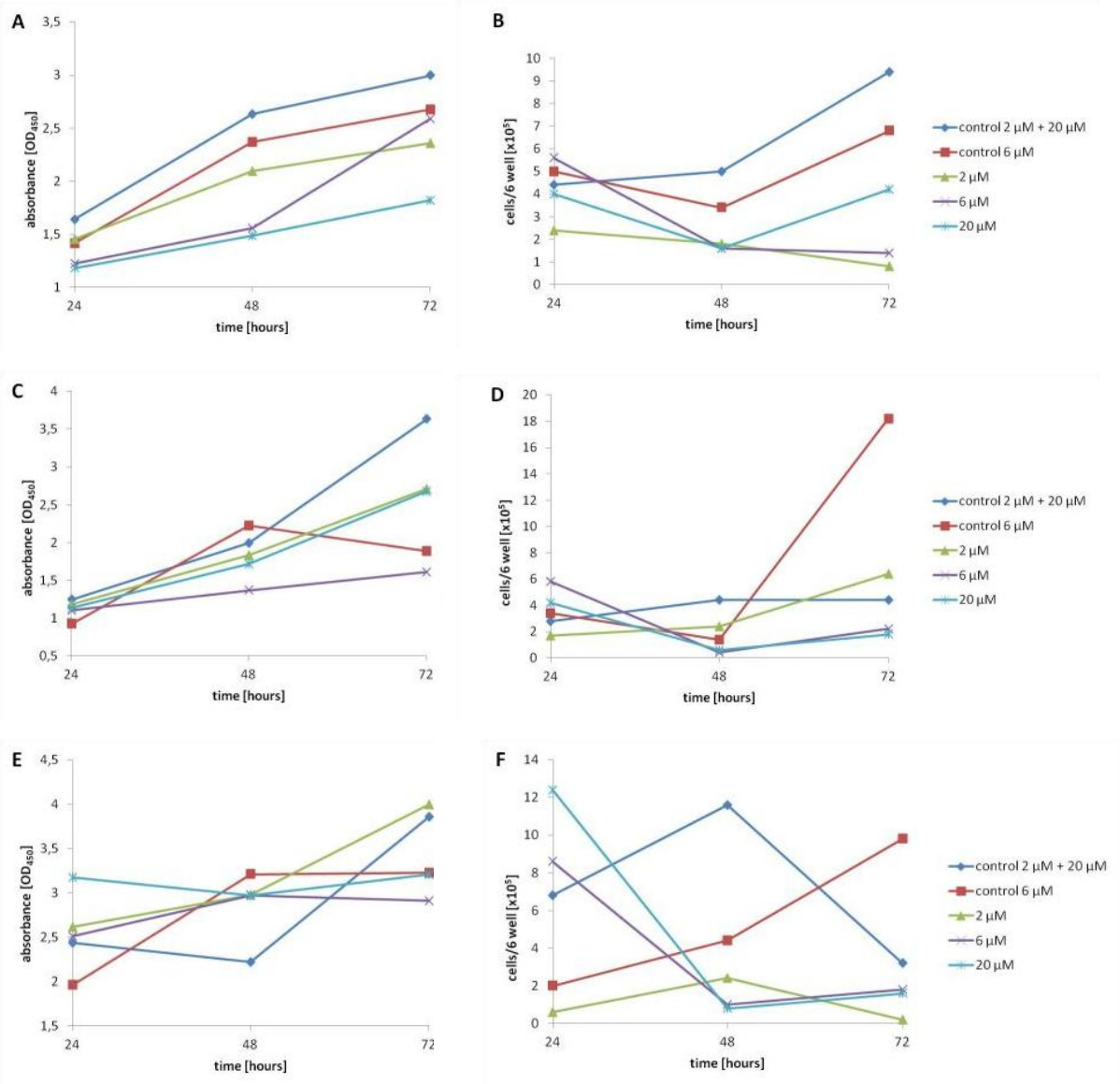
Fig. 33 EZ4U assay (left panels) and cell count (right panels) of FLO-1 (A, B), SK-GT-4 (C, D), and TE-1 cells (E, F) after 24, 48, and 72 hours of PF-3644022 hydrate treatment.

3.6 Effect of MK2 Gene Silencing on Proliferation and Migration of Esophageal Cancer Cells

3.6.1 Optimization of Cell Electroporation for Transient MK2 Silencing

Efficacy of MK2 gene silencing by transient transfection with siRNA was determined with qRT-PCR using ACTB as a reference gene (Fig. 35). MK2 gene expression levels were normalized to the highest value (set to 100%) of the sample treated with control siRNA. Three distinct siRNA oligonucleotides were tested at a concentration of 1 µM (20 µl per electroporation).

FLO-1 cells showed the highest level of MK2 silencing, regardless of the used siRNA, when compared to SK-GT-4 and TE-1. The combination of all three siRNAs led to the highest silencing efficacy in all cell lines. Relative expression data normalized to ACTB are listed in Tab. 5 and indicate that FLO-1 cells have higher endogenous MK2 mRNA levels than SK-GT-4 and TE-1 cells.
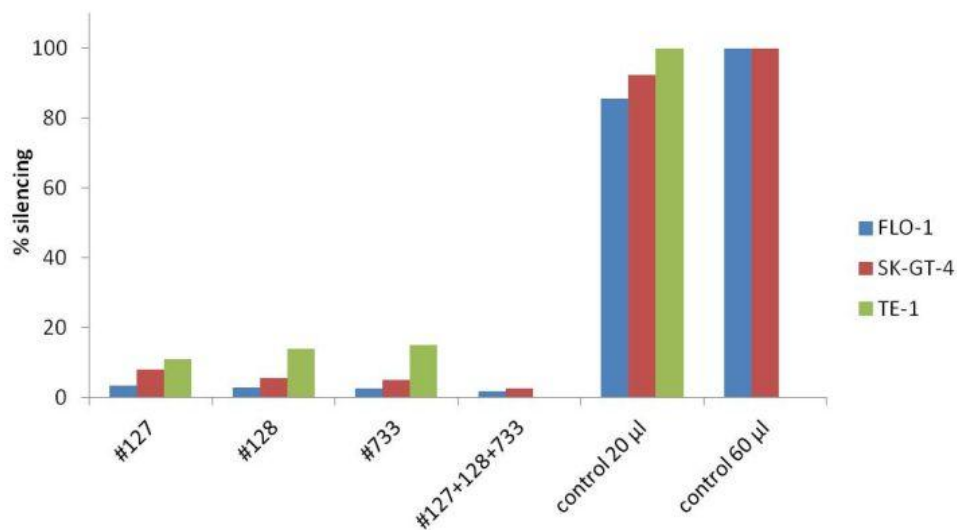

Fig. 34 MK2 silencing efficacy as determined via qRT-PCR and illustrated by bar chart. Esophageal cancer cell lines were transfected with 20 µl MK2 siRNAs #127, #128, and #733 or with negative control siRNA. Values of MK2 mRNA expression were normalized to ACTB and the highest value of MK2 mRNA in control samples was set to 100%.

sample	relative MK2 expression
FLO-1 siRNA #127	9,0
FLO-1 siRNA #128	8,0
FLO-1 siRNA #733	7,2
FLO-1 siRNA #127+128+733	5,1
FLO-1 siRNA control 20 µg	227,6
FLO-1 siRNA control 60 µg	265,7
SK-GT-4 siRNA #127	9,1
SK-GT-4 siRNA #128	6,2
SK-GT-4 siRNA #733	5,7
SK-GT-4 siRNA #127+128+733	2,9
SK-GT-4 siRNA control 20 µg	105,0
SK-GT-4 siRNA control 60 µg	113,5
TE-1 siRNA #127	11,1
TE-1 siRNA #128	13,9
TE-1 siRNA #733	15,2
TE-1 siRNA control 20 µg	98,8

Tab. 5 MK2 silencing efficacy as determined via qRT-PCR. MK2 expression levels were normalized to ACTB values for each cell line (but were not expressed in % of control) to allow for a comparison of MK2 transcript levels between cell lines.

3.6.2 Effect of MK2 Silencing on Proliferation of Esophageal Cancer Cells

After siRNA transfection, the cell suspension was seeded into three 6-wells. Medium was changed after 9 hours. After 24, 48, and 72 hours pictures were captured, an EZ4U assay measuring absorbance at 450 nm was performed, and cell count was determined.

FLO-1 cells (Fig. 35) showed a moderate cell growth rate and did not reach confluence within 72 hours. Growth of SK-GT-4 cells (Fig. 36) was considerably faster, with confluent cultures within 24 hours. TE-1 cells (Fig. 37) exhibited a very fast cell growth in all cases, which led to an almost confluent cell layer already after 24 hours. None of the transfected MK2 siRNAs led to substantial changes in the growth pattern of the esophageal cancer cell lines.
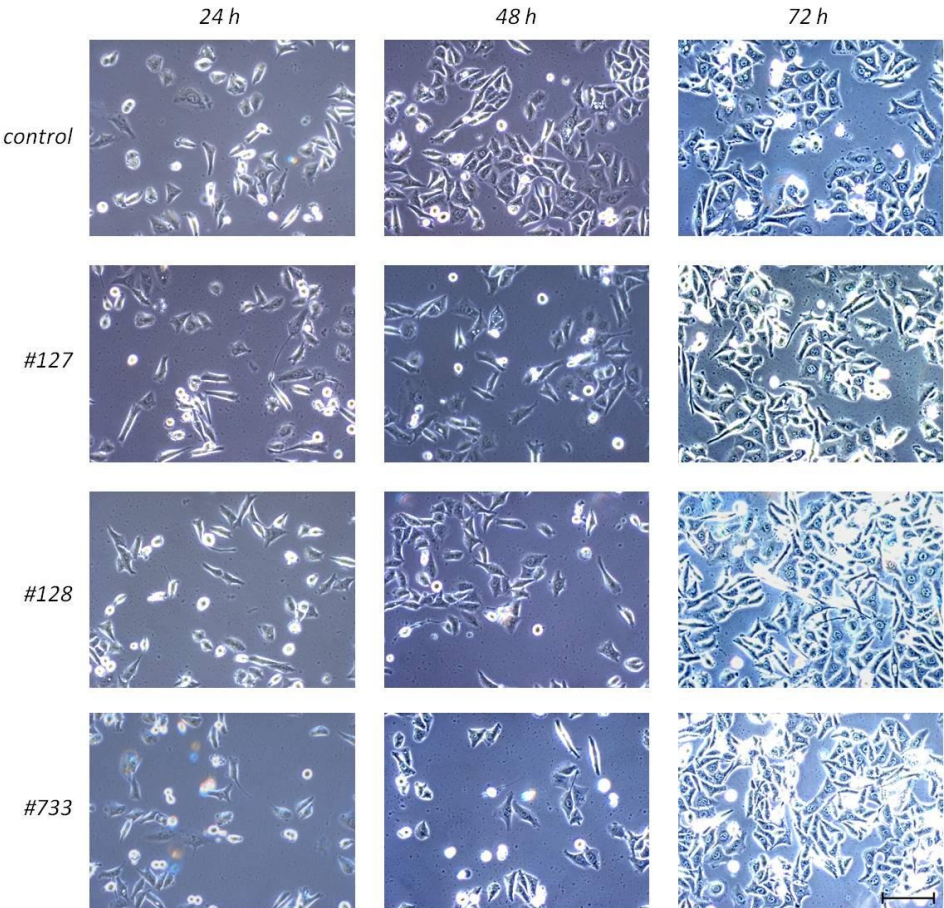
Fig. 35 Cell growth of FLO-1 cells 24, 48, and 72 hours after transfection with MK2 siRNAs #127, #128, and #733 or with negative control siRNA. Scale bars 100 µm, valid for all images.
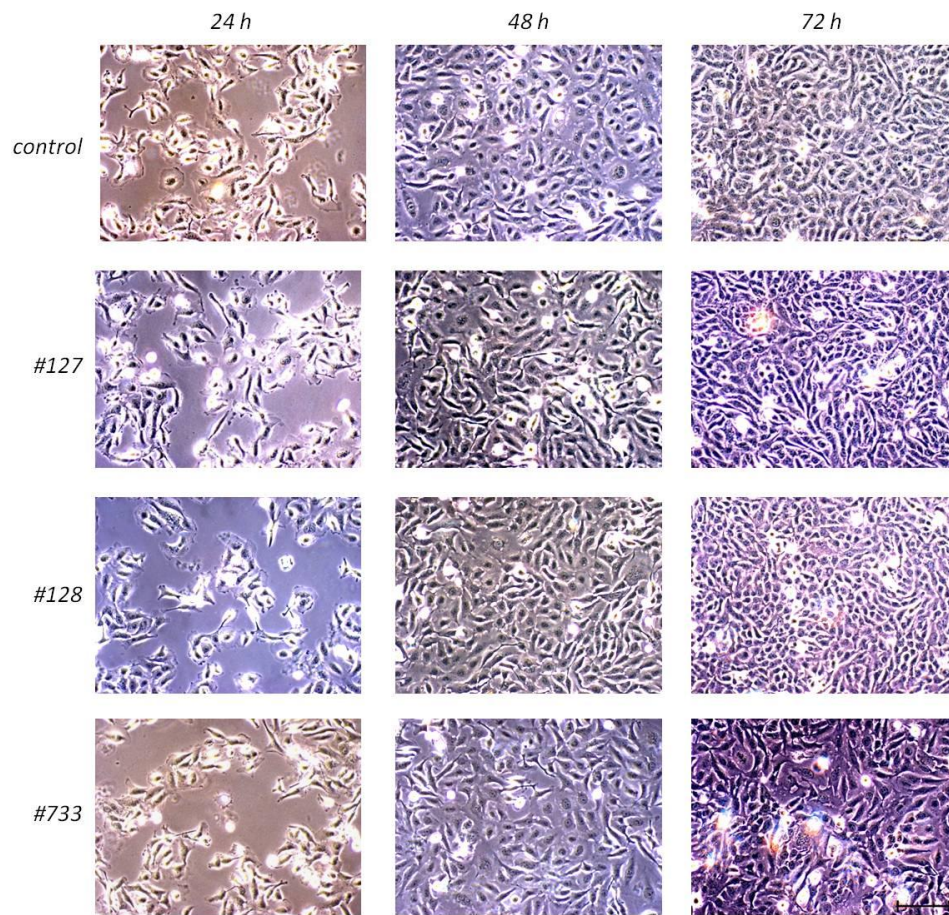
Fig. 36 Cell growth of SK-GT-4 cells 24, 48, and 72 hours after transfection with MK2 siRNAs #127, #128, and #733 or with negative control siRNA. Scale bars 100 μm, valid for all images.
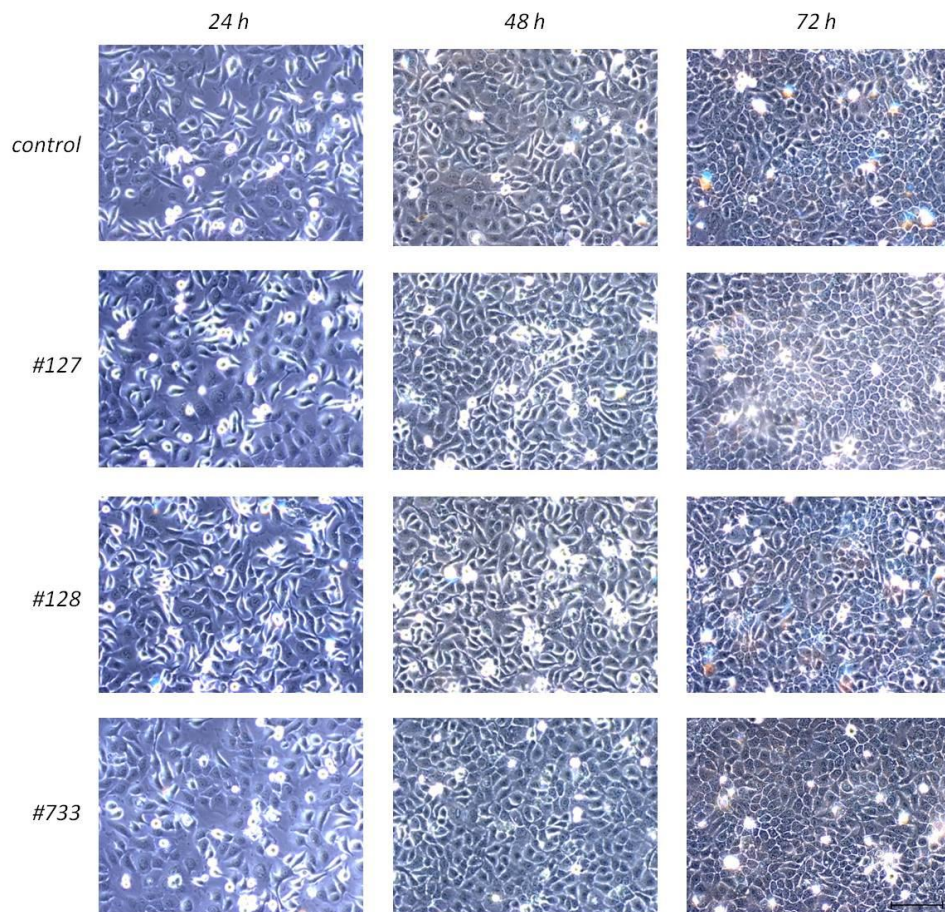
Fig. 37 Cell growth of TE-1 cells 24, 48, and 72 hours after transfection with MK2 siRNAs #127, #128, and #733 or with negative control siRNA. Scale bars 100 μm, valid for all images.

When measuring metabolic activity by EZ4U assay (Fig. 38A, C, E), all cell lines showed moderate increases from 24 to 48 hours, but a decrease by 72 hours which may be due to a reduction in metabolism after reaching confluence and after nutrient (medium) consumption. There was no consistent effect of MK2 silencing observed in EZ4U assays. A moderate reduction in cell growth and metabolism was recorded for SK-GT-4 cells when transfected with #733 siRNA.

Similarly, cell growth of SK-GT-4 cells as determined by cell count was slightly decreased by transfection with #733 siRNA (Fig. 38D). FLO-1 cells showed no substantial effect of MK2 silencing on cell count (Fig. 38B), whereas for TE-1 cells all three MK2 siRNAs resulted in a somewhat reduced cell growth based on cell counting (Fig. 38F).
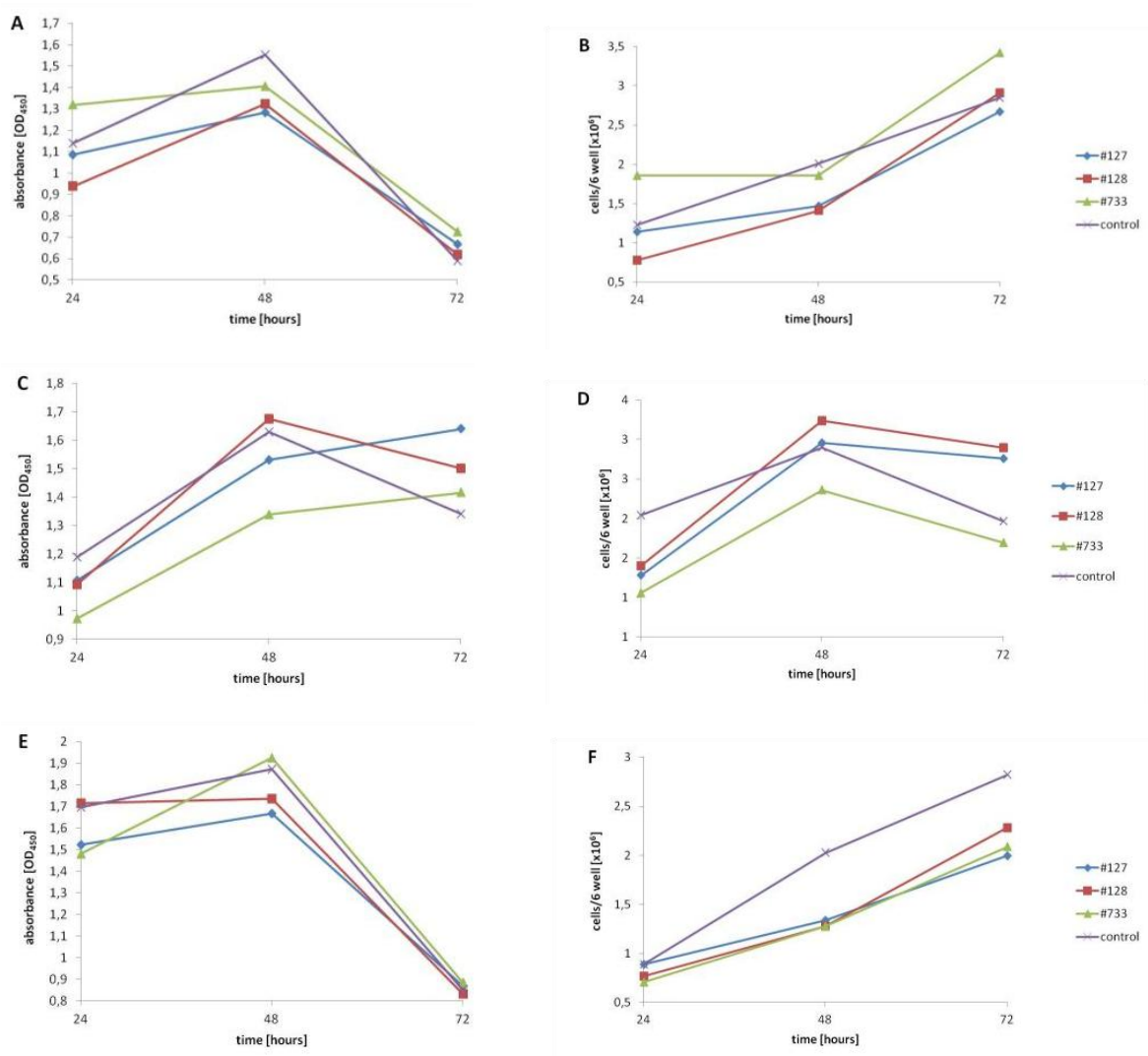
Fig. 38 EZ4U assay (left panels) and cell count (right panels) of FLO-1 (A, B), SK-GT-4 (C, D), and TE-1 cells (E, F) after transfection with three distinct MK2 siRNAs or with negative control siRNA.

3.6.3 Effect of MK2 Silencing on Migration of Esophageal Cancer Cells

To investigate the effect of different MK2 siRNAs on the migratory behavior of esophageal cancer cells, a scratch-wound assay was performed as described in Methods 2.4.1. Fig. 39-41 show cell migration after transfection of FLO-1 cells with siRNA #127, #128, or #733 on migration. No substantial effect of MK2 gene silencing on the migration of FLO-1 cells was detectable. Analogous experiments were conducted for SK-GT-4 and TE-1 cells with comparable results (data not shown).
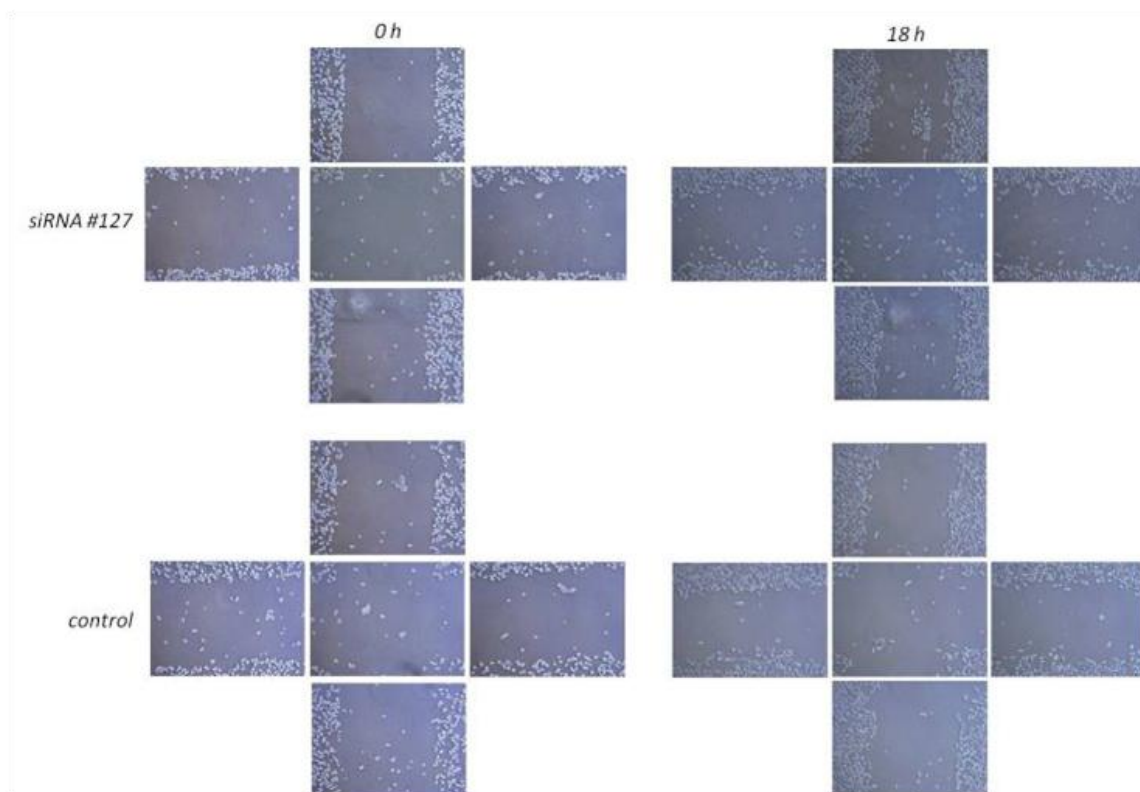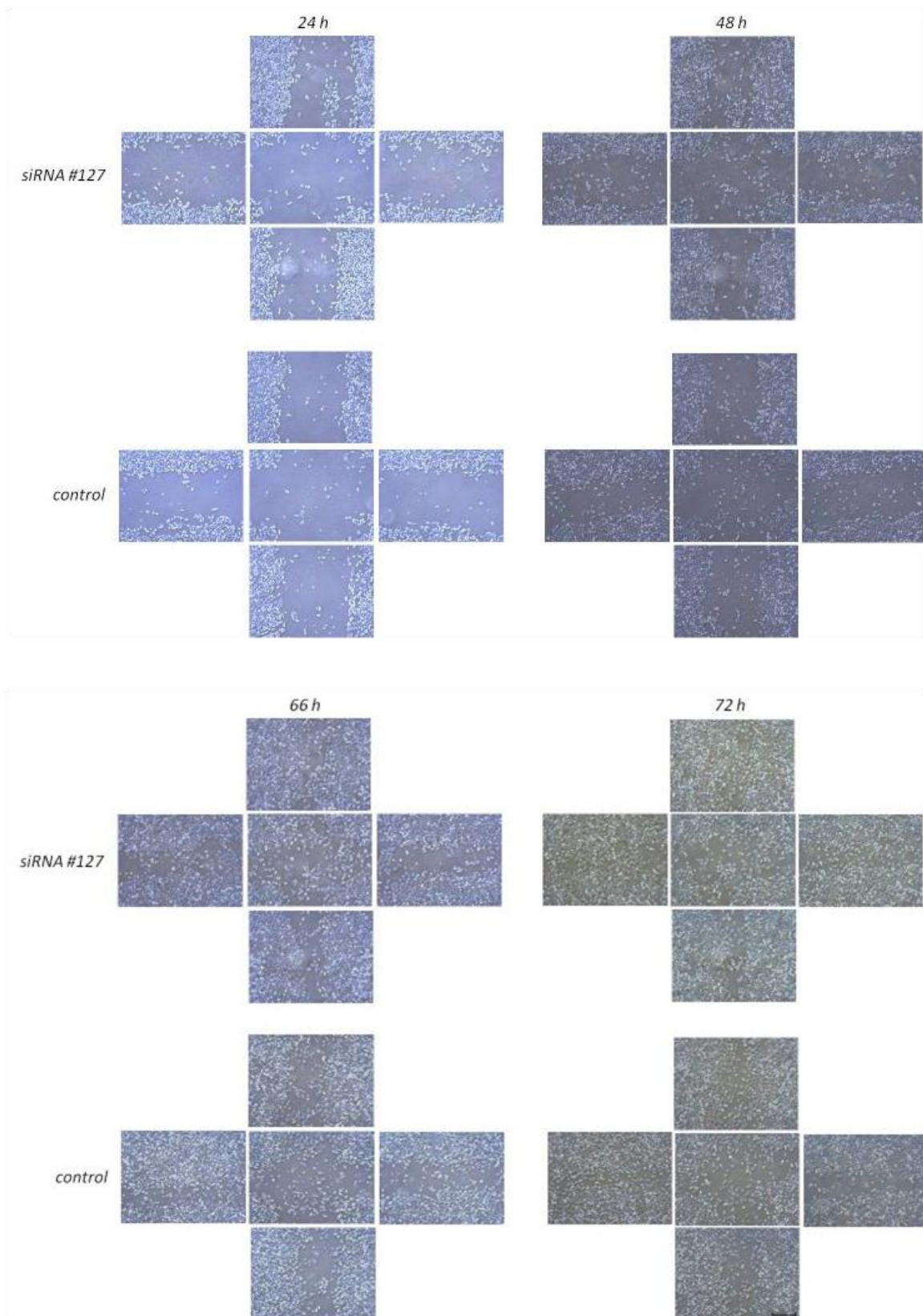
Fig. 39 Migration of FLO-1 cells after transfection with siRNA #127. Scale bar 100 µM, valid for all images of this figure.
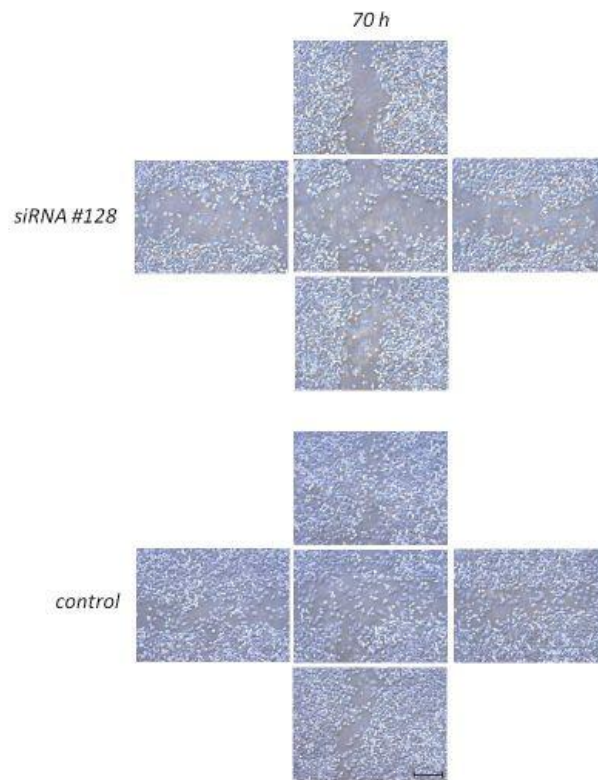
Fig. 40 Migration of FLO-1 cells after transfection with siRNA #128. Scale bar 100 µM, valid for all images of this figure.

0 h   24 h

siRNA #733

control

30 h   48 h

siRNA #733

control

79
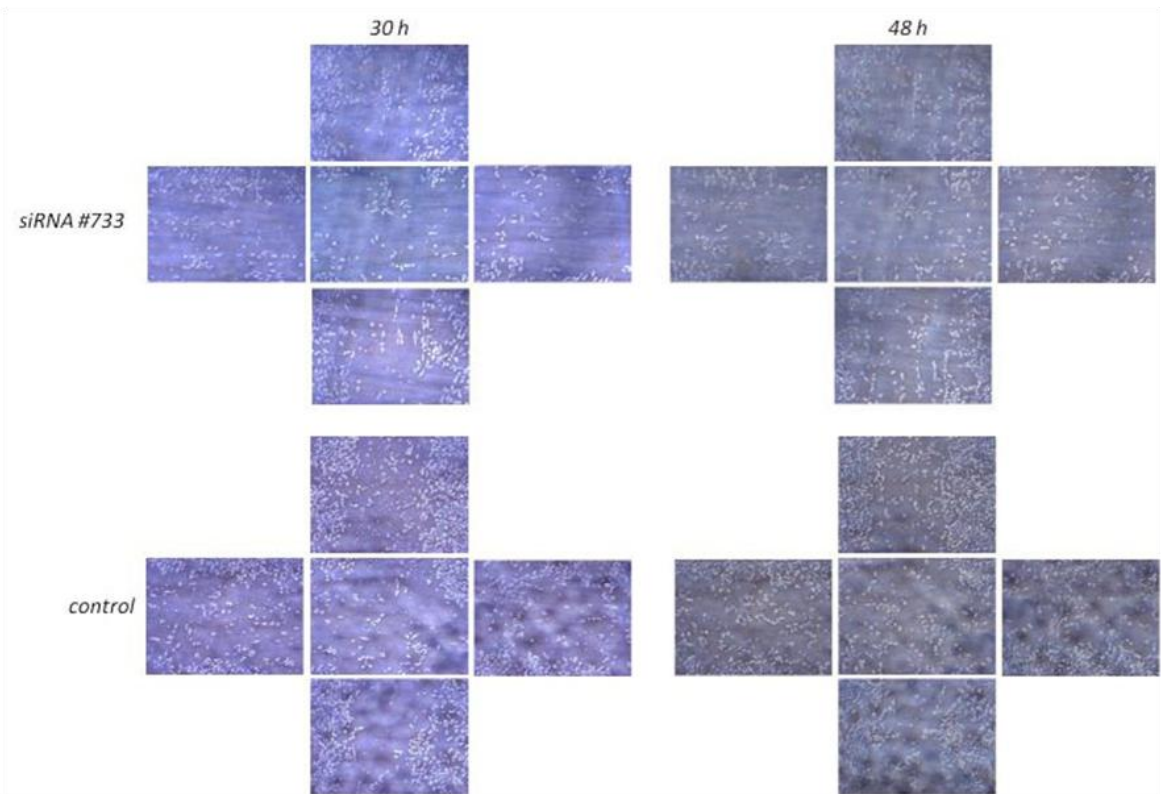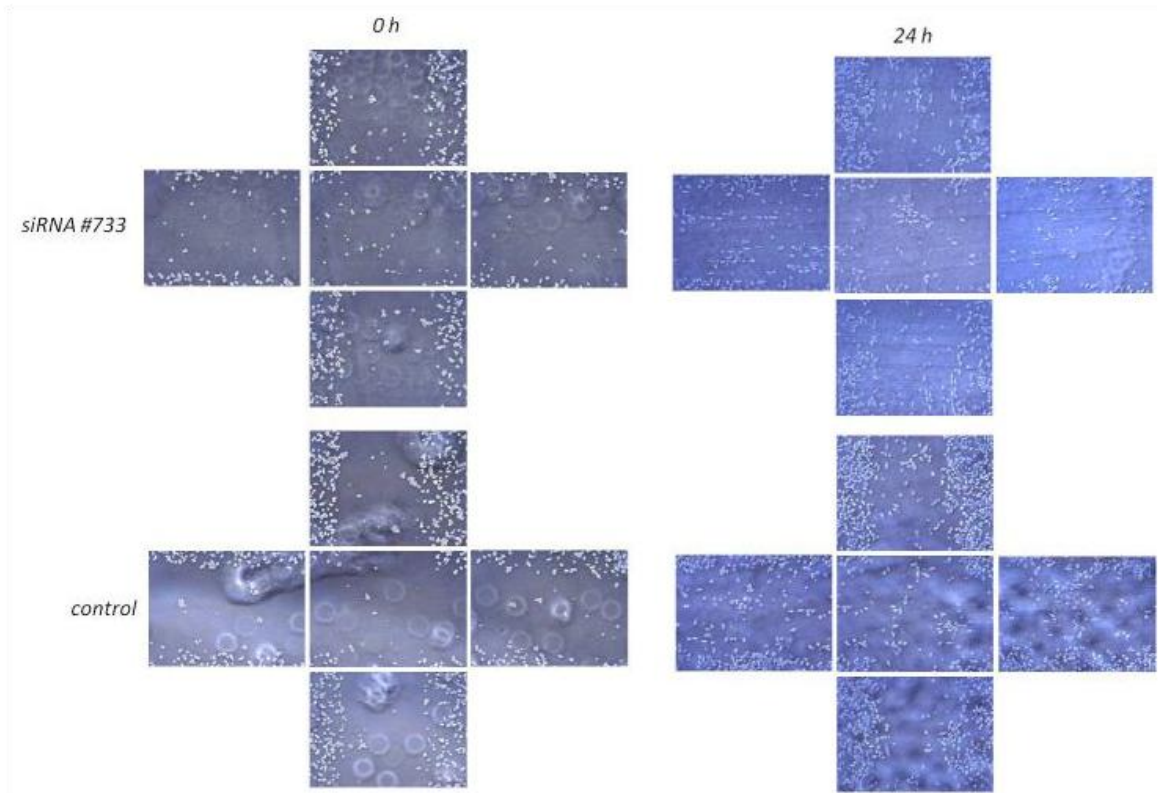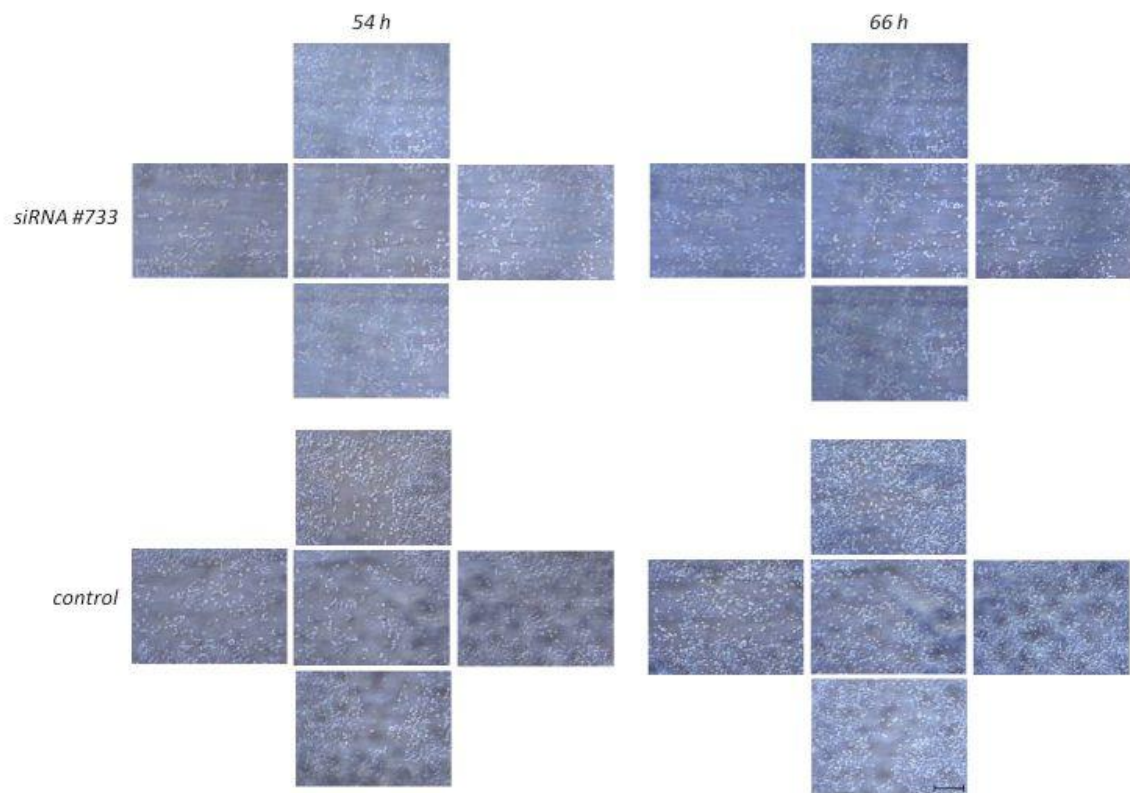
Fig. 41 Migration of FLO-1 cells after transfection with siRNA #733. Scale bar 100 µM, valid for all images of this figure.

3.7 Overexpression of MK2 in Esophageal Cancer Cells

3.7.1 Optimization of Cell Electroporation for Transient MK2 Overexpression

Before transient MK2 overexpression was repeatedly applied, the transfection conditions for the esophageal cancer cell lines had to be optimized. Therefore, cells were transfected with pEGFP-C3 plasmid, while control cells were mock-transfected with aqua dest. to gain a negative control. The electroporation was conducted as described in Methods 2.6.2 and the cells were seeded in 6-wells. The following conditions were tested: 1000 µF/200 V, 1000 µF/250 V, 1200 µF/200 V, and 1200 µF/250 V. After 24, 48, and 72 hours cells were prepared for flow cytometric analysis according to Methods 2.16. For determination of the best electroporation condition, the percentage of EGFP positive cells and the mean fluorescence intensity of EGFP positive cells were compared.

After 24 hours FLO-1 cells (Fig. 42A) showed an EGFP uptake of about 75 to 90% which decreased to 50 to 80% on day 3. Highest EGFP expression levels (mean fluorescence of EGFP positive cells) were seen on the first day (Fig. 42B) and dropped rapidly after 48 and 72 hours. The EGFP expression in SK-GT-4 cells (Fig. 42C and D) was found to be more stable. The percentage of EGFP positive SK-GT-4 cells ranged between 70-90% over the entire observation period, and EGFP expression levels (mean fluorescence) dropped only moderately after 48 and 72 hours. TE-1 cells (Fig. 42E) similarly showed a consistent transfection efficiency of 70-90% within 3 days after electroporation, but EGFP expression levels dropped to about half from 24 to 48 hours and remained at this level after 72 hours (Fig. 42F).
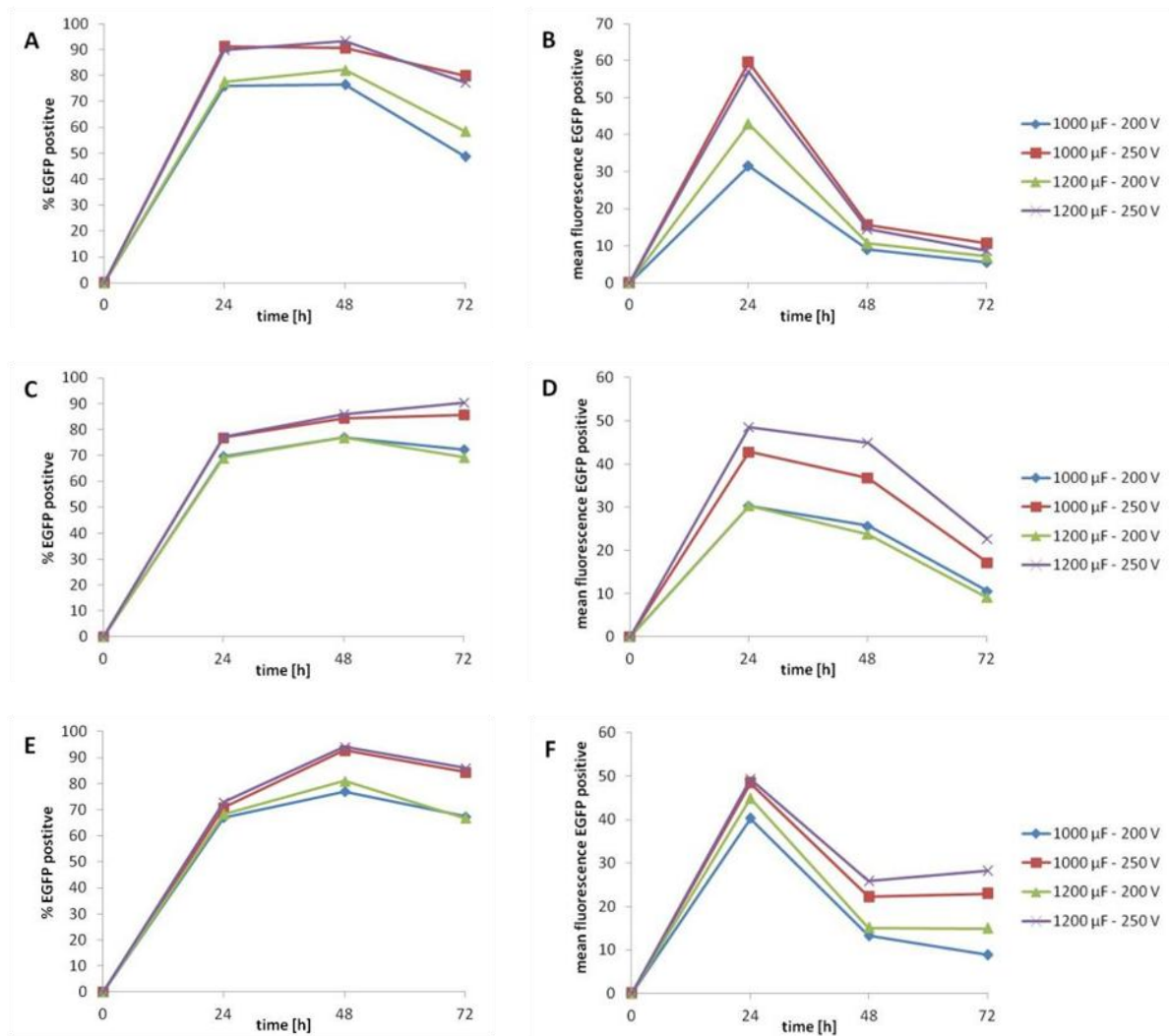
Fig. 42 Percentage of EGFP positive cells (left panels) and mean fluorescence intensity of EGFP positive cells (right panels) in FLO-1 (A and B), SK-GT-4 (C and D), and TE-1 cells (E and F) at 24, 48 and 72 hours after electroporation with pEGFP-C3 expression plasmid.

When comparing the electroporation conditions, exposure to 250 V as opposed to 200 V consistently gave higher transfection values, while varying the capacity between 1000 and 1200 µF had no major impact. However, exposure of cells to 250 V resulted in considerably more cell death (loss) than electroporation with 200 V (data not shown).

These results led to the conclusion that for optimized electroporation conditions a compromise had to be made between high plasmid uptake which should persist as long as possible and cell death through transfection which wanted to be kept as low as possible. Therefore, the conditions used in the subsequent experiments were set to 1000 µF and 200 V.

After optimization of transfection conditions with an EGFP expression plasmid, the efficacy of MK2 overexpression was tested and determined by qRT-PCR, where the results were normalized to ACTB. MK2 transcript levels of each cell line were further normalized to the values of the corresponding EFpLink control sample which was set to 1. As presented in Fig. 43, the increase in MK2 mRNA expression at 18 hours after transfection was highest in MK2 transfected FLO-1 cells (765 fold). SK-GT-4 cells showed a 338 fold higher expression when transfected with MK2 and TE-1 cells displayed a more than 290 fold higher MK2 mRNA expression when compared to control transfected cells. Data of relative MK2 expression are listed in Tab. 6 below.
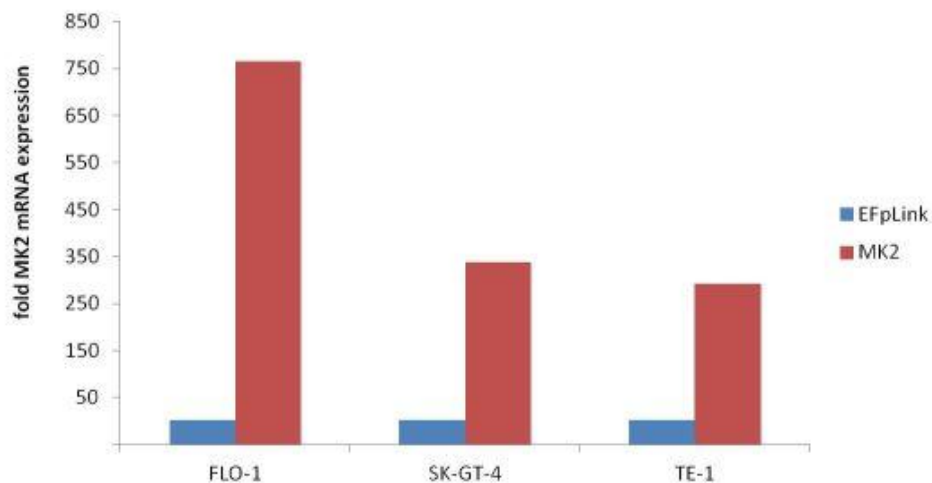
Fig. 43 Efficacy of MK2 overexpression (as analyzed by qRT-PCR) after transient transfection of esophageal cancer cell lines with MK2 expression plasmid. Ordinate shows the level of MK2 overexpression compared to the respective control (transfection with EFpLink vector).

sample	relative MK2 expression
FLO-1 EFp 18 h	522,3
FLO-1 MK2 18 h	399507,4
SK-GT-4 EFp 18 h	241,6
SK-GT-4 MK2 18 h	81626,6
TE-1 EFp18 h	228,3
TE-1 MK2 18 h	66609,6

Tab. 6 MK2 mRNA expression levels as detected by qRT-PCR and normalized to ACTB levels for each cell line.

3.7.2 Effect of MK2 Overexpression on Proliferation of Esophageal Cancer Cells

Electroporation was performed according to Methods 2.6.2 and optimized as described in Results 3.7.1. EFpLink was used as a control plasmid. After electroporation the cells were seeded into two 6-wells. After 18 and 42 hours pictures were taken, an EZ4U assay was implemented, and cell count was determined.

As depicted in Fig. 44 MK2 transfected FLO-1 cells showed a marginally lower cell density at 18 and 42 hours when compared to control conditions. SK-GT-4 cells presented with similar cell densities for control as well as MK2 transfected cells at both time points. TE-1 cells showed a slightly reduced cell number at 18 hours after MK2 transfection whereas at 42 hours the cell density was comparable to the control.
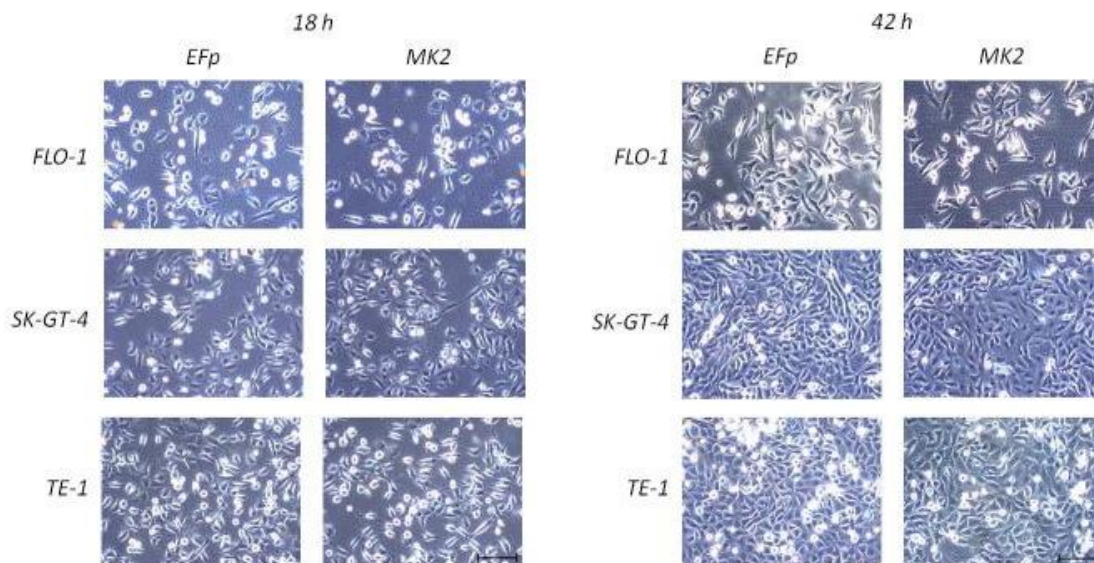
Fig. 44 Microscopic images of cells transfected with EFpLink or MK2 as taken 18 and 42 hours after electroporation. Scale bars 100 µm, valid for all shown pictures.

Evaluation of cell metabolism and growth after MK2 transfection using the EZ4U assay (Fig. 45A) revealed that TE-1 cells showed the highest absorption values. Here, MK2 transfected cells displayed a decrease after 42 hours, whereas the absorbance of control electroporated cells increased. SK-GT-4 cells exhibited similar metabolic values at 18 hours after transfection, whereas MK2 transfection led to a slightly reduced metabolic activity compared to the control at 42 hours. MK2 transfected FLO-1 cells showed the lowest value which was clearly reduced as compared to control transfected FLO-1 cells at both time points.

The findings of the lowest metabolic levels for FLO-1 cells in the EZ4U assay were also reflected in the cell count data depicted in Fig. 45B where FLO-1 again showed the lowest values. In contrast, SK-GT-4 control cells presented the highest cell count after 42 hours, while MK2 transfected SK-GT-4 cells showed a clearly reduced cell concentration. Similarly, TE-1 cells transfected with MK2 expression plasmid had lower cell counts than control treated TE-1 cells at both observation time points.
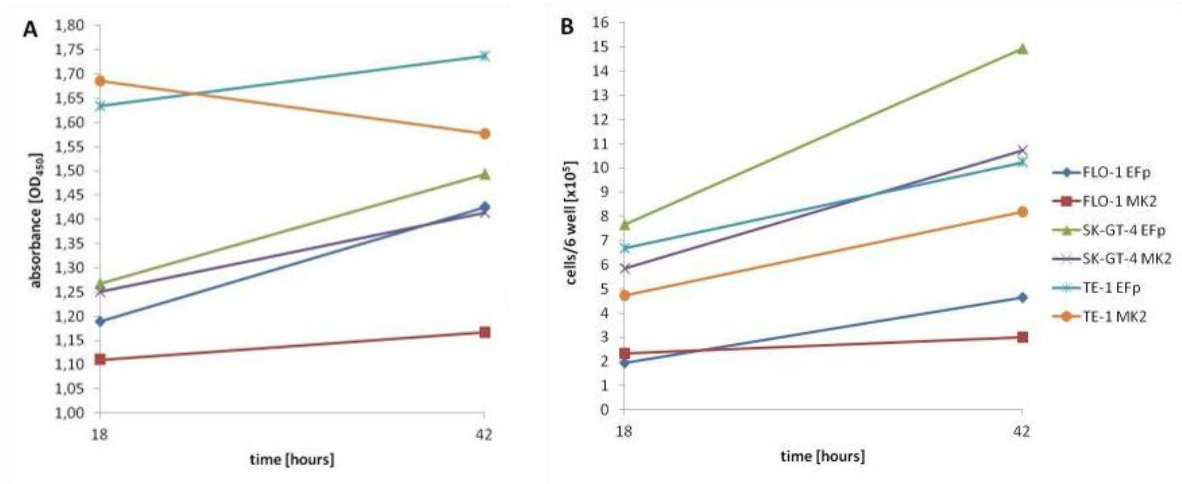
Fig. 45 EZ4U assay (A) and cell count (B) results for the cell lines FLO-1, SK-GT-4, and TE-1 at 18 and 42 hours after transfection with MK2 expression plasmid or empty control vector EFpLink.

3.7.3 Effect of MK2 Overexpression on Migration of Esophageal Cancer Cells

To investigate the effect of MK2 overexpression on the migratory behavior of MK2 transfected esophageal cancer cells, a scratch-wound assay was performed as described in Methods 2.4.1. To monitor the closure of the scratch, microscopic images were taken directly after scratching and 17, 24, and 42 hours later.

Fig. 46 visualizes that wound closure of MK2 transfected FLO-1 cells proceeded more slowly as compared to the control transfected cells. However, differences were small and under both conditions the scratch was not closed after 42 hours.
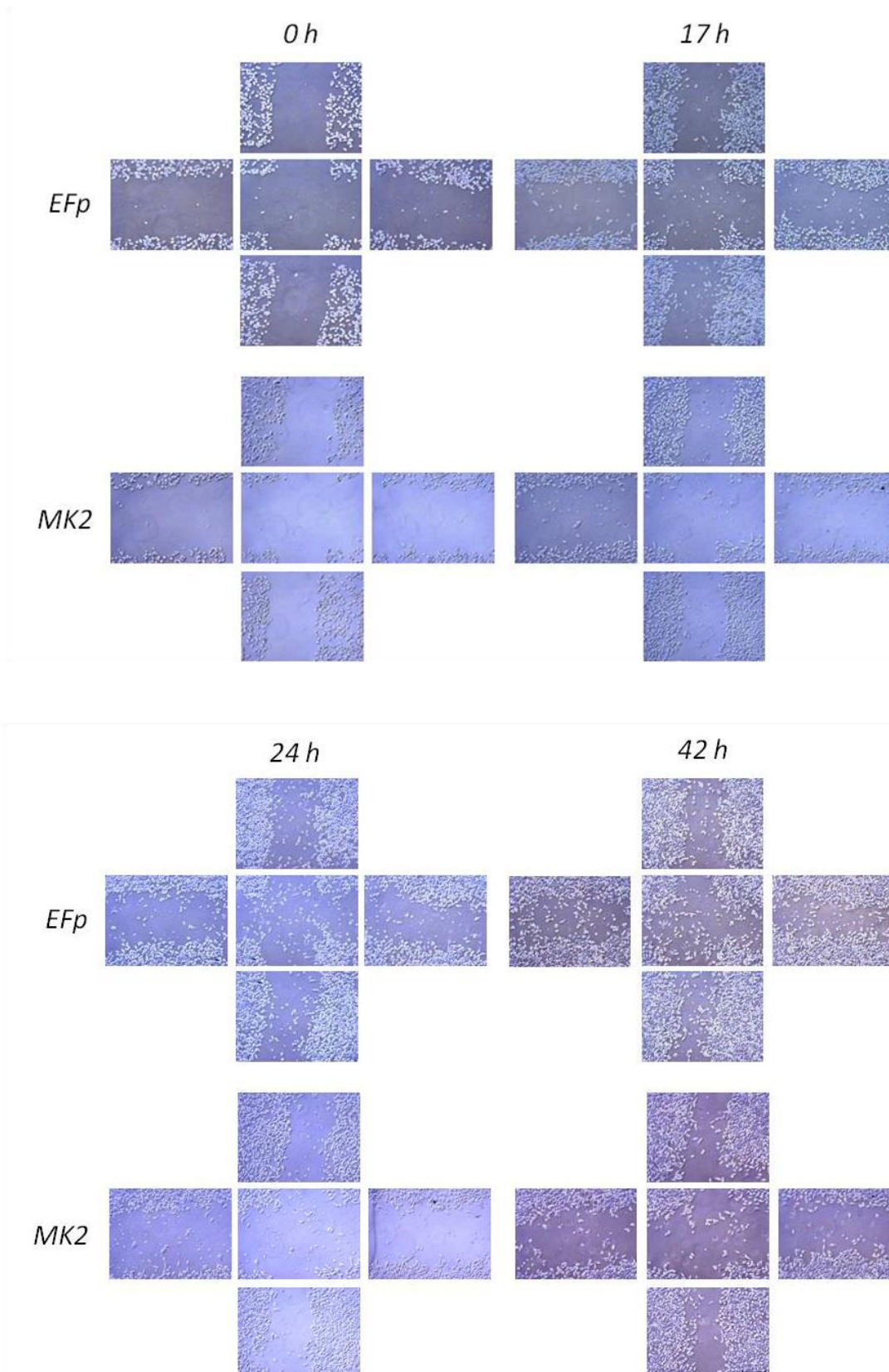
Fig. 46 Microscopic images of MK2 and EFpLink transfected FLO-1 cells at the indicated time points after introducing the scratch-wound. Scale bar 100 μm, valid for all images.

SK-GT-4 control cells were migrated and grown to confluence within 17 hours, whereas the MK2 transfected cells did not completely close the scratch (Fig. 47). However, it should be noted that the initial scratch (cell free area) was larger in case of cells transfected with the MK2 plasmid.
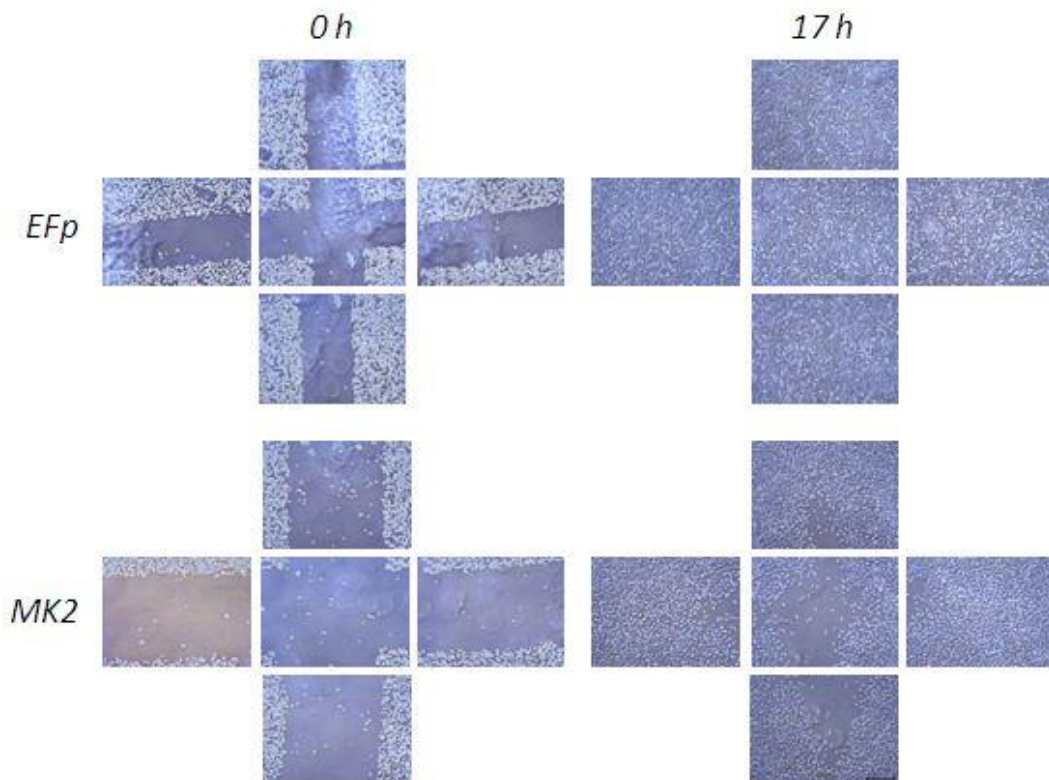
Fig. 47 Microscopic images of MK2 and EFpLink transfected SK-GT-4 cells at the indicated time points after introducing the scratch-wound. Scale bar 100 μm, valid for all pictures shown above.

The monitoring of scratch closure was difficult in TE-1 cells due to the high amount of unattached (floating) cells (Fig. 48). In this case, a small cell free area was still observable in MK2 transfected cells after 42 hours, whereas the control cells had essentially closed the gap.

In summary, the effects of MK2 overexpression on the migratory behavior of esophageal cancer cells were minor, showing only a slight reduction after transfection with MK2 expression plasmid. Therefore, the differences in gap closure were not further quantified by an imaging software.
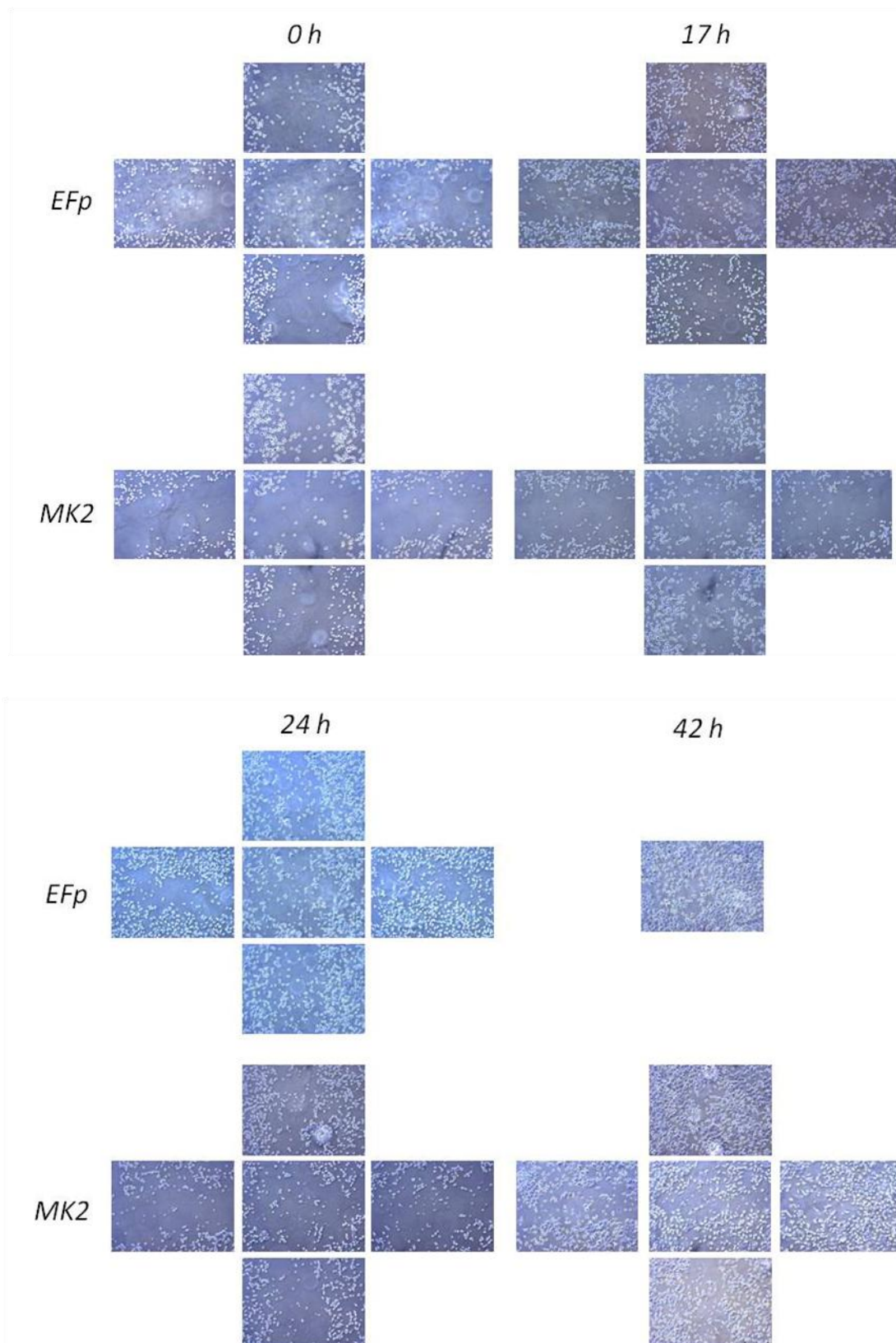
Fig. 48 Microscopic images of MK2 and EFpLink transfected TE-1 cells at the indicated time points after introducing the scratch-wound. Scale bar 100 μm, valid for all images.

4   DISCUSSION

The aim of this project was to investigate the role of MK2 in proliferation, survival and migration of gastroesophageal cancer cells. Therefore, three main research aims were defined. The first task was to characterize the expression and distribution of MK2 as well as phospho-MK2 in the chosen esophageal cancer cell lines. This was achieved by immunofluorescence staining and examination by confocal laser scanning microscopy. Also, immunoblotting was used to detect the levels of MK2 and phospho-MK2. The second aim addressed the question whether commercially available MK2 inhibitors or gene silencing by specific siRNAs would alter cell proliferation and migration. Therefore, the pharmacological inhibitors Hsp25 kinase inhibitor and PF-3644022 hydrate were added at different concentrations to esophageal carcinoma cultures followed by image acquisition, EZ4U cell metabolism assay, and determination of cell count. The same analytical procedure was performed in experiments of MK2 gene silencing, where 3 different siRNAs were tested. To investigate migration of esophageal cancer cells under the influence of MK2 siRNAs, a scratch-wound assay was performed. With respect to the third aim, we addressed the question if MK2 overexpression has an effect on the migratory and proliferative behavior of gastroesophageal cancer cells. Again microscopic images were taken, cell proliferation and metabolism were examined with the EZ4U assay, and the number of cells was determined. In addition, migration was investigated using the scratch-wound assay.

In their studies Birner et al. showed that MK2 was highly expressed in GISTs and an upregulation was associated with poor prognosis of cancer patients [15]. A comparable observation was made for esophageal cancer (unpublished data). Hence, it was planned to reproduce these findings using different antibodies for MK2 and phospho-MK2. After careful optimization of antigen retrieval and immunohistochemical procedures, positive staining was obtained for 3 of the 4 tested antibodies. However, in contrast to the originally applied MK2 antibody ab63574 where strong cytoplasmic staining of esophageal cancer cells was observed, the Thr^{334}-phosphorylation specific antibodies #3041 and #3007 only detected p-MK2 in the normal esophageal squamous epithelial tissue

The MK2 antibody #3042 did not give positive staining in any of the tested conditions for immunohistochemistry. It has to be pointed out that upon personal inquiry the manufacturing company stated that this antibody had been tested in immunohistochemistry which had led to unsatisfying results and which is why they did not recommend it for this application.

In conclusion, the results of immunohistochemical staining of esophageal cancer sections gave contradictory results. The MK2 antibody ab63574 would be expected to detect both, non-phosphorylated and phosphorylated MK2 protein. However, the normal esophageal epithelium which was prominently stained with the two p-MK2 antibodies did not present positive for MK2 antibody ab63574. In contrast, the cancer cells recognized by MK2 antibody ab63574 were negative in IHC staining with p-MK2 antibodies. While this may indicate that cytosolic MK2 detected in the esophageal cancer cells is not phosphorylated, we also have to consider the possibility that the MK2 antibody ab63574 cross-reacts unspecifically with another protein.

Esophageal cancer cell lines were then selected for in vitro experiments based on their MK2 expression profiles as well as their growth rates. Thus, all following experiments were performed with the cell lines FLO-1, SK-GT-4, and TE-1. By immunofluorescence staining and confocal microscopy it was shown that the MK2 antibody ab63574 led to cytoplasmic staining, whereas the alternative MK2 antibody #3042 displayed nuclear staining of all esophageal cancer cell lines. With respect to phosphorylated (activated) MK2, the p-MK2 antibodies #3041 and #3007 led to mainly nuclear staining. Similarly, phosphorylated p38 was found to be predominantly nuclear in the tested cell lines. Thus, with exception of the MK2 antibody ab63574, all other MK2 and p-MK2 antibodies document that MK2 is mainly found in the nucleus of esophageal cancer cells. It is (at least in part) phosphorylated and co-localizes with phosphorylated p38 in the nucleus. These findings were highly unexpected. In the literature it is stated that MK2 is present in its inactive and unphosphorylated form in the nucleus of resting cells and a stimulation by activated p38 leads to phosphorylation and export of the phosphorylated p38/MK2 complex into the cytosol [9].

Based on these results, next Jurkat cells were stained for MK2, phospho-MK2 and phospho-p38 for control, as these cells should reportedly contain the phosphorylated p38/MK2 complex in the cytosol [6].

We could confirm that Jurkat cells had a high amount of cytoplasmic MK2, phospho-MK2, and phospho-p38 which was detectable with all tested antibodies. For the phospho-MK2 antibody #3007 it was shown that p-MK2 was additionally present in the nuclei of Jurkat cells. TNFα stimulation of Jurkat cells did not substantially alter this expression pattern (as Jurkat cells seemed to have constitutively active MK2), but increased the level of detectable nuclear MK2 and p-MK2. Thus, in line with the literature, phosphorylated p38/MK2 complexes were predominantly found in the cytosol of control Jurkat cells, indicating that the applied antibodies were functional and our contrasting findings in esophageal cancer cells were a cell-type specific phenomenon. In conclusion, it could be the case that MK2 in esophageal cancer cells is activated and regulated in a different way than is the case for leukocytes like Jurkat cells.

With respect to the fact that only the MK2 antibody ab63574 stains the cytosol of esophageal cancer cells, whereas all other tested antibodies detect a nuclear protein, a possible explanation could be that the applied antibodies might exhibit differential cross-reactivity with MK3 or other family members of the calcium/calmodulin-dependent Ser/Thr protein kinases which might be present in esophageal cancer cells. According to the datasheet cross-reactivity with MK3 and MK5 can be excluded for the MK2 antibody #3042. However, for the p-MK2 #3041 it is quoted that a cross-reaction with the MK3 phosphorylation site at Thr^{313} might be observed. Alternative explanations for the controversial results are that MK2 possibly owns a particular modification or that another isoform of MK2 is present in esophageal cancer cells which is particularly recognized by the MK2 antibody ab63574 but is not detected by the other antibodies. To clarify which antigen actually binds to the MK2 antibody ab63574, immunoprecipitation and mass spectrometry could be further approaches.

The detection of MK2 and phospho-MK2 by immunoblotting was very challenging. Due to heavy background (artifact bands by the secondary antibody which could not be improved by changing the secondary reagent) only weak signals at 46 kDa were observed which corresponded to the predicted size of MK2. SDS lysis buffer (instead of RIPA buffer) combined with heat and sonication gave a higher protein yield. In addition to this modification, membrane activation and blocking technique were refined.

An important factor was that the membrane should never dry, neither in the process of activation by methanol nor during the blocking procedure which was always performed overnight at a shaker and 4°C. Membranes had to be consistently moistened and should not touch or "overlap". Furthermore, the incubation with antibodies was always performed with a sufficient amount of antibody solution to guarantee complete immersion of the membrane.

Using the optimized cell extract and immunoblotting conditions, double bands at 46 kDa could be detected with MK2 antibody #3042. Immunoblotting with the phospho-MK2 antibody #3007 led to a very weak single band at 46 kDa.

The next step was to use MK2 overexpression to solve the problem of low detection by increasing the amount of MK2 expressed in esophageal cancer cells. To further address the time course of MK2 overexpression, the MK2 protein was analyzed at several time points (12, 24, and 48 hours) after transient transfection. Surprisingly, despite a high level of MK2 mRNA detected in transfected cancer cells, the level of MK2 protein (46 kDa bands on immunoblots) was only weakly and transiently increased. Similarly, overexpression of MK2 protein was not readily detectable by confocal microscopy (data not shown). This observation points to a possible negative regulation of MK2 protein translation or stability upon MK2 overexpression in esophageal cancer cells which is in contrast to the observed endogenous protein.

To investigate the functional role of MK2 in esophageal cancer cells, the effect of pharmacological MK2 inhibitors, two commercially available substances (Hsp25 kinase inhibitor and PF-3644022 hydrate) was tested on cell proliferation and migration. Experiments with the Hsp25 kinase inhibitor showed that SK-GT-4 and TE-1 cells were sensitive to the DMSO solvent. However, no specific effect of the Hsp25 kinase inhibitor was detected on the growth of esophageal cancer cell lines. These findings were also confirmed by EZ4U measurements of metabolic activity.

The second tested inhibitor was PF-3644022 hydrate. With respect to the microscopic images it can be said that this substance clearly inhibited cell growth in a dose dependent manner. These findings were supported by cell counts and partly by EZ4U assay. However, EZ4U values showed high variation which may be due to cell toxicity and cell debris interfering with the assay detection system.

Thus, the two MK2 inhibitors tested gave contradictory results. While Hsp25 kinase inhibitor had no impact on esophageal cancer cell growth, PF-3644022 hydrate showed a remarkable blocking effect. To determine whether PF-3644022 hydrate may exert an unspecific, off-target effect leading to cell toxicity or whether the observed inhibition of cell proliferation was indeed due to the reduction in MK2 activity, further experiments were conducted with selective MK2 gene silencing.

Silencing efficacy after siRNA transfection was confirmed by mRNA quantitation via qRT-PCR. The results led to the conclusion that every used siRNA resulted in more than 90% silencing and the combination of all three siRNAs gave rise to the highest silencing values. The effect of MK2 siRNAs on proliferation and migration of esophageal cancer cells was then investigated. To sum up the results of microscopic images, the EZ4U proliferation assays and cell count determination, it can be said that all tested siRNAs did not lead to substantial effects on cell proliferation and migration.

In comparison to the results obtained with the pharmacological MK2 inhibitors, we may thus conclude that the growth inhibitory impact observed for PF-3644022 hydrate is most likely due to unspecific, off-target effects unrelated to MK2. Furthermore, expression of MK2 in esophageal cancer cells does not seem to be required for their normal cell growth, despite the fact that MK2 has a documented functional role in the regulation of cell cycle [25]. Previous investigations have shown that MK2 may exert a protective effect in stress situations (such as cell starvation, hypoxia or exposure to DNA-damaging agents like chemotherapeutics) [27, 39]. In future experiments, it may thus be of interest to test the effect of MK2 silencing in esophageal cancer cells exposed to stress situations. In particular, the p53 mutant cell lines (FLO-1 and SK-GT-4) may show increased sensitivity to stressors in the absence of MK2.

As endogenous MK2 protein levels in the investigated esophageal cancer cell lines were moderate, we further attempted to characterize the functional role of MK2 in esophageal cancer cells by MK2 overexpression. Before starting with overexpression experiments, the transfection conditions had to be established.

After optimization of the electroporation protocol the setting of 1000 µF and 200 V was chosen for further transfections because it resulted in sufficient transfection rates (75%) coupled to a minimized cytotoxic effect due to the jolts of electricity during electroporation.

The efficacy of MK2 overexpression was confirmed by qRT-PCR. The analysis revealed a high MK2 mRNA level in all cell lines, where FLO-1 exhibited a remarkably high value with a 765 fold higher MK2 expression when compared to control transfected cells. SK-GT-4 cells showed a 338 fold and TE-1 cells a 290 fold higher MK2 mRNA expression. However, we have to emphasize once more that overexpression resulted in very high MK2 transcript levels while protein induction was rather moderate. To address the question if overexpression of MK2 influences proliferation esophageal cancer cells FLO-1, SK-GT-4, and TE-1 cells were transfected with the MK2 expression plasmid or an empty control vector. Summing up the results of microscopic images, the EZ4U proliferation assays and cell count determination it can be said that MK2 overexpression led to a small reduction of cell growth when compared to control transfected cells.

Also, the results of the scratch-wound assays revealed that MK2 transfected cells exhibited marginally reduced migration when compared to control transfected cells.

Thus, transient transfection of esophageal cancer cells with MK2 expression plasmid did not show a major impact on the proliferative or migratory capacity of these cells. This may, again, indicate that MK2 has no functional role in these processes. Alternatively, the level of protein overexpression achieved may not be sufficient to trigger functional changes. A more elaborate investigation on regulatory feedback loops would be required to address this issue and possibly yield higher levels of MK2 protein overexpression (in line with highly elevated transcript levels).

With respect to cell migration, it was unexpected that neither MK2 silencing nor MK2 overexpression resulted in any aberration of cancer cell migration. In previous studies it has clearly been shown that MK2 regulates Hsp27 phosphorylation for actin polymerization and that both, excessive or insufficient actin remodeling blocks cell migration [29]. Again, the role of MK2 in esophageal cancer cells seems to be cell type specific and distinct from the role observed in other cell types, which warrants further investigation.

Concerning the future project design for subsequent studies, it would be of interest to further investigate cancer cell invasion by scratch-wound assays with matrix overlay to study the importance of MK2 in MMP activity in cancer cell invasion. As MK2 has previously been shown to regulate MMP-2 and MMP-9 in other cell types [19, 20], an impact on the invasive properties of esophageal cancer cells is feasible. Furthermore, the cytokines and chemokines which are secreted by esophageal cancer cells could be analyzed with bead arrays following silencing or overexpression of MK2 in esophageal cancer cells. In particular chemokines like IL-8 known to favor tumor growth and angiogenesis are known as MK2 targets [34] and may also be subject to regulation by MK2 in esophageal cancer cells.

In summary, our study has shown that MK2 protein is detectable in esophageal cancer cells but seems to be subject to regulation and cellular localization distinct from other cell types. Silencing or overexpression of MK2 in esophageal cancer cells had no substantial effect on cell proliferation and migration. Further studies are warranted investigating the role of MK2 in cell invasion, chemokine expression and stress protection.

ABBREVIATIONS

AA/Bis	acrylamide/bis-acrylamide
ACTB	beta-actin
APS	ammonium persulfate
aqua dest.	aqua destillata
ARE	AU-rich element
ATM	ataxia telangiectasia mutated
ATR	ataxia telangiectasia and Rad3-related protein
BCA	bicinchoninic acid
Cdc	cell division cycle
Cdk	cyclin-dependent kinase
Chk	checkpoint kinase
CLSM	confocal laser scanning microscopy
CMV	cytomegalovirus
CNV	copy number variation
DMSO	dimethyl sulfoxide
DTT	dithiothreitol
ECACC	European Collection of Cell Cultures
EDTA	ethylenediaminetetraacetic acid
EGFP	enhanced green fluorescent protein
EGFP	enhanced green fluorescent protein
ERK	extracellular signal-regulated kinase
ETV1	E twenty-six translocation variant 1
FCS	fetal calf serum
GFP	green fluorescent protein
GIST	gastrointestinal stromal tumor
HRP	horseradish peroxidase
Hsp25	Heat shock protein 25
Hsp27	Heat shock protein 27
IFNγ	interferon gamma
IgG	immunoglobulin G

IL	interleukin
JNK	c-Jun amino (N)-terminal kinase
LPS	lipopolysaccharide
mAb	monoclonal antibody
MAPK	mitogen activated protein kinase
MAPKAPK	mitogen activated protein kinase-activated protein kinase
MAPKK	mitogen-activated protein kinase kinase
MAPKKK	mitogen-activated protein kinase kinase kinase
MEKK	mitogen activated protein kinase kinase kinase
MK2	mitogen activated protein kinase-activated protein kinase 2
MMP	matrix metalloproteinase
MNKs	MAPK-interacting kinases
MSKs	mitogen- and stress-activated kinases
NES	nuclear export signal
NLK	Nemo-like kinase
NLS	nuclear localization signal
PBR	polybasic region
PBS^{++}	Dulbecco's phosphate-buffered saline with Ca^{2+} and Mg^{2+}
PBSdef	Dulbecco's phosphate-buffered saline without Ca^{2+} and Mg^{2+}
phospho-MK2	phosphorylated MK2
p-MK2	phosphorylated MK2
PP2A	protein phosphatase 2A
PVDF	polyvinylidene fluoride
qRT-PCR	quantitative real-time polymerase chain reaction
ROS	reactive oxygen species
RSKs	ribosomal S6 kinases
RT	room temperature
SDS	sodium dodecyl sulfate
SH3	Src-homology-3
siRNA	small interfering RNA
SUMO	small ubiquitin-like modifier
TC	tissue culture

TEMED	tetramethylethylenediamine
TGFβ	transforming growth factor beta
TIC	tumor-inducing cell
TNFα	tumor necrosis factor alpha
TRIS	tris(hydroxymethyl)aminomethane
TTP	tristetraprolin
VPR	viral protein R

REFERENCES

1.   Pearson G, Robinson F, Gibson TB, Xu BE, Karandikar M, Berman K, Cobb MH: **Mitogen-activated protein (MAP) kinase pathways: Regulation and physiological functions**. *Endocr Rev* 2001, **22**(2):153-183.

2.   Cargnello M, Roux PP: **Activation and function of the MAPKs and their substrates, the MAPK-activated protein kinases**. *Microbiol Mol Biol Rev* 2011, **75**(1):50-83.

3.   Meng W, Swenson LL, Fitzgibbon MJ, Hayakawa K, Ter Haar E, Behrens AE, Fulghum JR, Lippke JA: **Structure of mitogen-activated protein kinase-activated protein (MAPKAP) kinase 2 suggests a bifunctional switch that couples kinase activation with nuclear export**. *J Biol Chem* 2002, **277**(40):37401-37405.

4.   Benlevy R, Leighton IA, Doza YN, Attwood P, Morrice N, Marshall CJ, Cohen P: **Identification of Novel Phosphorylation Sites Required for Activation of Mapkap Kinase-2**. *Embo Journal* 1995, **14**(23):5920-5930.

5.   Stokoe D, Campbell DG, Nakielny S, Hidaka H, Leevers SJ, Marshall C, Cohen P: **MAPKAP kinase-2; a novel protein kinase activated by mitogen-activated protein kinase**. *The EMBO journal* 1992, **11**(11):3985-3994.

6.   Ben-Levy R, Hooper S, Wilson R, Paterson HF, Marshall CJ: **Nuclear export of the stress-activated protein kinase p38 mediated by its substrate MAPKAP kinase-2**. *Curr Biol* 1998, **8**(19):1049-1057.

7.   Parra-Palau JL, Scheper GC, Wilson ML, Proud CG: **Features in the N and C termini of the MAPK-interacting kinase Mnk1 mediate its nucleocytoplasmic shuttling**. *J Biol Chem* 2003, **278**(45):44197-44204.

8.   Scheper GC, Parra JL, Wilson M, van Kollenburg B, Vertegaal ACO, Han ZG, Proud CG: **The N and C termini of the splice variants of the human mitogen-activated protein kinase-interacting kinase Mnk2 determine activity and localization**. *Molecular and Cellular Biology* 2003, **23**(16):5692-5705.

9.   Gaestel M: **MAPKAP kinases - MKs - two's company, three's a crowd**. *Nat Rev Mol Cell Biol* 2006, **7**(2):120-130.

10.   Stokoe D, Engel K, Campbell DG, Cohen P, Gaestel M: **Identification of MAPKAP kinase 2 as a major enzyme responsible for the phosphorylation of the small mammalian heat shock proteins**. *FEBS letters* 1992, **313**(3):307-313.

11.   ter Haar E, Prabhakar P, Liu X, Lepre C: **Crystal structure of the p38 alpha-MAPKAP kinase 2 heterodimer**. *J Biol Chem* 2007, **282**(13):9733-9739.

12.   Su AI, Wiltshire T, Batalov S, Lapp H, Ching KA, Block D, Zhang J, Soden R, Hayakawa M, Kreiman G *et al*: **A gene atlas of the mouse and human protein-encoding transcriptomes**. *Proc Natl Acad Sci U S A* 2004, **101**(16):6062-6067.

13.   Hegen M, Gaestel M, Nickerson-Nutter CL, Lin LL, Telliez JB: **MAPKAP kinase 2-deficient mice are resistant to collagen-induced arthritis**. *Journal of immunology* 2006, **177**(3):1913-1917.

14.   Feng YJ, Li YY: **The role of p38 mitogen-activated protein kinase in the pathogenesis of inflammatory bowel disease**. *J Dig Dis* 2011, **12**(5):327-332.

15. Birner P, Beer A, Vinatzer U, Stary S, Hoftberger R, Nirtl N, Wrba F, Streubel B, Schoppmann SF: **MAPKAP kinase 2 overexpression influences prognosis in gastrointestinal stromal tumors and associates with copy number variations on chromosome 1 and expression of p38 MAP kinase and ETV1**. *Clin Cancer Res* 2012, **18**(7):1879-1887.

16. Lin SP, Lee YT, Yang SH, Miller SA, Chiou SH, Hung MC, Hung SC: **Colon cancer stem cells resist antiangiogenesis therapy-induced apoptosis**. *Cancer Lett* 2013, **328**(2):226-234.

17. Wang HW, Boshoff C: **Linking Kaposi virus to cancer-associated cytokines**. *Trends Mol Med* 2005, **11**(7):309-312.

18. Liu B, Yang L, Huang B, Cheng M, Wang H, Li Y, Huang D, Zheng J, Li Q, Zhang X *et al*: **A functional copy-number variation in MAPKAPK2 predicts risk and prognosis of lung cancer**. *American journal of human genetics* 2012, **91**(2):384-390.

19. Xu L, Chen S, Bergan RC: **MAPKAPK2 and HSP27 are downstream effectors of p38 MAP kinase-mediated matrix metalloproteinase type 2 activation and cell invasion in human prostate cancer**. *Oncogene* 2006, **25**(21):2987-2998.

20. Kumar B, Koul S, Petersen J, Khandrika L, Hwa JS, Meacham RB, Wilson S, Koul HK: **p38 mitogen-activated protein kinase-driven MAPKAPK2 regulates invasion of bladder cancer by modulation of MMP-2 and MMP-9 activity**. *Cancer Res* 2010, **70**(2):832-841.

21. Chen CC, Chen LC, Liang Y, Tsang NM, Chang YS: **Epstein-Barr virus latent membrane protein 1 induces the chemotherapeutic target, thymidine phosphorylase, via NF-kappaB and p38 MAPK pathways**. *Cell Signal* 2010, **22**(7):1132-1142.

22. Yang L, Liu B, Qiu F, Huang B, Li Y, Huang D, Yang R, Yang X, Deng J, Jiang Q *et al*: **The effect of functional MAPKAPK2 copy number variation CNV-30450 on elevating nasopharyngeal carcinoma risk is modulated by EBV infection**. *Carcinogenesis* 2013.

23. Engel K, Kotlyarov A, Gaestel M: **Leptomycin B-sensitive nuclear export of MAPKAP kinase 2 is regulated by phosphorylation**. *The EMBO journal* 1998, **17**(12):3363-3371.

24. Neininger A, Thielemann H, Gaestel M: **FRET-based detection of different conformations of MK2**. *Embo Rep* 2001, **2**(8):703-708.

25. Reinhardt HC, Yaffe MB: **Kinases that control the cell cycle in response to DNA damage: Chk1, Chk2, and MK2**. *Curr Opin Cell Biol* 2009, **21**(2):245-255.

26. Huard S, Elder RT, Liang D, Li G, Zhao RY: **Human immunodeficiency virus type 1 Vpr induces cell cycle G2 arrest through Srk1/MK2-mediated phosphorylation of Cdc25**. *J Virol* 2008, **82**(6):2904-2917.

27. Reinhardt HC, Aslanian AS, Lees JA, Yaffe MB: **p53-deficient cells rely on ATM- and ATR-mediated checkpoint signaling through the p38MAPK/MK2 pathway for survival after DNA damage**. *Cancer cell* 2007, **11**(2):175-189.

28. Landry J, Lambert H, Zhou M, Lavoie JN, Hickey E, Weber LA, Anderson CW: **Human Hsp27 Is Phosphorylated at Serines-78 and Serines-82 by Heat-Shock and Mitogen-Activated Kinases That Recognize the Same Amino-Acid Motif as S6 Kinase-Ii**. *Journal of Biological Chemistry* 1992, **267**(2):794-803.

29.   Chang E, Heo KS, Woo CH, Lee H, Le NT, Thomas TN, Fujiwara K, Abe J: **MK2 SUMOylation regulates actin filament remodeling and subsequent migration in endothelial cells by inhibiting MK2 kinase and HSP27 phosphorylation**. *Blood* 2011, **117**(8):2527-2537.

30.   Hedges JC, Dechert MA, Yamboliev IA, Martin JL, Hickey E, Weber LA, Gerthoffer WT: **A role for p38(MAPK)/HSP27 pathway in smooth muscle cell migration**. *J Biol Chem* 1999, **274**(34):24211-24219.

31.   Huang C, Jacobson K, Schaller MD: **MAP kinases and cell migration**. *J Cell Sci* 2004, **117**(Pt 20):4619-4628.

32.   Kotlyarov A, Neininger A, Schubert C, Eckert R, Birchmeier C, Volk HD, Gaestel M: **MAPKAP kinase 2 is essential for LPS-induced TNF-alpha biosynthesis**. *Nat Cell Biol* 1999, **1**(2):94-97.

33.   Neininger A, Kontoyiannis D, Kotlyarov A, Winzen R, Eckert R, Volk HD, Holtmann H, Kollias G, Gaestel M: **MK2 targets AU-rich elements and regulates biosynthesis of tumor necrosis factor and interleukin-6 independently at different post-transcriptional levels**. *J Biol Chem* 2002, **277**(5):3065-3068.

34.   Winzen R, Kracht M, Ritter B, Wilhelm A, Chen CY, Shyu AB, Muller M, Gaestel M, Resch K, Holtmann H: **The p38 MAP kinase pathway signals for cytokine-induced mRNA stabilization via MAP kinase-activated protein kinase 2 and an AU-rich region-targeted mechanism**. *The EMBO journal* 1999, **18**(18):4969-4980.

35.   Ronkina N, Menon MB, Schwermann J, Tiedje C, Hitti E, Kotlyarov A, Gaestel M: **MAPKAP kinases MK2 and MK3 in inflammation: complex regulation of TNF biosynthesis via expression and phosphorylation of tristetraprolin**. *Biochem Pharmacol* 2010, **80**(12):1915-1920.

36.   Hitti E, Iakovleva T, Brook M, Deppenmeier S, Gruber AD, Radzioch D, Clark AR, Blackshear PJ, Kotlyarov A, Gaestel M: **Mitogen-activated protein kinase-activated protein kinase 2 regulates tumor necrosis factor mRNA stability and translation mainly by altering tristetraprolin expression, stability, and binding to adenine/uridine-rich element**. *Mol Cell Biol* 2006, **26**(6):2399-2407.

37.   Brook M, Sully G, Clark AR, Saklatvala J: **Regulation of tumour necrosis factor alpha mRNA stability by the mitogen-activated protein kinase p38 signalling cascade**. *FEBS letters* 2000, **483**(1):57-61.

38.   Ricci-Vitiani L, Lombardi DG, Pilozzi E, Biffoni M, Todaro M, Peschle C, De Maria R: **Identification and expansion of human colon-cancer-initiating cells**. *Nature* 2007, **445**(7123):111-115.

39.   Lin SP, Lee YT, Wang JY, Miller SA, Chiou SH, Hung MC, Hung SC: **Survival of cancer stem cells under hypoxia and serum depletion via decrease in PP2A activity and activation of p38-MAPKAPK2-Hsp27**. *PLoS One* 2012, **7**(11):e49605.

40.   Kobayashi Y, Qi X, Chen G: **MK2 Regulates Ras Oncogenesis through Stimulating ROS Production**. *Genes & Cancer* 2012, **3**(7-8):521-530.

41.   Dolado I, Swat A, Ajenjo N, De Vita G, Cuadrado A, Nebreda AR: **p38alpha MAP kinase as a sensor of reactive oxygen species in tumorigenesis**. *Cancer cell* 2007, **11**(2):191-205.

42. Hamasaki T, Hattori T, Kimura G, Nakazawa N: **Tumor progression and expression of matrix metalloproteinase-2 (MMP-2) mRNA by human urinary bladder cancer cells**. *Urological research* 1998, **26**(6):371-376.

43. Johansen C, Vestergaard C, Kragballe K, Kollias G, Gaestel M, Iversen L: **MK2 regulates the early stages of skin tumor promotion**. *Carcinogenesis* 2009, **30**(12):2100-2108.

44. Janknecht R: **Cell type-specific inhibition of the ETS transcription factor ER81 by mitogen-activated protein kinase-activated protein kinase 2**. *J Biol Chem* 2001, **276**(45):41856-41861.

45. Anderson DR, Meyers MJ, Vernier WF, Mahoney MW, Kurumbail RG, Caspers N, Poda GI, Schindler JF, Reitz DB, Mourey RJ: **Pyrrolopyridine inhibitors of mitogen-activated protein kinase-activated protein kinase 2 (MK-2)**. *J Med Chem* 2007, **50**(11):2647-2654.

46. Mourey RJ, Burnette BL, Brustkern SJ, Daniels JS, Hirsch JL, Hood WF, Meyers MJ, Mnich SJ, Pierce BS, Saabye MJ *et al*: **A benzothiophene inhibitor of mitogen-activated protein kinase-activated protein kinase 2 inhibits tumor necrosis factor alpha production and has oral anti-inflammatory efficacy in acute and chronic models of inflammation**. *The Journal of pharmacology and experimental therapeutics* 2010, **333**(3):797-807.

47. Chotani MA, Touhalisky K, Chiu IM: **The small GTPases Ras, Rac, and Cdc42 transcriptionally regulate expression of human fibroblast growth factor 1**. *J Biol Chem* 2000, **275**(39):30432-30438.

48. Pfaffl MW: **A new mathematical model for relative quantification in real-time RT-PCR**. *Nucleic Acids Research* 2001, **29**(9).

49. Duggan SP, Gallagher WM, Fox EJ, Abdel-Latif MM, Reynolds JV, Kelleher D: **Low pH induces co-ordinate regulation of gene expression in oesophageal cells**. *Carcinogenesis* 2006, **27**(2):319-327.

50. Barretina J, Caponigro G, Stransky N, Venkatesan K, Margolin AA, Kim S, Wilson CJ, Lehar J, Kryukov GV, Sonkin D *et al*: **The Cancer Cell Line Encyclopedia enables predictive modelling of anticancer drug sensitivity**. *Nature* 2012, **483**(7391):603-607.

51. Mahidhara RS, De Oliveira PEQ, Kohout J, Beer DG, Lin JY, Watkins SC, Robbins PD, Hughes SJ: **Altered trafficking of Fas and subsequent resistance to Fas-mediated apoptosis occurs by a wild-type p53 independent mechanism in esophageal adenocarcinoma**. *J Surg Res* 2005, **123**(2):302-311.

52. Altorki N, Schwartz GK, Blundell M, Davis BM, Kelsen DP, Albino AP: **Characterization of Cell-Lines Established from Human Gastric-Esophageal Adenocarcinomas - Biologic Phenotype and Invasion Potential**. *Cancer* 1993, **72**(3):649-657.

53. Yamada Y, Yoshida T, Hayashi K, Sekiya T, Yokota J, Hirohashi S, Nakatani K, Nakano H, Sugimura T, Terada M: **P53 Gene-Mutations in Gastric-Cancer Metastases and in Gastric-Cancer Cell-Lines Derived from Metastases**. *Cancer Research* 1991, **51**(21):5800-5805.

ABSTRACT

Mitogen activated protein kinase-activated protein kinases (MAPKAPKs or MKs) play an important role in signal transduction and regulate cellular processes like cell cycle control, apoptosis, migration and inflammatory response. Elevated levels of MK2 have been found in cancer cells. The focus of this master thesis was to investigate MK2 expression and its role in the proliferation and migration of gastroesophageal cancer cells. MK2 expression was first determined with immunohistochemical staining of tumor tissue retrieved from esophageal carcinoma patients as well as with immunofluorescence staining of esophageal cancer cell lines. Another aim was to assess the influence of pharmacological MK2 inhibitors, gene silencing via siRNA and MK2 overexpression on the proliferation and migration of tumor cells. The efficacy of silencing and overexpression was assessed by quantitative RT-PCR of MK2 transcripts. To determine the effect on proliferation, the cell count was determined, a metabolic assay was performed, and microscopic images were taken. To verify a possible effect of MK2 siRNA or MK2 overexpression on tumor cell migration, a scratch assay was performed. The results on MK2 expression provided data which were partially contradictory to the literature: While phosphorylated (activated) MK2 is generally expected to localize to the cytosol, it was primarily found in the nucleus of esophageal cancer cells pointing to a distinct MK2 regulation in this cell type. Concerning the role of MK2 in cell proliferation, gene silencing, overexpression or pharmacological inhibition with the Hsp25 kinase inhibitor did not alter survival or proliferation of esophageal cancer cells. In contrast, for the pharmacological MK2 inhibitor PF-3644022 hydrate a dose-dependent growth reduction was observed which, however, seemed to be an off-target effect. Furthermore, MK2 gene silencing or overexpression did not lead to substantial changes in the migratory behavior of these cancer cells. Summarizing it can be said that despite its prominent expression in esophageal cancer, no functional role of MK2 in cell proliferation or migration was evident which may relate to its aberrant protein distribution and warrants further investigation.

ZUSAMMENFASSUNG

Mitogen-aktivierte Proteinkinase-aktivierte Proteinkinasen (MAPKAPKs oder MKs) spielen eine wichtige Rolle in der Signaltransduktion und steuern zelluläre Prozesse wie Zellzyklus, Apoptose, Migration und Entzündungsreaktion. Eine erhöhte MK2 Expression wurde für Tumorzellen beobachtet. Der Forschungsfokus dieser Masterarbeit lag auf der Charakterisierung von MK2 in gastroösophagealen Tumoren und deren Rolle in der Zellproliferation und Migration. Hierfür wurden immunhistochemische Färbungen von Patientengewebe sowie Immunfluoreszenzfärbungen von ösophagealen Tumorzelllinien durchgeführt. Eine weiteres Ziel in diesem Forschungsprojekt war es, den Einfluss von pharmakologischen MK2-Inhibitoren, Abschaltung des MK2-Gens mittels siRNA sowie MK2-Überexpression auf die Proliferation und Migration der Tumorzellen festzustellen. Die Effizienz von Silencing und Überexpression wurde mittels quantitativer RT-PCR von MK2 mRNA ermittelt. Zur Messung der Proliferation wurden die Zellzahl und der Zellmetabolismus bestimmt, sowie der Wachstumsverlauf fotografisch dokumentiert. Um einen möglichen Effekt von MK2 siRNA und MK2-Überexpression auf die Tumorzell-Migration festzustellen, wurde ein so genannter *Scratch Assay* durchgeführt. Die Untersuchung der MK2 Expression in ösophagealen Tumorzellen ergab der Literatur teilweise widersprechende Ergebnisse: Anders als erwartet, war die phosphorylierte (aktive) Form von MK2 nicht im Zytosol sondern im Kern der Zellen zu finden, was auf eine Zelltyp-spezifische Proteinregulation hindeutet. Weder die Anwendung von MK2 siRNA noch die MK2 Überexpression führten zu nennenswerten Effekten auf die Proliferation und Migration der untersuchten Zellen. In Bezug auf Proliferation unter dem Einfluss von pharmakologischen Inhibitoren konnte für den Inhibitor PF-3644022 eine dosisabhängige Wachstumsreduktion festgestellt werden, nicht jedoch für den Hsp25 Kinase Inhibitor, was darauf hindeutet dass es sich bei dem PF-3644022 Effekt vermutlich um eine unspezifische (nicht MK2-vermittelte) Wirkung handelt. Zusammenfassend kann festgestellt werden, dass MK2 trotz der prominenten Expression keine evidente Rolle in der Proliferation oder Migration ösophagealer Tumorzellen spielt, was im Zusammenhang mit der aberranten Proteinverteilung stehen könnte und weitere Untersuchungen erfordert.

Curriculum Vitae

Personal Data

Name Jasmin Stieger

Date and Place of Birth August 18th, 1986, Bad Ischl, Austria

Citizenship Austrian

E-Mail jasminstieger@gmx.net

Education

1992 - 1996 Elementary school, St. Agatha

1996 - 2000 Secondary modern school, Bad Goisern

2000 - 2005 Federal Secondary College for Economy, Major Social Management, Bad Ischl

2005 - 2007 Medical University of Innsbruck, Human Medicine

2007 - 2010 Paris Lodron University of Salzburg, Bachelor of Science in Genetics

since 2010 University of Vienna, Masters program in Genetics and Developmental Biology, Major Genetics and Molecular Pathology

12/2012 - 11/2013 Master thesis on the Role of Mitogen Activated Protein Kinase-Activated Protein Kinase 2 in Gastroesophageal Cancer Cells, Anna Spiegel Center of Translational Research, Department of Surgery, Medical University of Vienna

Scientific and other Work Experience

summer of 2005, 2006, 2007, 2008 and 2010

Hoffmann & Co. Elektrokohle AG, Chemical and Physical Laboratory, Bad Goisern

Titrimetric and photometric analyses, raw material examination, surface structure analysis by scanning electron

microscopy and energy-dispersive X-ray microanalysis, quality assessment of finished products

3/2009 - 6/2009, 3/2010-6/2010   Paris Lodron University of Salzburg

Tutor; support of course-participating students

9/2010 - 9/2011   Ludwig Boltzmann Institute for Experimental and Clinical Traumatology, Vienna (Histology)

Processing of histological specimens, histochemistry, immunohistochemistry

7/2012 - 10/2012   Ludwig Boltzmann Institute for Experimental and Clinical Traumatology, Vienna (Group Holnthoner)

Cell culture, immunofluorescence, flow cytometry, endothelial cell isolation

Further Qualifications

Language Skills   German: first language

English: fluent

Swedish: basic knowledge

Austrian Sign Language: basic knowledge

Computer Literacy   MS Office, ECDL

Personal Interests

Hobbies   Photography, Literature, Archery

Research Interests   Human Medicine, Forensic Science, Behavioral Biology